DESIGN AND SYNTHESIS OF PHOTOSWITCHABLE MOLECULES FOR BIOLOGICAL APPLICATIONS.

Antonio Bautista Barrufet

Antonio Bautista Barrufet

Design and Synthesis of Photoswitchable Molecules for Biological Applications

DOCTORAL THESIS

Supervised by:

Prof. Dr. Pau Gorostiza Langa (director)
Institut de Bioenginyeria de Catalunya (IBEC)

Prof. Dr. Miquel Àngel Pericàs Brondo (co – director)
Institut Català d'Investigació Química (ICIQ)

UNIVERSITAT ROVIRA I VIRGILI

Tarragona, 2014

Institut de Bioenginyeria de Catalunya
Baldiri Reixac, 10-12
08028 Barcelona,
Tel. +34(93)403 97 06

UNIVERSITAT ROVIRA I VIRGILI

Departament de Química Orgànica i Analítica
C/ Marcel.lí Domingo s/n
Campus Sescelades
43007 - Tarragona
Tel. + 34 977 559 769
Fax. 977 558 446

Institut Català d'Investigació Química
Av. Països Catalans
43007 Tarragona
Tel. 977 920 200
Fax 977 920 225

Prof. PAU GOROSTIZA LANGA as the director and Prof. MIQUEL A. PERICÀS BRONDO as the co – director, both Group Leaders of a Research Group,

CERTIFY, that the present Doctoral Thesis entitled: "**Design and Synthesis of Photoswitchable Molecules for Biological Applications**", presented by Antonio Bautista Barrufet to receive the degree of Doctor, has been carried out under their supervision between the Institute of Chemical Research of Catalonia (ICIQ) and the Bioengineering Institute of Catalonia (IBEC), and fulfils all the requirements to be awarded with the "European Doctor" mention.

Barcelona, 3rd September 2014.

PhD Supervisors

Prof. Pau Gorostiza Langa
(director)

Prof. Miquel Àngel Pericàs Brondo
(co – director)

UNIVERSITAT ROVIRA I VIRGILI
DESIGN AND SYNTHESIS OF PHOTOSWITCHABLE MOLECULES FOR BIOLOGICAL APPLICATIONS.
Antonio Bautista Barrufet
Dipòsit Legal: T 1920-2014

I am personally grateful to:

- Spanish Ministry of Science and Innovation for an FPI predoctoral fellowship (ref. BES-2009-025077).

List of Publications

1. "Optical Control of Enzyme Enantioselectivity in Solid Phase"

Bautista-Barrufet, **A**., López-Gallego, F., Rojas-Cervellera, V., Rovira, C., Pericàs, M.A., Guisán, J.M., Gorostiza, P.

ACS Catalysis **2014**, *4* (3), 1004-1009.

2. "Photoswitchable Ion Channels and Receptors"

Bautista-Barrufet, **A**., Izquierdo-Serra, M., Gorostiza, P.

F. Benfenati et al. (eds.), Novel Approaches for Single Molecule Activation and Detection. Advances in Atom and Single Molecule Machines. DOI 10.1007/978-3-662-43367-6_9. Springer-Verlag Berlin Heidelberg 2014.

3. "Photocontrol of Endogenous Receptors using Targeted Covalent Ligands"

Izquierdo-Serra, M., **Bautista-Barrufet**, **A**., Trapero, A., Garrido-Charles, A., Valbuena, S., Camarero, N., Pérez-Gimenez, A., Lerma, J., Rodríguez-Escrich, C., Pericàs, M.A., Llebaria, A., Gorostiza, P.,

Manuscript in preparation

Acknowledgments

Esta tesis, no sólo es un recopilatorio de capítulos ya que al ser "itinerante" se suman lugares, vivencias, personas y sentimientos distintos en cada uno de ellos aunque algunos comunes, por suerte. Con eso no quiero dar a entender que haya sido malo, sino todo lo contrario, sumándole intensidad y variedad.

Artífice de este viaje fué Pau al que conocí por un anuncio colgado en la facultad donde se necesitaba un estudiante durante el verano, para hacer la síntesis de *unas moléculas sencillas*...y me lo creí.

La primera parada fue el ICIQ, dónde conocí a Miquel, ya director del instituto, que nos cedió un espacio y facilidades para poder trabajar así como haciéndome sentir parte de su grupo como si fuera uno más. Allí conocí a Patri, Félix, Dani, Carolina, Xisco, Rafa, Rocío, Ciril, Xacobe, Sonia, Esther, Christian y Carles Rodríguez que buenamente intentó transmitirme su experiencia, aprendiendo a trabajar en un laboratorio, asistiéndome con buenos consejos sin esperar nada a cambio.
Más tarde algunos se fueron, entre ellos yo mismo, pero al volver, después de finalizar la licenciatura, algunas caras habían cambiado, conociendo a Laura, Míriam, Diana, Paola, Jagjit, Carles Ayats, Erik, Julien, Erhan, Pinar, Irina, Xinyuan y Andrea con quién compartimos des de colas en el rotavapor o la máquina del café hasta noches dónde el tiempo se comprimía alternando con partidos de volley y San/ta Magís/Teclas irrepetibles.
Fuera del grupo e incondicionales de los nombrados eventos sociales y que si no los había, espontáneamente organizaban; Mariona, Txepo, David, Jorge, grupo del Dr. Martín (Joan, Asraa, Paula, Arkaitz, Petr, Pep).
No me gustaría dejar a las personas de "soporte" que, con mucha paciencia, nos soportan. Entre ellos está el personal administrativo, Ricard Rius (IBEC), Mercé y Sara, que no perecí entre papeles, trámites y gestiones gracias a ellos. También gracias al personal de soporte a la investigación; Kerman, Israel, Gabriel, Fernando, Gisela, Ivette, Eduardo, Simona, Enrique, Noemí y Sofía ayudándonos y facilitándonos el día a día.
No podia olvidarme a las chicas de limpieza, que con su salero marcado por la música nos alegraban los días más largos a los nocturnos, no Somnath?

Fuera del ICIQ, me gustaría recordar el piso de Sant Antoni Maria Claret del que nunca me aprendería el numero, compartiéndolo con Rico, Carlos, Jordi, Patrik, Abelina y Bara, una fémina de uñas muy largas!, llenando la mochila de buenos recuerdos, preparándome para el siguiente destino sin olvidar a Marta, Rafa, Estefi, Alba, Roser, Antonella, Emilio, Delfín y Jaumet que me obsequiaron con un buen kit de supervivencia, del todo útil fuera de Tarragona.

La segunda parada fue Madrid, en el Instituto de Catálisis y Petroleoquímica (UAM), donde pasé de ser el nuevo a el nuevo que se cortó y que pronto me recuperé gracias al apoyo de Fer, Javi, José Manuel y Mari Carmen y del que siempre estaré muy agradecido. El grupo aunque no tan grande era muy internacional coincidiendo también con Susana, Tanja, Oscar, Marita, Eri, Andreina, Manuela, Sonia, Cleiton, Cristina, Munilla, César, Gloria y Palomo, a los que se juntarían los fines de semana Víctor y Violeta Gong, mis compañeros de Begoña para conocer el Madrid de los madrileños del que muchas veces había oído hablar pero que nunca había visto.
De vuelta, antes de coger un avión para ir a Regensburg paré en Barcelona, para trabajar un par de meses en el laboratorio del Dr. Amadeu, a quién ya conocía. Allí compartí vitrina y risas con Ana Trapero, Ana Alcaide, Ester, Roser, Jousef, Xavi, Joan y Carme.

Al terminar el verano empezó una nueva etapa en el sud de Baviera, en Regensburg donde la familia Gajek tenia una bonita casa para acogerme durante mi estancia. Allí conocí a Angelo, Gabi i Ferdinand con los que compartí un Dult, agradable convivencia, sabrosas cenas, reciclaje y compra de los sábados.
En la Universidad de Regensburg estaba el grupo del Profesor Burkhard König, a quién agradezco los cuatro meses de estancia. En una planta entera se encontraban Manuel, Ana, Carolyn, Peter Raster, Tamal, Melanie, Thea, Stephanie, Ramona, Andreas, Michal, Peter Schroll, Thomas, Maksim ,Tomas, Simone Stark, Qui, Daniel, Stephan, Durga, Natascha, Marsel, Indrajit, Petra, Viola, Rudolf, Susanne, Britta, Regina, Ernst, Simone Strauss y Javier, que junto a Gracia compartimos buenos ratos, cervezas, viajes y paseos en bici por el Danubio. Un poco más tarde llegó Max, un máster de estudiante que me ayudó en el tercer capítulo de esta tesis, haciéndome el trabajo más ameno y productivo hasta el final. Fuera del laboratorio, compartí también muy buenos ratos con Paula, Alessio, Salvattore, Matthias y Alicia, pudiendo ser aún mejores con Alessio recuperado.

Ya de vuelta, este libro se materializó en Barcelona, compartiendo despacho de Bellvitge y comidas con Núria, Santi, Mercè, Silvia, Dentxo, Aida, Ariadna, Natalia, Joan y Diana. Fuera de él aprendiendo a cocinar de Iris Silvia y Julio, conviviendo también junto a Alba, Pio, Gay, Debi y Charlotte en un espacioso piso de l'Eixample muy bién situado.

Por último me gustaría agradecer la oportunidad y confianza que Pau me brindó, su trato cercano durante estos años y su asistencia en cualquiera de las etapas del viaje.
También me gustaría dar las gracias a las personas que amablemente han corregido este manuscrito así como los asistentes en los ensayos de la defensa de la presente tesis, aportando útiles consejos y sugerencias.

Y sobretodo, agradecer a mis padres su empeño, consejos y apoyo mostrado, necesario en cada viaje y siempre.

Structure of the thesis

The content is divided in two main parts, in accordance with the biological system-type employed to confer light-sensitive properties.

The first part, divided in three chapters, is focused on the development of efficient photochromic compounds for the modulation of important brain receptors, as kainate and $GABA_A$ channel proteins.

The second part deals with the light-modulation of the catalytic site of lipase 2 using photochromic molecules, to analyse the change in the hydrolytic enantiopreference and the mechanism involved.

As an introductory summary, each part starts with an updated overview about light-sensitive type-related biological system classified by families and cronologically.

A compilation of conclusions is covered at the end of the thesis highlighting the main findings of this work.

Table of contents

PART I

CONTROLLING ENDOGENOUS RECEPTORS WITH LIGHT

This section is adapted from a book chapter published in *Novel Approaches for Single Molecule Activation and Detection* in the series entitled *Advances in Atom and Single Molecule Machines*.[35] It provides an overview of the field of opto (genetic) pharmacology for the last four years, classified by receptor families using PCLs and PTLs as an introduction to the three chapters of this Part I.

PHOTOSWITCHABLE ION CHANNELS AND RECEPTORS

Antoni Bautista-Barrufet[a,b,+], Mercè Izquierdo-Serra[a,+] and Pau Gorostiza[a,c,d,*]

[a] *Institut de Bioenginyeria de Catalunya (IBEC), Barcelona, Spain.*

[b] *Institut Català d'Investigació Química (ICIQ), Tarragona, Spain.*

[c] *Centro de Investigación Biomédica en Red en Bioingeniería, Biomateriales y Nanomedicina (CIBER-BBN), Zaragoza, Spain.*

[d] *Institució Catalana de Recerca i Estudis Avançats (ICREA), Barcelona, Spain.*

[+] *Equal contribution*

[*] *Corresponding author. E-mail: pau@icrea.cat*

Abstract

The development of photochromic and photoswitchable tethered ligands for ion channels and receptors have made important contributions to optopharmacology and optogenetic pharmacology. These compounds provide new tools to study ion channel proteins and to understand their function and pathological implications. Here we describe the design, methodology and light-regulated applications of the available photoswitches, classified according to the target family, with special emphasis on ligand- and voltage-gated channels.

CHAPTER 3: Photochromic ligands for GABA$_A$ receptors

This work is the result of a short stage granted by the Spanish Ministery within the FPI subprogram support EEBB-I-13-07742, carried out during 2013 (September-December period), at Prof. Dr. Burkhard König's laboratories (Regensburg Universität, Germany).

1. OBJECTIVES

In this chapter we will present an approach for the synthesis of different photochromic ligands (PCL's) for controlling $GABA_A$ protein channel activity with light. For this purpose, we aimed at combining a benzodiazepine scaffold, as the pharmacophore, with an azo group as the light-sensitive unit.

2. BACKGROUND

The pentameric ligand-gated receptor family is a superfamily of receptors located at the postsynaptic cell membrane which shows both excitatory and inhibitory effects on the mammalian central nervous system (CNS).[44] This superfamily includes nicotinic acetylcholine receptors (nAChr), serotonin receptors ($5\text{-}HT_3$), γ-aminobutyric acid receptors ($GABA_A$) and glycine receptors (GlyR).[45]

The receptors of this family are organized by four different subunits such as α, β, γ and δ and have different stoichiometries. In heteromers, the neurotransmitter binding sites are usually located at the interface between α and β subunits and three conserved domains can be distinguished in this protein family.[47, 48] Allosteric ligands are also bound in the same region, but to a different protein spot than the neurotransmitter (orthosteric ligand), for the regulation of receptor's activity. Benzodiazepines and the anesthetic propofol are allosteric modulators of $GABA_A$ receptors.[48, 49]

The receptors of γ-aminobutyric acid ($GABA_A$ and $GABA_C$) and glycine (GlyRs) are chloride-selective channel proteins, and thus have an inhibitory effect on the neuronal activity in the central nervous system. They are important targets for anxiety treatment and anesthesia,[1] and controlling their activity with light is attractive because it would allow the inhibition of neuronal tissue using designed spatiotemporal patterns, for example to functionally isolate specific neuronal circuits. This can be achieved with naturally light-gated ion pumps like halorhodopsin or archaerhodopsin,[103, 151] however they require continuous illumination, which is not convenient for certain applications.[152] In principle, photoswitchable glycine or $GABA_A$ receptors with slow relaxation lifetimes could be stimulated with a short light pulse, allowing the inhibition of neurons in the dark. Tethered glycine or GABA receptor ligands are required to design PTLs of these receptors, but adding a tether reduces the affinity in the case of $GABA_A$ agonists.[153] However, a photoswitchable antagonist inhibitor has been used to regulate $GABA_A$ receptors with light.[38] Kramer et al. have developed a photoswitchable maleimide-azo-muscimol ligand (MAM-6) that conjugates covalently with cysteine introduced residues in the α_1 subunit. Reversible interconversion between states occurs at 380 and 500 nm, modulating from the functional *t*rans stable form to the inactive *c*is state, obtaining photocontrol over neuron excitation in response to presynaptic stimulation.[154]

As an alternative to the orthosteric place, an allosteric binding site like that of propofol[48, 49] can be the target of photoswitch design. Two recent articles reported a PCL[155] and a PTLs[144] that potentiate GABA currents in a light-dependent fashion. A series of azo-derived propofol ligands were developed and applied to $\alpha_1\beta_{2/3}\gamma_2$ heteropentamers. These compounds were active in *trans* and inactive in *cis*, but differ in photostability, therefore in their potential applications. The photochromic AP-2 ligand, synthesized using the classical diazo coupling, presented a red-shifted *cis*-isomerization (404 nm) and a fast *trans* restoration due to para-substituted electro-donating groups that decrease the *cis* thermal stability.[155] The compound was tested in tadpoles where it controlled the anesthetic action of propofol using one wavelength.[92] On the other hand, the PTL MPC088[144] showed *cis-trans* reversibility between 365 and 440 nm respectively, and allowed modulating GABA currents in retinal and cerebellar Purkinje neurons. Spatiotemporal control of neuronal spike rate was demonstrated using this allosteric PTL.

The lack of crystal structures with the benzodiazepine allosteric ligands family bound to the receptor has delayed the development of light modulators providing this

pharmacophore. This is due to the non-selective drug action in each α subunit isoforms.[156-159]

In our approach for the synthesis of different PCLs for the $GABA_A$ ionic channel, we combined a benzodiazepine with an azo group as the photoswitchable moiety.

3. RESULTS AND DISCUSSION

Among the variety of tranquilizers known, benzodiazepines are the most important group in the inhibition of neuronal transmission, thus the structure-activity relationship is well studied and characterized. The results reported an important effect on the activity of these molecules when possessing electron withdrawing groups at the position 2 of the benzyl ring (**Figure 1**).[160]

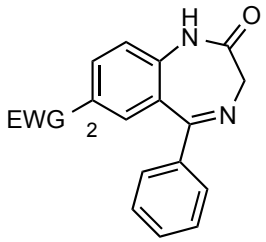

Figure 1. Positive allosteric GABAA activator.

Previous *in vitro* results obtained by PhD Peter Raster, at Regensburg University with diarylethene-based photochromic ligands (**Figure 2**) were not conclusive due to their poor solubility on cell culture conditions. Therefore, we aimed our research at the synthesis of a benzodiazepine family containing an azo group at position 2. It is important to note that azo group has already been widely applied onto biological systems to bestow light sensitivity[37, 161] due to its good physicochemical properties, easy photophysical tuning, and synthetic accessibility.[1]

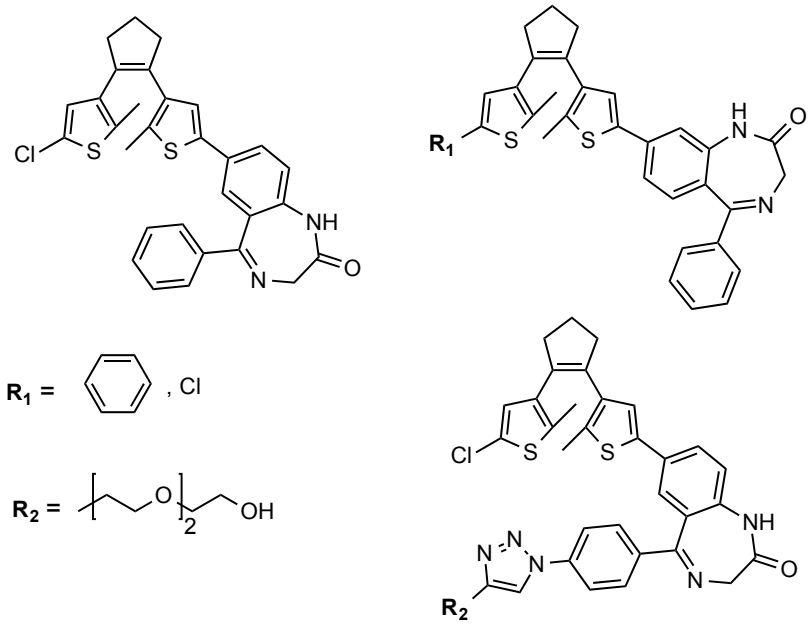

Figure 2. Benzodiazepine-dithienylethene derivatives prepared by Peter Raster.[162]

However, the aforementioned groups have associated both advantatges and disadvantatges. Azo compounds show the largest geometrical change when isomerizing but their photostationary states show rarely complete isomerization and the *cis* isomer thermally re-isomerizes back to the more stable *trans* form. Dithienylethenes can be stable in both isomeric forms but the isomerization wavelenghts are shorter (UV shifted, between 310-350 nm) and they switch the molecule between a flexible and a rigid conformation.[5]

Although 2-azo-benzodiazepines have been reported in the literature, obtained from decomposition of Nitrazepam[163] in a structure-activity study[164] and in the azo-coupling with phenols,[165] neither photochromic properties nor pharmacological activity of the corresponding photo-isomers have been investigated so far. We proposed the synthesis of three benzodiazepine derivatives **41-43** varying the R group, at position 2 of the benzyl ring, which displayed different solubility and photoisomerization properties (**Figure 3**) respect dithienylethene derivates (**Figure 2**).

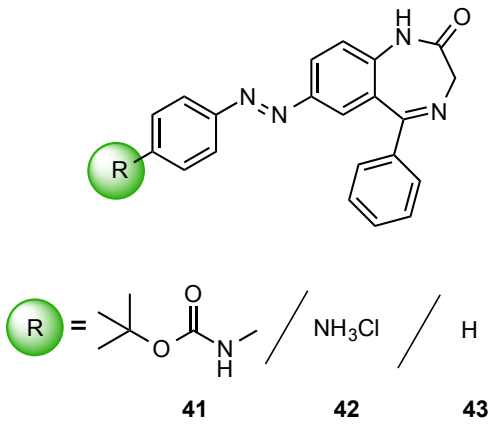

Figure 3. Representation of the structures proposed PCLs

3.1– Synthesis of the azo precursor 47

The retrosynthetic strategy used for the synthesis of the different azo derivates **41-43** is depicted in **Scheme 1**. Interestingly, all desired products were obtained starting from the same commercially available benzophenone derivative **44**.

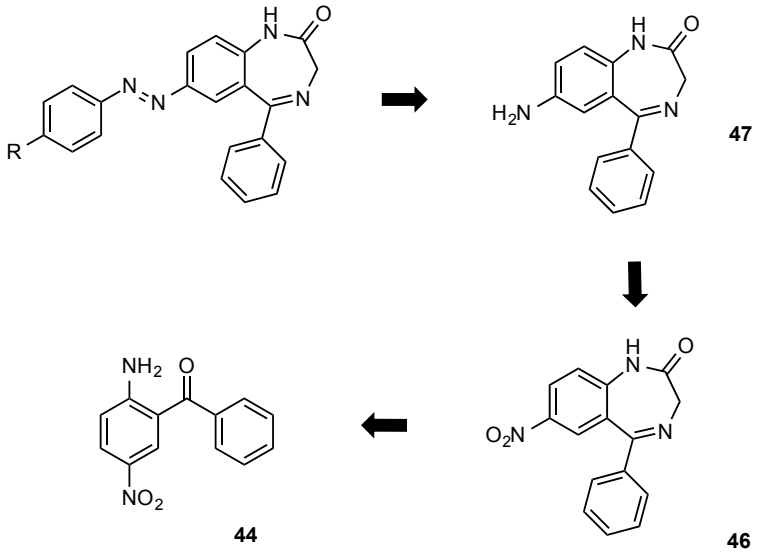

Scheme 1. General retrosynthetic route for the synthesis of azo compounds.

The reaction of benzophenone derivative **44**, with chloroacetyl chloride in presence of triethylamine gave amide **45**, which was transofrmed to 7-membered ring compound **46** by treatment of ammonium acetate and hexamethylenetetramine under reflux. Although the

yield was very low (only 14 % yield was obtained), the purification only required a crystallization with toluene and ethanol mixture. The last step for the formation of **47** involves the reduction of nitro group of compound **46**. The reduction step was performed using Iron in EtOH/HCl as a solvent mixture, giving rise the desired product **47** in a quantitative yield. Worthy of note, a previous hydrogenation using the catalytic Pd/C result in a complex mixture to separate where the imine group was partially reduced.

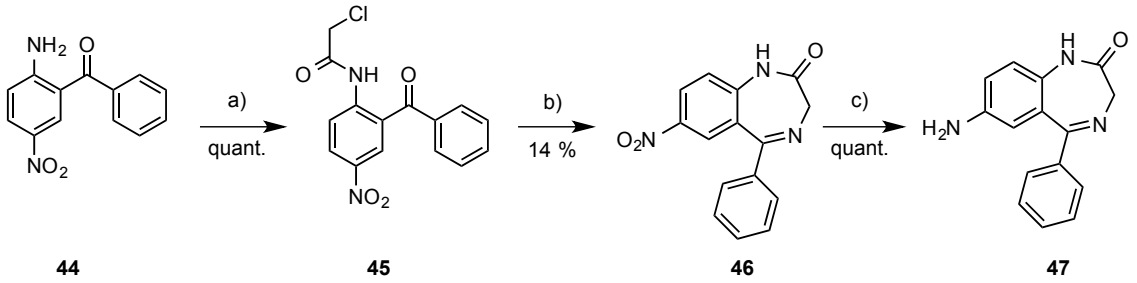

Scheme 2. *a*) Chloroacetyl chloride, Et_3N, THF (18h. rt). *b*) Hexamethylenetetramine, NH_4OAc in EtOH (reflux, N_2, overnight). *c*) Fe, EtOH/HCl (2.5 h, reflux).

3.2– Previous to the synthesis of the azo derivatives

In the literature there are several methods to obtain azo functional groups from amines.[13] One of the most employed methods is the diazotization reaction which involves the direct formation of the diazonium salt by treatment of the amine with sodium nitrite in strong acid media. However, this method was discarded due to the fact that diazepine ring can be hydrolyzed in the presence of strong acidic aqueous media (**Scheme 3**).[166, 167]

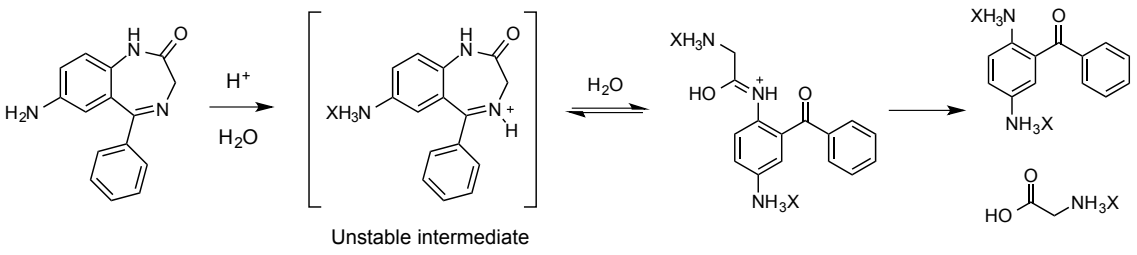

Scheme 3. Benzodiazepine hydrolysis reaction in strong acid aqueous media.

Following the Mills reaction as the selected procedure, we need an amine acting as a nucleophile to attack a nitroso derivative in acetic acid media. Among several methods, using oxidazing agents[131] or metals,[134, 168] the simplest way to prepare a nitroso compound is using potassium peroxymonosulfate (oxone),[135] also used in chapter 1 (see section 3.1.1) and 2

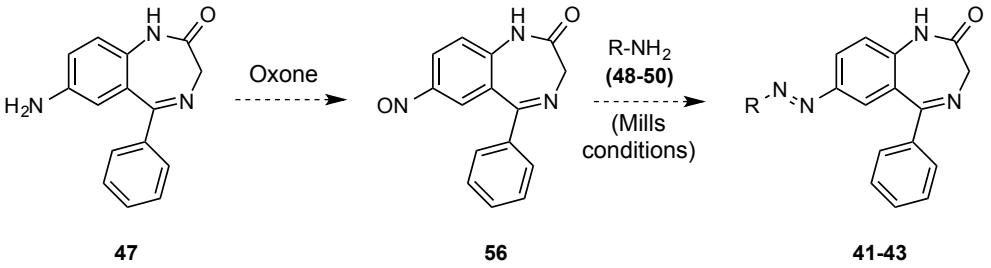

Scheme 4. Strategy of the azo compound synthesis through the common 2-nitroso-benzodiazepine intermediate.

At this point, two different possibilities for the nitroso derivative preparation appeared. One option (**Scheme 4**) was the reaction of **47** with oxone, but we obtained instead the over oxidized nitro compound **46** (**Scheme 7**)**.**

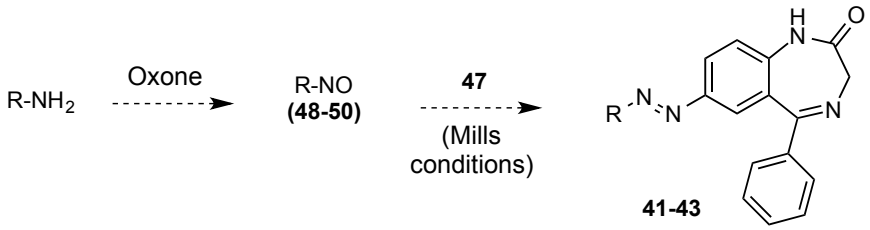

Scheme 5. Strategy of the azo compound synthesis through **48-50** nitroso intermediate.

The other alternative (**Scheme 5**) was the formation of nitroso compounds **48-50** which would react with **47** to afford azo compounds **41-43**.

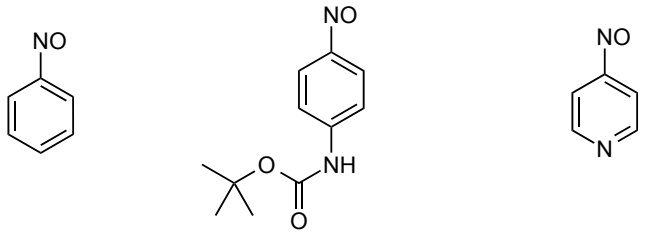

48 **49** **50**

Figure 4. Nitroso precursors for the azo coupling reaction.

Compound **48** is a commercially available compound for its long storage stability. Worthy to note, this is a particular case of stable nitroso compound, due to the fact that its stability depends on the substituents and the position occupied in the ring.[131, 135] Compound **49** was prepared from the *tert*-Butyl carbamate monoprotected *p*-aniline with oxone in 47% yield.

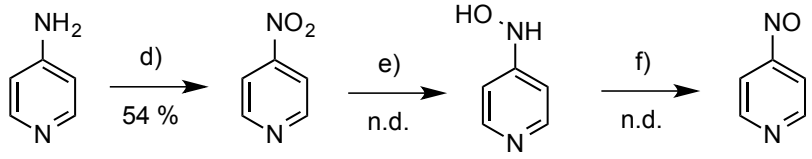

51 **52** **53** **50**

Scheme 6. d) H_2SO_4 conc., H_2O_2 (30%) rt, overnight, e) NH_4Cl, Zn in MeOH rt, 30 min., f) $Na_2Cr_2O_7$, H_2SO_4 (10%) at 0 ºC, 5 min.

The third nitroso compound **50** (**Figure 4**) was obtained using a different strategy, to avoid the easy formation of the pyridine *N*-Oxide as a main product with oxone. The synthesis started by treatment of the available 4-amino pyridine **51** with strong oxidizing conditions,[169] to give **52** in a 54% yield. Further reduction with metallic Zn and subsequent oxidation of the formed hydroxylamine with sodium dichromate allowed us to obtain the desired nitroso compound **50** (**Scheme 6**).[170]

The coupling between nitroso compound **50** and precursor **47** gave rise a mixture of products. Experimental analysis showed no coincidence between the fractions isolated and the expected azo containing substance **54** (**Figure 5**).

Important to note is that compound **55** (**Figure 5**) also attracted our interest as a potential PCL. Unfortunately, this compound was not able to be obtained due to the lack of ability to prepare the 2-nitrosobenzodiazepine **56** (**Scheme 4**)**.**

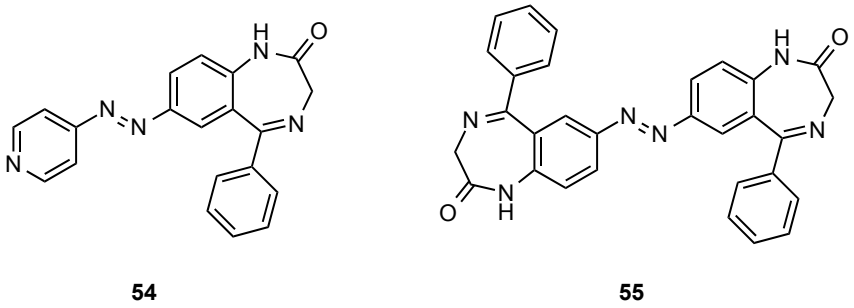

Figure 5. Other PCL candidates

Also, an interesting reductive coupling protocol was carried out to obtain the symmetric **55**[171] (**Scheme 7**), but instead, the reduced compound **47** was obtained (**Scheme 7**). Importantly, this method was a clean and selective reduction of a complex structure without the presence of metals, however a very similar procedure was reported recently in the literature.[172]

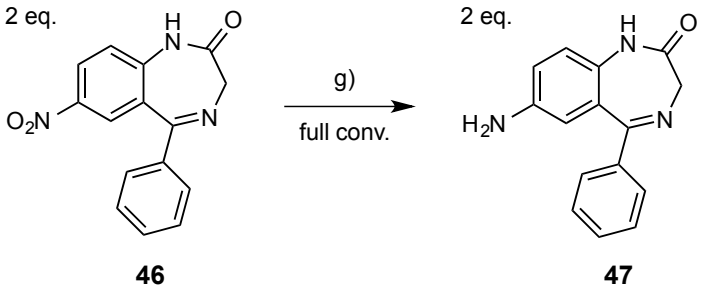

Scheme 7. g) Glucose, NaOH EtOH/H_2O, 70 ºC, 24h.

3.3– Synthesis and UV-vis characterization of azo compounds

Compounds **41**, **42** and **43** were synthesized, according to protocols described in the experimental part, in an overall yield of 11% and 7% for **41** and **43** respectively. This information is fully confirmed by the characterization data for compounds **41** and **43**. ^{1}H and ^{13}C NMR data for compound **42** (signals at 1.56 and 28.64 ppm respectively), revealed the presence of a CH_3, probably due to the incomplete deprotection of *tert*-Butoxy carbamate precursor, obtaining a mixture with **41** in a ratio of 3:1 (determined by ^{1}H NMR). HRMS analysis confirmed the presence of structure **42**.

Photo-physical properties of compounds **41** and **43** differed from solubility and relaxation times, mainly showing a 390 - 410 nm range of *cis* to *trans* isomerization and around 500 nm to recover back the *trans* state (**Table 1**). It is important to note that a more precise wavelength and relaxation time values can be determined using Flash-Photolysis technique, with the possibility to record up to milliseconds.

Compound	**THF solvent**		**[a]buffer + 1% DMSO**		**τ**	**Laser Scattering**	**ε ($M^{-1}cm^{-1}$)**
	λ_{cis}	**λ_{trans}**	**λ_{cis}**	**λ_{trans}**			
41	400	530	≅390-410	≅500	hours	no	20330
43	400	500	≅390-410	≅500	seconds	yes (60 μM)	21406

Table 1. Physical properties for azo compounds 41 and 43. *a* = Buffer was prepared according to protocol described by Sigel, E., in *The Journal of Physiology* **386**, 73-90 (1987), for *in-vitro* assay conditions. *τ* and *ε* determined in organic solvents. Laser scattering observed in buffer conditions. Isomerization, relaxation and laser scattering experiments of compounds **41** and **43** were at [30 μM], otherwise noted.

All switches in buffer solution[173] behave as a fast chromophores, relaxing before the measurement took place (τ < few seconds). Regarding stability issues in organic solvents, compound **41** exhibited slow relaxation times (hours in THF), therefore obtaining the two distinct isomer spectra with the corresponding isosbestic points when overlapped.[174] This is not the case of compound **43**, where nearly all the molecules are in the *trans* form after UV irradiation. This was confirmed by determination of τ showing a value of few seconds in

THF. For compound **42** we can only conclude an increased solubility character due to the partial carbamate deprotection.

Other irradiation experiments at a shorter wavelenght (312 nm and 30 μM concentration) for all the compounds flanked by an azo group, revealed a photolytic tendency; **43** > **41** > **42** in physiological conditions. Compound **43** was completely degraded after 15 min of irradiation. Photolysis was also observed in substance **41**, although 10% of bleaching was observed after 60 min. However, for compound **42** (containing **41)** any photolysis was observed. This tendency can be correlated with the group solubility character.

4. CONCLUSIONS

- A photochromic derivative of benzodiazepine, compound **47** was prepared using a three steps sequence from commercially available benzophenone **44** in 14% yield.

- We designed a convergent approach to synthesize benzodiazepine-PCLs bearing an azo group for the photomodulation of GABAA receptors. Two analogues were synthesized (**41** and **43**) from precursor **47** following this strategy.

- The PCLs **41** and **43** were obtained and characterized with different solubility properties and similar isomerization wavelenghts, showing fast relaxation in physiological conditions. They are ready to be tested *in vitro*.

- Compound **42** was not pure enough and it was isolated as a mixture of **41** (ratio 3:1 respectively, determined by ^{1}H NMR). The partial free amine in position 4 respect to the azo group, gave an increased solubility character in physiological conditions to the PCL. Other deprotection conditions or methods should be tried in order to obtain the compound **42** pure.

5. SUPPORTING INFOMATION

INDEX

SUPPLEMENTARY EXPERIMENTAL DETAILS.

5.1– General Experimental Conditions

All reagents were obtained from commercial sources. Unless otherwise noted, solvents (analytical grade) were purchased from commercial suppliers and used without further purification. **Melting points** were obtained using a Lambda Photometrics Optimelt MPA100 apparatus (Lambda Photometrics, Harpenden, UK), and are not corrected. **IR spectra** were obtained using a Varian Biorad FT-IR Excalibur FTS 3000 spectrometer. ^{1}H NMR spectra were recorded at 400 and 600 MHz and ^{13}C NMR spectra were recorded at 100 MHz and 150 MHz on a Bruker Avance 400 spectrometer and Bruker Avance III Br600 with a cryogenic probe head (Bruker, Karlsruhe, Germany). The **NMR spectra** were recorded in $CDCl_3$, DMSO, THF and CD_3OD as solvents and chemical shifts are reported in ppm. The following abbreviations are used: *J* as a coupling constant reported in Hz. s: singlet, brs: broad singlet, d: doublet, dd: double doublet, t: triplet, dt: doublet of triplets, tt: triplet of triplets q: quadruplet, qt: quintuplet, m: multiplet. **UV/Vis spectra** were recorded using a Varian Cary BIO 50 UV/Vis/NIR spectrophotometer (Varian Inc., CA, USA). **Mass spectra** were obtained using Finnigan SSQ 710A (EI), Finnigan MAT 95 (CI) or Finnigan MAT TSQ 7000 (Thermo FINNIGAN, USA) (ES/LC–MS) instrumentation. Thin layer chromatography (TLC) was performed on alumina plates coated with silica gel (Merck silica gel 60 F245, thickness 0.2 mm). Column

chromatography was accomplished with Merck Geduran SI 60 silica gel as the stationary phase.

5.2– Synthetic protocols and analytical data.

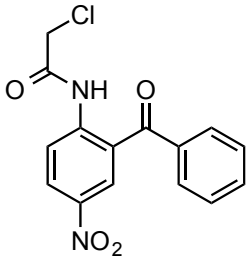

***N*-(2-Benzoyl-4-nitrophenyl)-2-chloroacetamide (45)**. Benzophenone derivative **44** (1.9 g, 7.84 mmol) and triethylamine (1.2 mL, 8.58 mmol) were dissolved in THF (50 mL). After stirring 30 min., the yellow solution was cooled down to 0°C and chloroacetyl chloride (1.28 mL, 16.38 mmol) was added dropwise. The clear solution became cloudy and the reaction mixture was stirred at room temperature for 18 h. The solid was filtered and obtained quantitatively (2.49 g) without further purification, as a pale beige powder. **mp:** 171-173 ºC. **Rf**: 0.4 (Hexane/EtOAc 2:1). **IR** (ATR): 3219, 2362, 1686, 1641, 1583, 1547, 1507, 1446, 1414, 1326, 1262, 1226, 1093 cm^{-1}. **^{1}H NMR** (400 MHz, $CDCl_3$): δ 11.91 (s, 1H), 8.91 (d, *J* = 9.1 Hz, 1H), 8.52 (d, *J* = 2.4 Hz, 1H), 8.45 (dd, *J* = 9.1, 2.4 Hz, 1H), 7.77–7.72 (m, 2H), 7.69 (tt, *J* = 1.3, 7.5 Hz, 1H), 7.59–7.53 (m, 2H), 4.25 (s, 2H). **^{13}C NMR** (100 MHz, $CDCl_3$): δ 197.6, 166.1, 144.7, 142.3, 137.2, 133.8, 130.1, 129.0, 128.8, 123.7, 121.8, 43.2. **HRMS** calculated for $C_{15}H_{11}N_2O_4Cl$: 319.0480 $[M+H]^+$. Found: 319.0481.

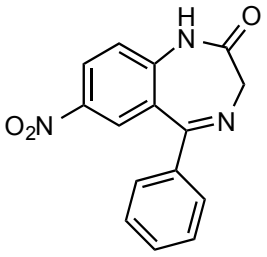

7-Nitro-5-phenyl-1,3-dihydro-2*H*-benzo[*e*][1,4]diazepin-2-one (46). A suspension of benzophenone-derivative **45** (3.92 g, 12.3 mmol) and hexamethylenetetramine (3.71 g, 26.43 mmol) in ethanol (80 mL) was heated to 40 °C. Then, ammonium acetate (2.05 g,

26.43 mmol) was added and the temperature was increased to reflux (turned into a clear red-brownish solution) and stirred for 17 h. The mixture was allowed to cool down to room temperature, water (300 mL) was added and the product was extracted with EtOAc (2 × 300 mL). The combined organic layers were dried over anhydrous Na_2SO_4, filtered and evaporated. The product was purified by recrystallization with toluene and ethanol (3-5 drops of ethanol for each 100 mL of toluene) to obtain pure product **46** (484 mg) in 14% yield as yellow fine particles. **mp:** 335 ºC decomp. **Rf**: 0.3 (Hexane/EtOAc 1:1) **IR** (ATR): 3489, 3347, 2848, 2360, 1657, 1579, 1525, 1481, 1398, 1323, 1282, 1081 cm^{-1}. **^{1}H NMR** (400 MHz, DMSO–d_6): δ 12.58 (s, 1H), 8.04 (dd, J = 2.6, 8.9 Hz,1H), 7.67 (d, J = 2.3 Hz, 1H), 7.65–7.69 (m, 2H), 7.56–7.52 (m, 1H), 7.43 (d, J = 8.9 Hz, 1H), 7.39–7.34 (m, 2H), 5.21 (s, 2H,). **^{13}C NMR** (100 MHz DMSO–d_6): δ 157.9, 141.9, 136.4, 135.7, 133.8, 129.8, 129.6, 128.4, 121.8, 119.3, 118.2, 116.8, 115.8. **HRMS** calculated for $C_{15}H_{12}N_3O_3$: 282.0873 $[M+H]^+$. Found: 282.0874.

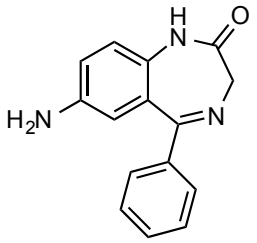

7-Amino-5-phenyl-1,3-dihydro-2*H*-benzo[*e*][1,4]diazepin-2-one (47). Iron powder (200 mg, 3.52 mmol) and aqueous HCl solution (0.18 M, 0.27 mL) were added to a previously dissolved nitrazepam **46** (100 mg, 0.35 mmol) in ethanol (1.08 mL) and the mixture was heated to reflux (bath temperature: 90°C) and stirred for 2.5 h. The reaction progress was monitored by TLC. The solution was filtered through Celite® (to remove iron particles). The solvent was evaporated under reduced pressure afterwards to obtain pure product **47** (88 mg, quantitative) as a brown syrup. **mp:** 356 ºC. **Rf**: 0.15 (100% EtOAc). **IR** (ATR): 3437, 3340, 2972, 2861, 1651, 1567, 1503, 1429, 1393, 1304, 1236 cm^{-1}. **^{1}H NMR** (400 MHz, DMSO–d_6,): δ 11.60 (s, 1H), 7.59–7.52 (m, 2H), 7.45 (dt, J = 1.2, 7.6 Hz, 1H), 7.30–7.25 (m, 2H), 7.00 (d, J = 8.5 Hz, 1H), 6.52 (dd, J = 2.4, 8.5 Hz, 1H), 6.05 (d, J = 2.4 Hz, 1H), 4.73 (s, 2H), 4.55 (s, 2H). **^{13}C NMR** (100 MHz, DMSO-d_6): δ 156.7, 143.5, 135.6, 133.8, 129.7, 129.3, 127.6, 123.9, 122.5, 118.6, 115.6, 113.6, 105.9. **HRMS** calculated for $C_{15}H_{14}N_3O$: 252.1131 $[M+H]^+$. Found: 252.1135.

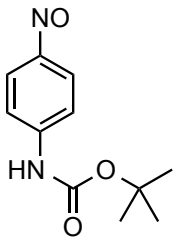

***tert*-Butyl(4-nitrosophenyl)carbamate (49).** See supporting information of chapter 1, section 5.2.1, compound (**4**) for the experimental data description.

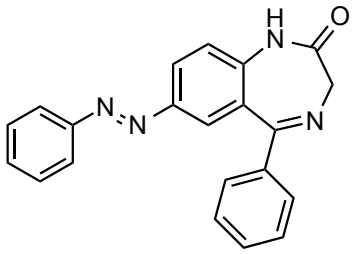

5-Phenyl-7-(phenyldiazenyl)-1,3-dihydro-2*H*-benzo[*e*][1,4]diazepin-2-one (43). To a flask containing **48** (17 mg 0.156 mmol), acetic acid (1 mL) and the precursor **47** (33 mg 0.131 mmol) were added and the reaction mixture stirred at room temperature for 5 days. After neutralization with a saturated aqueous $NaHCO_3$ solution (13 mL), the mixture was diluted with EtOAc (15 mL) and the resulting layers were separated. The aqueous layer was extracted with EA (3 × 10 mL) and the combined organic layers were washed with water (3 × 50 mL) and brine (3 × 50 mL). The organic layer was dried over anhydrous Na_2SO_4, filtered and concentrated in vacuo. Purification by column chromatography (from 1:1 Hexane/EtOAc to 9:1 EtOAc/MeOH) afforded the pure compound **43** (22 mg, 51%) as an orange solid. **mp:** 250.1°C. **Rf**: 0.7 (100% EtOAc). **IR** (ATR): 3472, 3339, 2965, 2922, 2854, 2358, 1740, 1651, 1578, 1576, 1397, 1159, 1057 cm^{-1}. **^{1}H NMR** (600 MHz, THF–d_8) δ 11.21 (s, 1H), 7.80–7.75 (m, 3H), 7.63 (d, J = 2.0 Hz, 1H), 7.61–7.56 (m, 2H), 7.47 (tt, J = 1.2, 7.6 Hz, 1H), 7.44–7.41 (m, 4H,), 7.39 (tt, J = 1.2, 7.6 Hz, 1H) 7.28 (d, J = 8.6, 1H), 4.86–4.77 (m, 2H). **^{13}C NMR** (150 MHz, THF–d_8) δ 159.0, 155.6, 153.8, 148.8, 136.5, 136.3, 135.9, 131.3, 131.1, 130.4, 129.8, 128.9, 123.5, 123.3, 119.3, 117.2, 116.3. **HRMS** calculated for $C_{21}H_{17}N_4O$: 341.1397 $[M+H]^+$. Found: 341.1400.

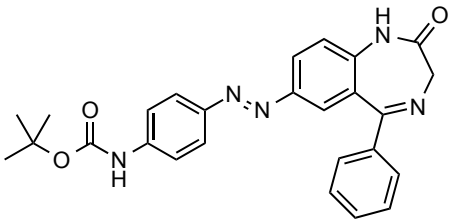

***tert*-Butyl-(4-((2-oxo-5-phenyl-2,3-dihydro-1*H*-benzo[*e*][1,4]diazepin-7-yl)diazenyl)phenyl)carbamate (41)**. To a flask containing **49** (35 mg 0.158 mmol), acetic acid (1 mL), the precursor **47** (33 mg 0.131 mmol) were added and the reaction mixture was stirred at room temperature for 4 days. After neutralization with saturated aqueous $NaHCO_3$ solution (13 mL), the mixture was diluted with EtOAc (15 mL) and the resulting layers were separated. The aqueous layer was extracted with EtOAc (3 × 10 mL) and the combined organic layers were washed with water (3 × 50 mL) and brine (3 × 50 mL). The organic layer was dried over anhydrous Na_2SO_4, filtered and concentrated in vacuo. Purification by column chromatography (from 1:1 Hexane/EtOAc to 9:1 EtOAc/MeOH) afforded **41** (47 mg, 78%) as a shiny orange solid. **mp:** 256.1 °C. **Rf**: 0.5 (100% EtOAc). **IR** (ATR): 3353, 2964, 2934, 2868, 2358, 2338, 1718, 1654, 1594, 1568, 1532, 1406, 1366, 1303, 1234, 1155, 1052 cm^{-1}. **^{1}H NMR** (600 MHz, THF–d_8): δ 11.31 (s, 1H), 8.74 (s, 1H), 7.77–7.71 (m, 3H) 7.61–7.53 (m, 5H), 7.47 (dt, *J* = 1.3, 7.5 Hz, 1H), 7.45–7.42 (m, 2H), 7.28 (d, *J* = 8.7 Hz, 1H), 4.85 (s, 2H), 1.50 (s, 9H). **^{13}C NMR** (150 MHz, THF–d_8): δ 157.6, 152.0, 147.5, 147.3, 142.0, 136.8, 135.1, 134.6, 133.9, 129.6, 128.9, 127.4, 123.0, 122.1, 121.3, 117.2, 115.7, 114.8, 78.8, 27.2. **HRMS** calculated for $C_{26}H_{26}N_5O_3$: 456.2030 $[M+H]^+$. Found: 456.2037.

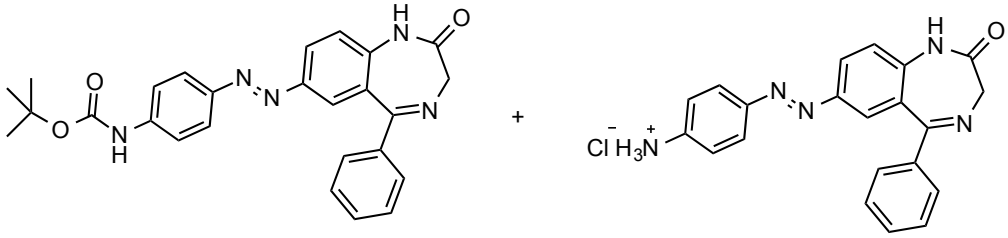

Both compounds are reported together as a mixture (ratio 1:3 as determined by NMR).

4-((2-oxo-5-phenyl-2,3-dihydro-1*H*-benzo[*e*][1,4]diazepin-7-yl)diazenyl) benzenaminium chloride (42)

To a flask containing **41** (24 mg, 1.12 mmol) was added a freshly prepared solution of HCl in EtOAc (2.17 M, 0.5 mL). At this moment, we observe a colour change from orange to strong purple. After 1 hour stirring, an argon flow passed through the solution to remove all HCl and the mixture was concentrated. The resulting purple solid was triturated with ethyl ether (3 × 5 mL) and filtered, to yield a mixture of **42** and **41** (12 mg, 57% for **42**) as a dark fine particles. **mp:** 251.6°C. **Rf**: 0.45 (Hexane/EtOAc 1:1). **IR** (ATR): 3356, 2826, 2364, 1656, 1578, 1526, 1499, 1367,1236, 1163 cm^{-1}. **^{1}H NMR** (600 MHz, MeOD) δ 7.91–7.86 (m, 2H), 7.82 (dd, *J* = 2.14, 8.76 Hz, 1H), 7.66–7.61 (m, 2H), 7.56 (d, *J* = 2.14 Hz, 2H) 7.44–7.41 (m, 3H), 7.37 (d, *J* = 8.76 Hz, 2H), 1.5 (s, 3H. minor compound). **^{13}C-NMR** (150 MHz, MeOD) δ 160.0, 154.9, 150.7, 135.7, 130.9, 130.8, 129.7, 126.5, 124.6, 123.9, 122.3, 118.5, 117.5, 28.6 (minor compound). **HRMS** calculated for $C_{21}H_{18}N_5O$: 356.1506 $[M+H]^+$. Found: 356.1509.

5.3- Selected examples of representative NMR spectra

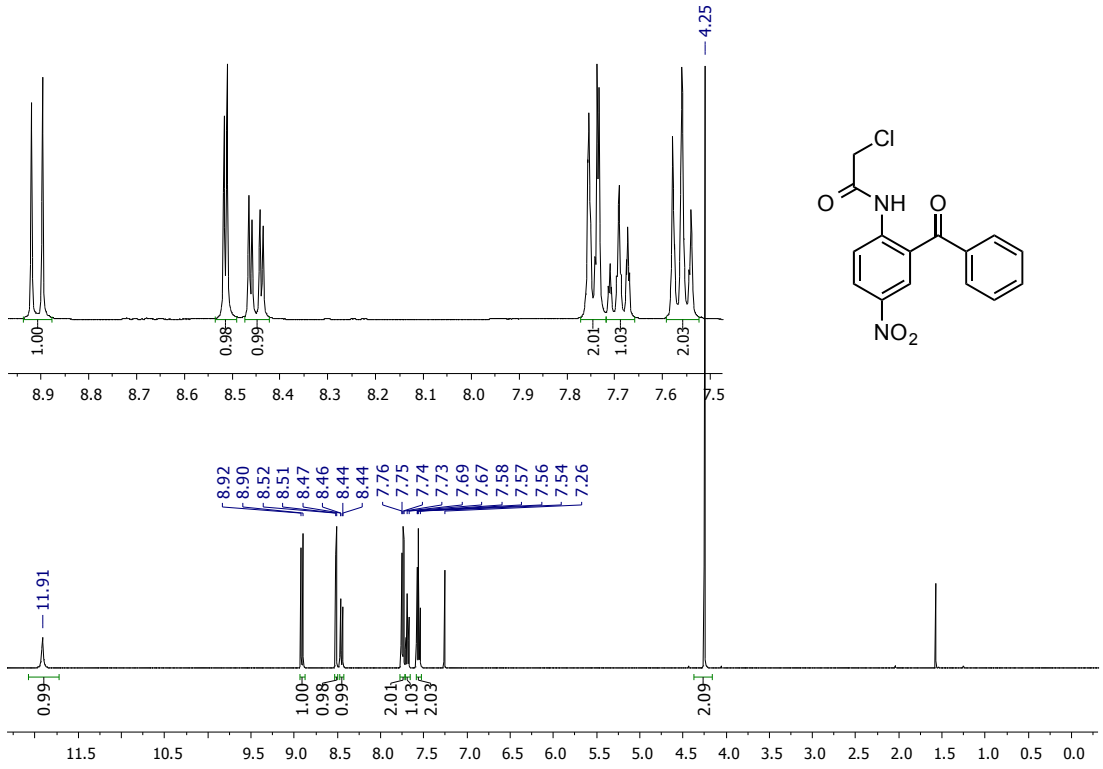

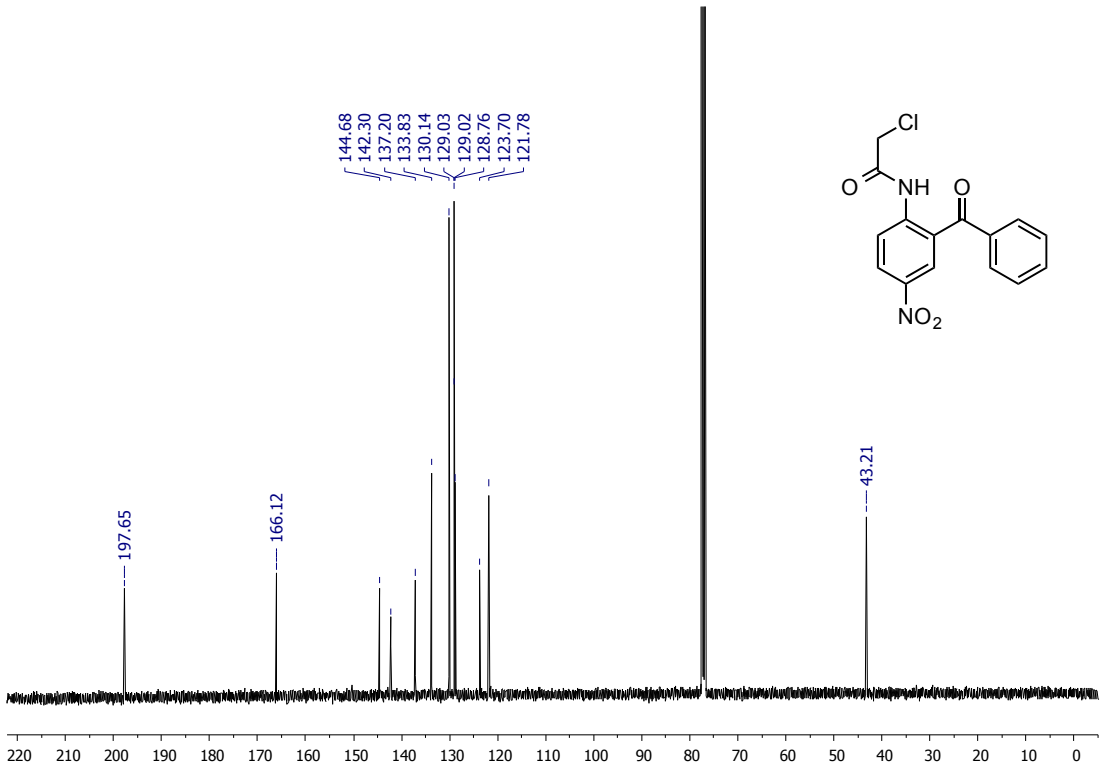

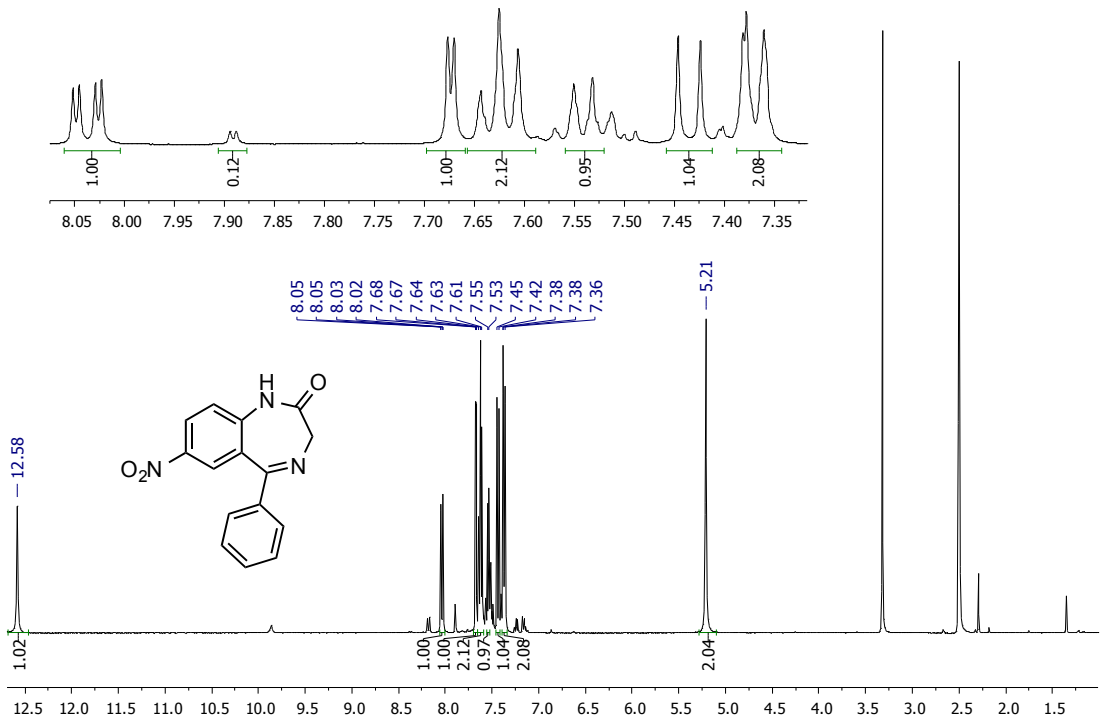

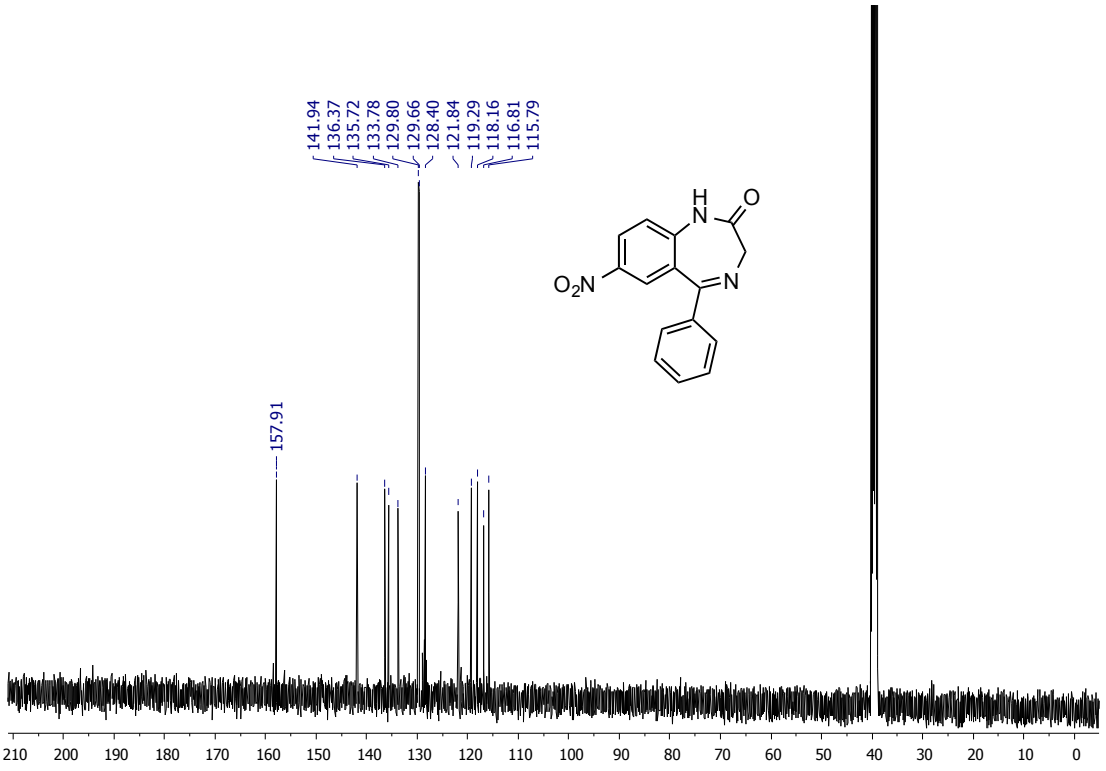

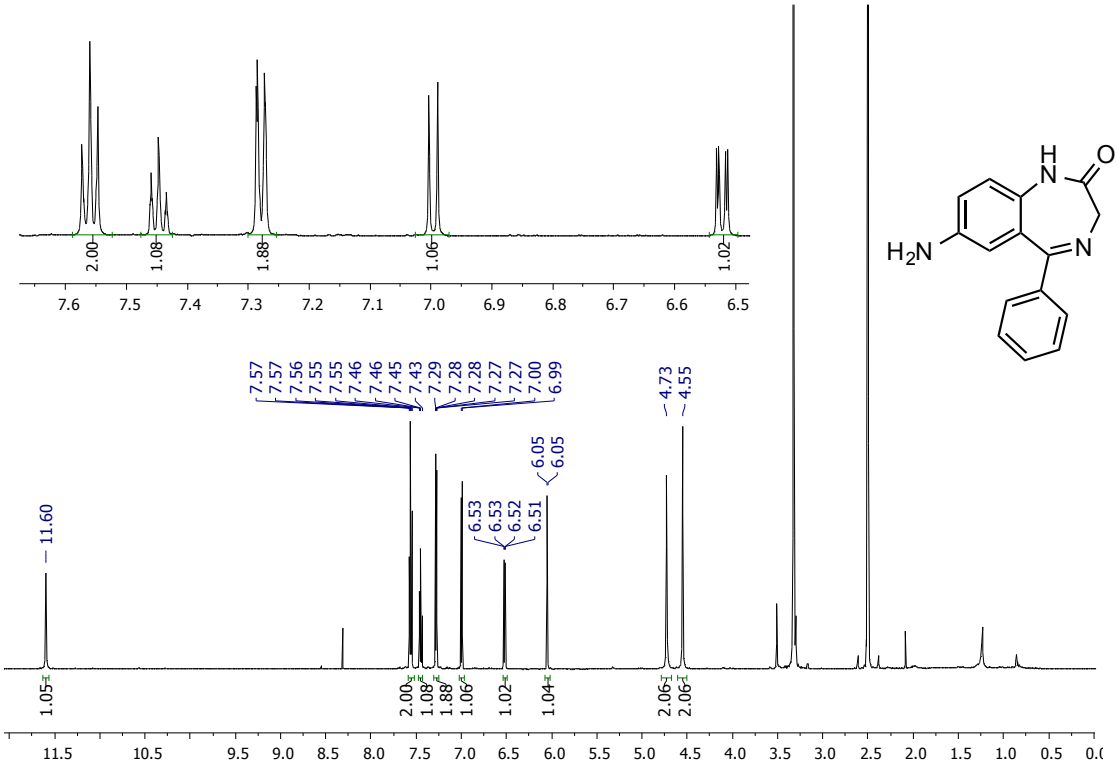

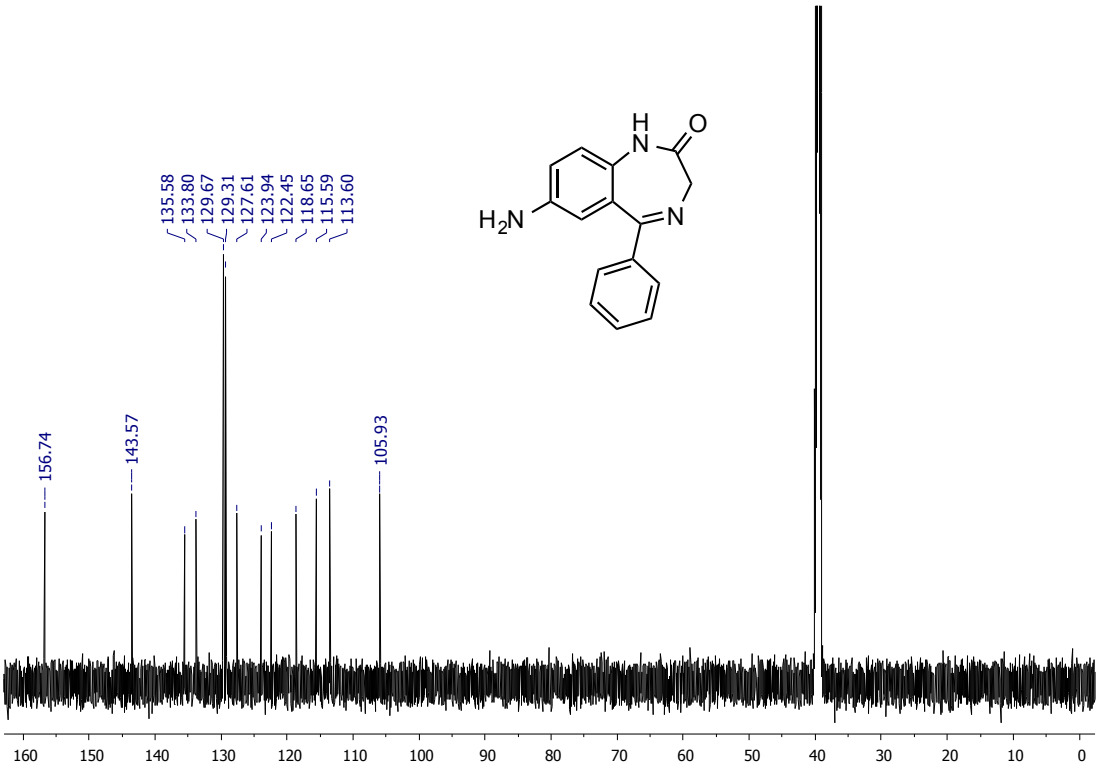

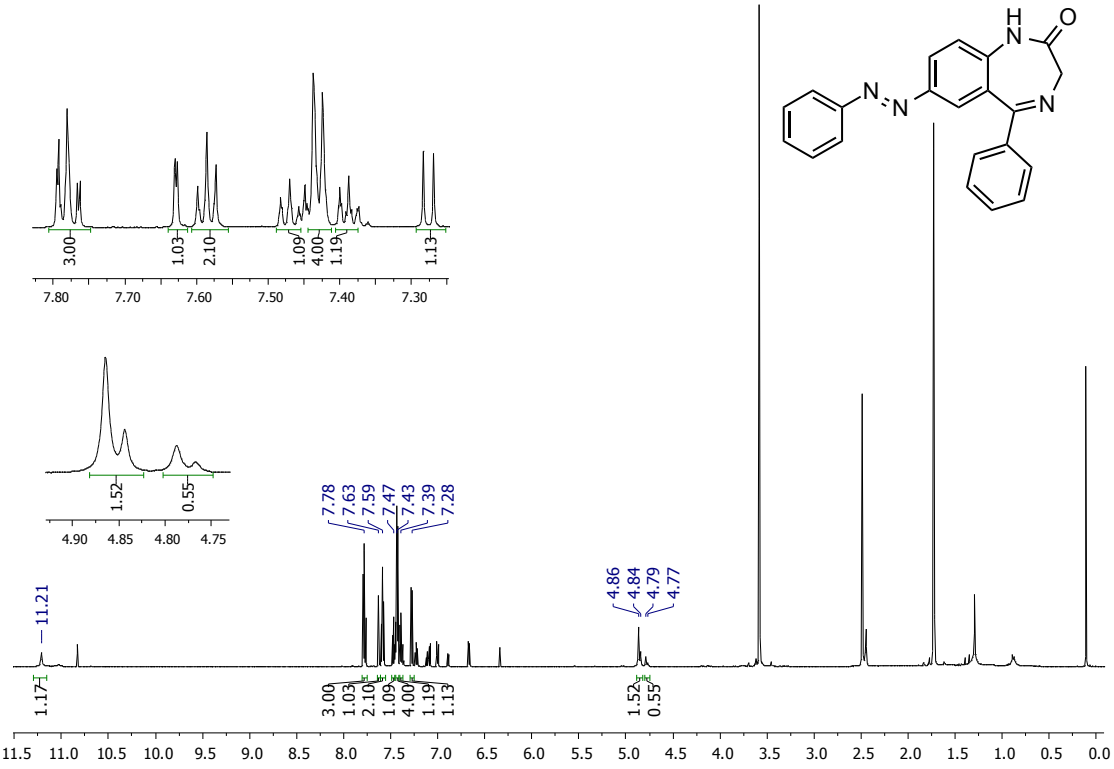

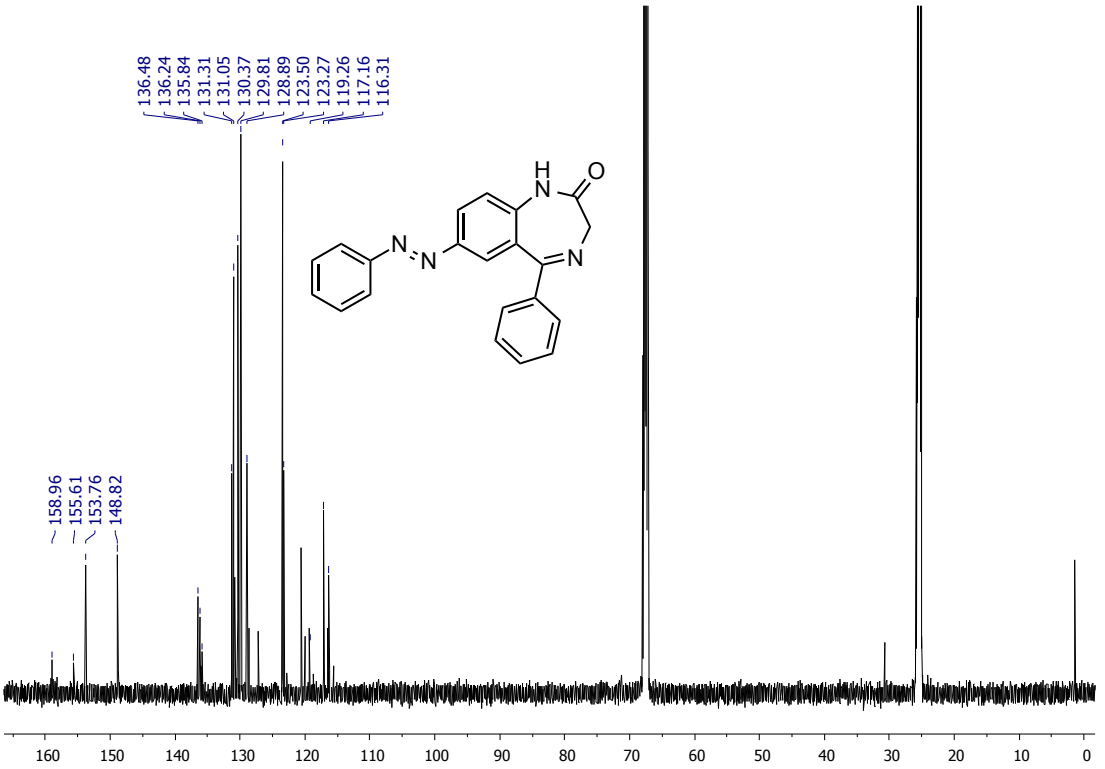

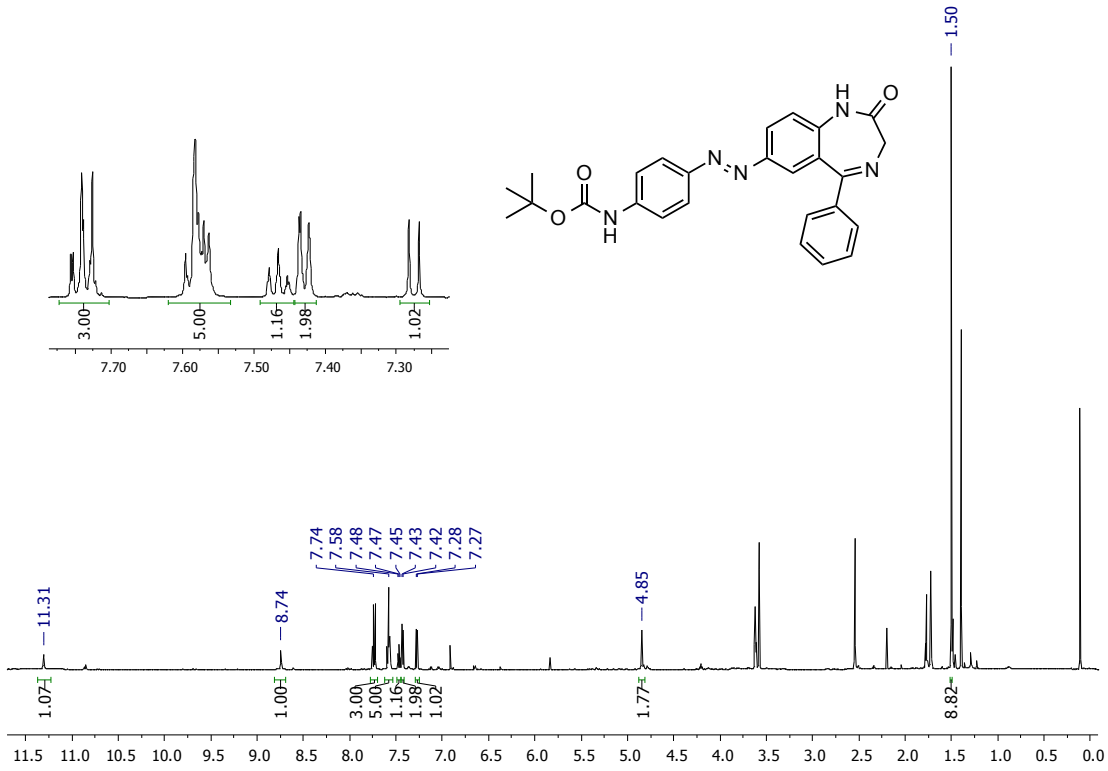

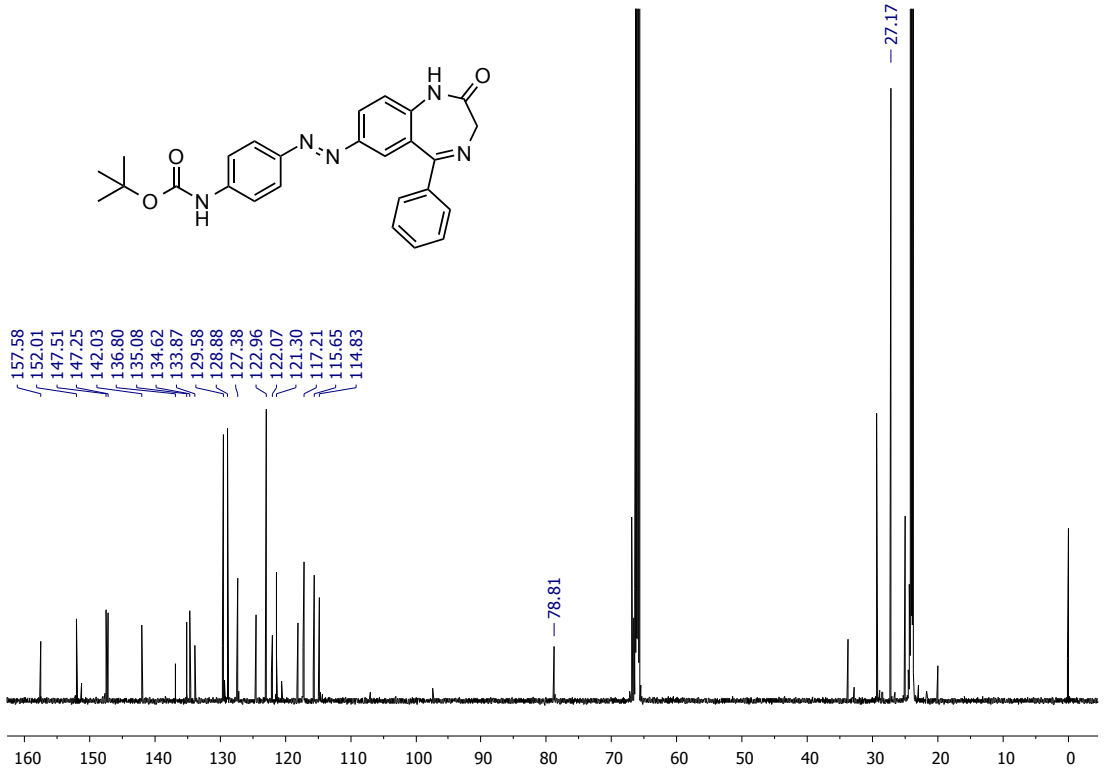

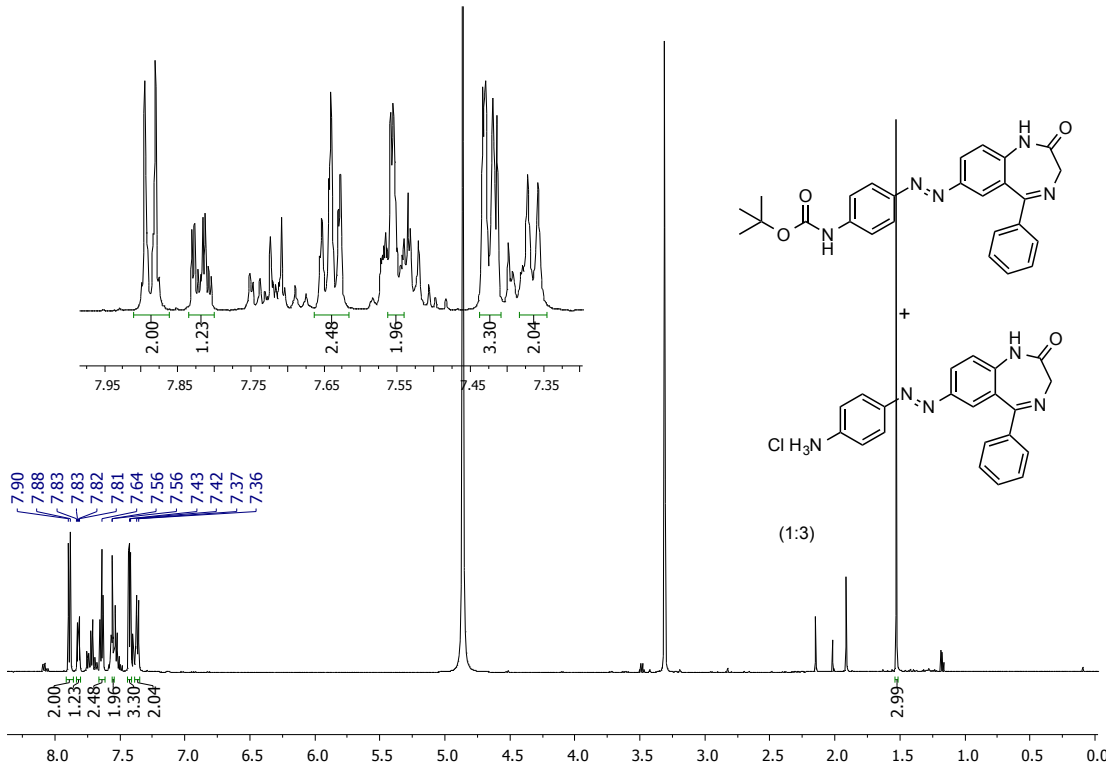

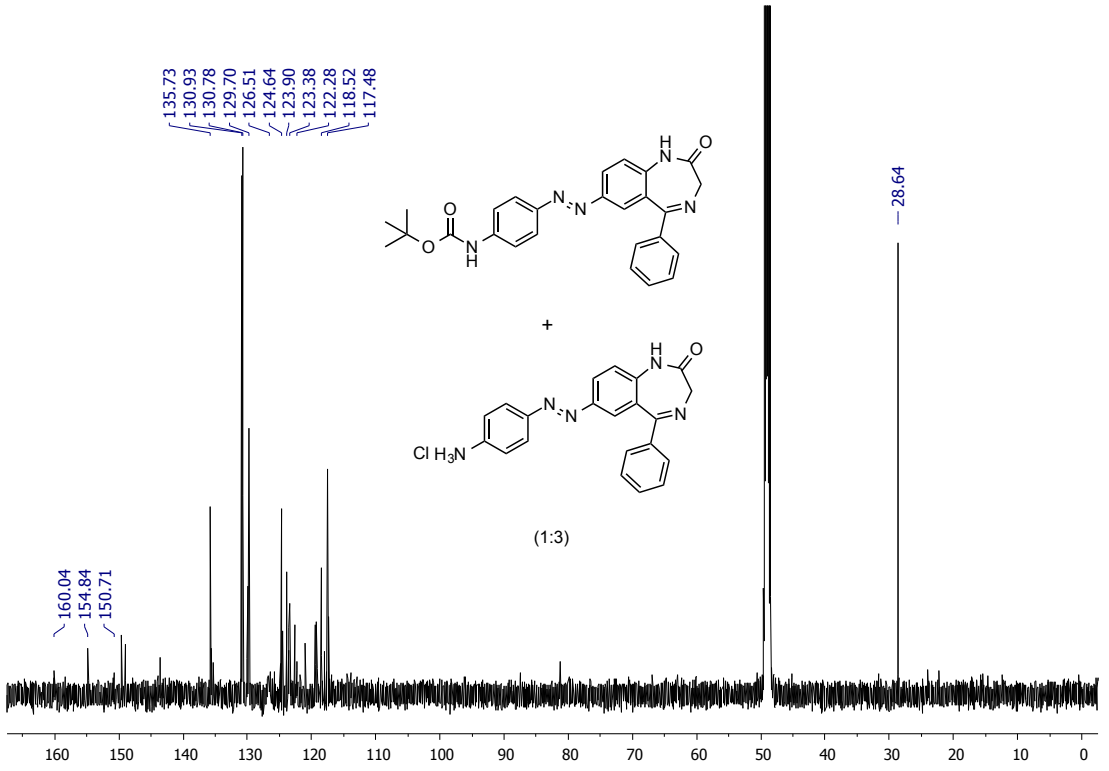

PART II

CONTROLLING ENZYMATIC PROPERTIES WITH LIGHT

This section, adapted as introductory part II, is an overview of light-modulated enzymes using synthetic switches. The classification has been done cronologically by families with EC number nomenclature, that stands for Enzyme Comission, and represent the arbitrarily assigned class, and sub-classes number respectively.[175] As with ion channels, the main strategies for enzyme photocontrol (PCLs and PTLs) are presented in each case.

PHOTOSWITCHABLE ENZYMES

1. LYASES

Lyases are a family of enzymes responsible for the cleavage or formation of C-C or C-X bonds, (where X is an heteroatom) through other reactions than hydrolysis or oxidation. An example is carbonic anhydrase (EC 4.2.1.1), a metalloenzyme that catalyzes the reversible reaction between carbon dioxide and water to give bicarbonate, responsible for CO_2 transport and pH regulation.[176] Glaucoma, epilepsy or cancer are related pathological diseases associated to dysfunction of this enzyme. Regulation using pharmacological inhibitors has not been always successful due to its rather spread localization in tissues/organs and the lack of drug specificity towards 16 isoforms existing in mammals.[176-179]

Due to its importance, the actvity of carbonic anhydrase I and II has been controlled with light using several approaches.

Harvey et al. reported a PTL that hinders the inhibition in the cis state increasing 2 fold the activity with respect to the trans state. This PTL has an epoxy tail for conjugation, a light sensitive azobenzene moiety for light controlled interconversion within states and a sulfanilamine head that interacts with the catalytically active zinc site of the enzyme type II.

The ligand conjugation occurs close to the receptor, by affinity labeling avoiding exogenous manipulation, where the epoxy group reacts with the histidine residues 2 or 3.[180] Irradiation with 380 and 460 nm allows reversible isomerization of the molecule during 4 cycles showed by colorimetric experiments using PNPA (p–nitrophenyl acetate) as a substrate.[34]

Using a different strategy to photocontrol carbonic anhidrase I, the group of König used a 1,2–dithienylethene scaffold to change the flexibility of the molecule upon light irradiation, obtaining an inhibition decrease of about two orders of magnitude. The central scaffold of the switch was derivatized with a sulfanilamine, inhibitting the active center as with the previous PTL and the other arm, with Cu (II) iminodiacetic acid (Cu (ida) complex), acting as an assistance group. This complex interactions causes a sulfanilamine undocking from the catalytic site in the rigid closed state with a ki = 0.3 μM. Otherwise, the open state shows and ki = 0.005 μM, due to a flexibility increase of the switch. Interconversion between states was achieved only by 312 nm (closed) and >420 nm (open) irradiation repeating the cycles 7 times without bleaching.[181] An Extension to other carbonic anhydrases II, IX, XII and XIV due to the best results obtained for I gave no better results, demonstrating the big differences between enzymatic isoforms and the selectivity for type I.[182]

2. TRANSFERASES

The transferases type enzymes are involved in bisubstrate reactions in which a specific functional group is transferred from one substrate to the other.[183] Among this family, spleen tyrosine kinase (Syk) (EC 2.7.10.2) has aroused the interest of researchers as a target for potential anti–allergic therapy because it plays an essential role in inmunoreceptor (IgE) pathway signaling which leads to mast cell degranulation manifested as urticarian disease.[184, 185]

A photo–controlled tool was developed towards Syk, to study the possibility of instantanously switch intracellular processes on and off with light.[186] Azo–ITAM candidate was developed bearing an azobenzene as the central core of about 12 Å (extended trans state). The ligand–enzyme interactions were studied by real time surface plasmon ressonance (SPR) technique for the first time, revealing 10 fold times difference in binding affinities between cis and trans isomers (*trans* k_D = 65 uM, *cis* k_D = 860 uM) reaching a 66 % cis PSS upon 366 nm light recovering back the trans state after visible irradiation. Soon after, different extends of the same switch were synthesized varying the central core lenght from 12 to 30.2 Å. Azo–ITAM with 18.6 Å, showed the largest differerence in affinity between the two isomers (100 fold times) being stronger in trans.[187]

3. ISOMERASES

Isomerases belong to a general class of enzymes which interconverts the spatial position or connectivity of an atom or functional group mantaining the same molecular formula between the substrate and the product. Among them, crucial transformations can be found, related either to prokaryotic or eukaryotic metabolism processes in living systems, but so far only an intramolecular oxidoreductase isomerization reaction has been modulated with light. In this work, the activity of the metabolic branch–point enzyme PriA from Mycobacterium tuberculosis (mtPriA) (EC 5.3.1.16) can be controlled reversibly, based on the dithienylethene bis–orthophosphate C_2 – symmetric scaffold. Switching from the flexible, ring–open to the rigid, ring–closed isomer reduces inhibition activity by one order of magnitude (from 4,4 to 0.5 μM realtive to *ki*) with 312 and >420 nm light respectively (synthetically analogous to the publication by König et al. showed above on Lyases.[188] Those results are specially valuable for the development of anti–tuberculosis drugs, as a result of modulating reversibly the biosynthesis of tryphtophan and histidine aminoacids processes.[189, 190]

4. OXIDOREDUCTASES

This protein family catalyse the exchange of electrons between two species from a donor, oxidizing itself to an acceptor being reduced. This family is divided in 13 subclasses where only the light sensitzed enzymes–type will be highlighted herein despite the importance of other oxidoreductase transformations. Light modulated enzymes comprise oxidoreductase,[8] peroxidase[191] and NADH deshydrogenase[192, 193] subfamilies, where the reductant is an alcohol, glucose and NADH respectively. Some applications were directed towards the development of enzymatic glucose biosensors for diabetes[194, 195] as a tool for neurobiologists to mark neurons[196] and ELISA (enzyme inmunoassay) colorimetric tests.
Among oxidorreductases, alcohol deshydrogenase was the first to be photocontrolled in 1994 by the group of Sisido. They were able to modulate the synthesis of aldehyde by using a synthetic NAD+ cofactor linked with an azobenzene moiety, which binds to an antibody in the trans form but not in cis. In this way, the system was blocked using visible light and activity – restored in a 72 % upon UV light irradiation.[192]

Willner, et al., one year after, showed an approach to control by light glucose oxidase (GOD, EC 1.1.3.4) oxidoreductase electron–transfer communication between redox–proteins and electrodes. GOD was attached by nitrospiropyran (40% effective attachement) and assembled as monolayer on a Au–electrode, acting as a supported biocatalyst for oxidation of the substrate and for the stimulation of an electrocatalytic anodic current. Upon 320–380 nm irradiation, the merocyanine state caused a half decrease in GOD activity. The closed spiro form didn't recover the full enzymatic performance with >475 nm wavelenght, caused by UV damage. This photoresponsive support provide an approximation for the amperometric transduction and amplification of recorded optical signals by means of a bio–electronic combination.[8]

Following with the use of spiropyran as a nanotool to photo–modulate oxidoreductases, an study with horseradish peroxidase (EC 1.11.1.7) presented the highest activity change at that time, reporting a 92% reduction in enzyme activity under visible illumination compared to UV illumination.

They prepared an acid terminated spiropyran derivative, covalently attached to all enzymatic lysine residues using a carbodiimide amidation agent (EDC). After incubation, spectroscopic studies confirm a complete accessible lysine labelling of 1:9 enzyme:molecule rate. Activity tests concluded that only a small fraction of the conjugated photochromic molecules are photo–switched to cause the reduced enzymatic activity. The dyes might influence in the activity via local hydrophobic/hydrophilic active site interaction.[191]

Later on, in 2006, Fujita et al. published a study with a photoresponsive inhibitor of Mitocondrial NADH ubiquinone oxidoreductase complex I (EC 1.6.5.3). They prepared an azo–Δlac–acetogenin derivate, with two azo groups in one molecule, highly active in tran–trans form (IC_{50} = 0.83 nM). The inhibition could not be reverted extensively due to the low photostationary state of the cis–cis isomer after 370 nm irradiation. Those results are valid to study the mechanistic changes in complex I closely associated with the mitochondrial respiratory system such as superoxide production and transport of various substances across the inner mitochondrial membrane.[193]

5. HYDROLASES

Hydrolytic enzymes assist the cleavage of organic bonds by the use of water. Despite mediating a wide range of relevant biological-related hydrolysis, herein we only report the light-modulated ones. Among them we find estearses, ureases, glycosidases, proteases, carboxylic ester hydrolases and lipases.

5.1– Estearases

Estearases are hydrolytic enzymes involved in the cleavage of ester bonds to give an alcohol and an acid as a reaction products. Among them, acetylcholinesterase (AChE), that belongs to acetylesterase subfamily (EC 3.1.1.6) is responsible for the splitting of acethylcholine neurotransmitter, found mainly at neuromuscular junctions and brain synapses mediating synaptic transmission.[197, 198]

Forty years ago, some approaches to photosensitize AChE for its biological relevance, gave rise to the first light–nanoengineered nicotininc acetylcholine receptor and the first PTL[51] at the same time, able to control nAChR currents reversibly with millisecond light pulses.[54, 199, 200]

In the first approaches developed to photomodulate AChE activity, Erlanger group synthesized a series of photochromic reversible inhibitors analogous to phenyl–trimethylammonium chloride.[201] With the incorporation of an azobenzene group (p–phenylazophenyltrimethylammonium chloride), both isomers acted as inhibitors being the trans isomer more potent with no more than 20% difference switching between reversible states with 320 and 420 nm light.[202] A following study with *N*–p–phenylazo–phenylcarbamyl choline chloride switch and the possible role in photoregulation of the electric eel electroplax with sunlight,[203] led to the first biologically relevant photochromic actuators. This study used the azo compounds described herein to photoregulate the electric potential difference across the excitable membrane of about 20–30 mV from electroplax cells.[204]

Forty years after, with the advanced biological and synthetical techniques available, the group of Trauner reported a tacrine structure based azo–switch (azo–THA) that modulates the neurotransmission by means of controlling optically AChE removing the neurotransmitter from the active zone. The switch is a photochromic ligand showing an inhibition upon blue light illumination (440 nm) that is 83 % higher than in the cis state

(350 nm), having only a small reduction in activity upon 5 irradiation cycles. Direct biological aplications showed a light–dependent effect on AChE kinetics in mouse trachea preparations with enanced characteristics compared to physostigmine.[205]

5.2 Ureases

Urease enzymes are responsible for the hydrolytic conversion of urea to bicarbonate and ammonium cation products. Direct applications in fast urease tests has been developed (as Campylobacter–like organism test) to detect the presence of urinary and gastrointestinal tract pathogens.[206]

Among ureases (EC 3.5.1), their activity has been controlled with light by inmobilization onto photoresponsive spiropyran–based biocatalysts reported by Suzuki.[9-11] Despite of having different inmobilization protocols, the results obtained after UV irradiation are nearly the same, showing 2 times more activity (referred to k_{cat} value) than after irradiation with 330 nm. Those results are in accordance to the change of the hydrophobicity that occurs from spiro to mero state, changing the affinity of the enzyme–substrate intermediate.[9-11]

But not only heterogenous light–sensitive biocatalysts urease–based have been developed. Recently, Korbus et al.[207] publised a reversible control of hystone bacterial deacetylase with azobenzenes through cysteine expression. Three variants were selected (M30C, S20C, M150C) showing the best light modulation responses after covalent conjugation with an azobenzene–maleimide linked reactive tail in the position 4 (4–PAM). Specially, position M30C present 50 % of activation in cis but not complete inactivation reverting back to trans, limitting possible applications. However, this position present a long–lived cis state of about 30 hours, attractive towards applicability due to avoidance of continous UV illumination causing photobleaching

5.3 Glycosidases

Those enzymes type catalyses the hydrolysis of α–glycosidic bonds in plants and humans, to obtain energy (glucose) from the ingested starch (found mainly in rice or potatoes) containing carbohydrates.[183]

In the study reported with ureases by Aizawa et al., (*see section 5.2*) it was also analysed the effect of β–glucosidase (EC 3.2.1.21) and α, β–amylases (EC 3.2.1.1, EC 3.2.1.2) conjugated with spyropiran anhydride reactive group. The influence of the open charged or

closed hydrophobic environment driven by light changes into linked spyro, cause a k_m decrease for hydrophilic catalytic pocket in the mero state for polar substrates and a k_m increase upon irradiation. This results reveal an strong influence of the spiro state interacting with the enzyme – substrate complex during the catalysis.[10]

5.4 Proteases

Cysteine Proteases

This subfamily encompasses the enzymes that degradate proteins by using a thiol to produce the catalysis in the active site. Among them, Papain or Calpain that are found in papayan fruit and in humans respectively, mediating several important physiological processes as cell motility, long-term potentiation in neurons, skeletal muscle breakdown, etc. and associated with cellular damage diseases as stroke, cataracts, among others.[208-211]

Willner et al. was the first to photo–sensitize the cys protease family with papain enzyme. They generated a serie of three azobenzene–substituted switches, with carboxylic acid group in benzene ring positions 2, 3 and 4, anchored to the enzyme through lysine residues by amidation reaction. The activities of the modified enzymes relative to native papain were lower and the extent of loading by the 4–carboxyazobenzene molecule had been determined, as 4.6 dye molecules per enzyme. Despite lowering enzymatic activity, this approach showed the highest hydrolytic difference rate between isomers, with 2.75 times increased activity in trans. The optical modulation was performed with 320 and >400 nm. They also observed a decrease in activity after several cycles, using a supported alginate beads version.[212] Shortly after was presented the photoresponsive polymeric version showing very similar results to the above described.[213]

Following those interesting results with papain, the group of Smith used a slightly different strategy to control cys and serine proteases taking advantage of their unique catalytic pocket. With papain, an azobenzene bearing a tail aldehyde was synthesised to allow a labile linkage with the catalytic cysteine. The trans isomer acted as a potent papain inhibitor (k_i = 2.1 μM) while, after irradiation between 330 and 370 nm, the inhibition was 40 times weaker, with an observed 83 % of the cis isomer in the photostationary state mixture. Irradiation with >400 nm reverts back the initial trans inhibition.[214]

In 2007, an extension of this strategy to m–Calpain enzyme was presented for the development of therapeutic anticataract agents, due to the important role on the protein

decomposition of crystalline lens. An structure-based diazodipeptide aldehyde and sulfanamide triazene ligand series were attached into S3 catalytic pocket site. Significant optical inhibition was achieved with a potent trans-enriched (4.8 *trans* : 1 *cis*) azo–aldehyde having an IC_{50} value of 45 nM. Irradiation with 340 nm reduced the potency until IC_{50} = 175 nM (nearly 4 times) with a major cis mixture (1 *trans* : 4.3 *cis)*, proved to be significantly less active.[215]

Serine Proteases

As cysteine proteases, serine proteases are enzymes that catalyse the cleavage of proteic amide bonds but using an alcohol instead of a thiol to initiate the process in the catalytic triad. They can be found either in eukaryotic systems with trypsin–like active site structure and in prokaryotic cells with subtilisin–like architecture, evolutionary convergent, not sharing common ancestors.[183, 216, 217]

This subfamily is the most extensively used for photocontrol with synthetic switches either inmobilized or in solution. The first serine proteases–like activity photomodulation was done by Erlanger et al., less than forty years ago. They synthesized the PTL bis–quaternary ammonium azobenezene dibromide and covalently attached to the catalytic site of chimotrypsin. An observed 4 times increase in the turnover number (k_{cat}) in trans form compared to the unmodified enzyme. Irradiation with 330 nm (80% cis PSS) caused a half decrease in k_{cat} respect to the trans isomer.[218]

One year later, a comparative study of the photocontrol of activity between ureases, glycosidases (*see section 5.2 & 5.3 respectively*) and chymotrypsin was performed using a synthetic spyropiran. The results revealed optical activity modulation of all covalently modified enzymes. Specifically, α–chymotripsin, having the most hydrophobic catalytic pocket, with this kind of substrates, showed a smaller k_m (4.3 mM) in the spyro state than in the merocyanine isomer (k_m = 15 mM) upon UV irradiation, indicating the stabilized enzyme–substrate interactions for the hydrophobic closed spyropiran state.[10]

More than ten years passed until a photoresponsive material was constructed. α–chymotrypsin was immobilized in acrylamide copolymer which contained a photoisomerizable azo group showing reversible permeabilities upon isomerization at 330–370 nm and >400 nm. The hydrolytic activity of α–chymotripsin with nitroanilide–peptide substrate was two times increased in cis and paused in trans. It was observed that the switching efficiency and the hydrolytic activity of α–chymotrypsin was strongly dependent

on the loading degree of the polymer and the substrate used respectively.[219] Further permeability studies were carried out, including a spyropiran and leucohydroxide switches to compare by light, its dipolar moment variation effect. A pronounced increase in fatigue resistance was observed on those photoresponsive materials.[220]

From then, a series of optical α–chymotrypsin inhibitors were developed. All of them acted as PTL, with azobenzene as the light sensitive actuator. The first, was a boronic acid derivate, showing a 4 times trans more potent inhibition (ki_{trans} = 11 μM) than in the cis state (ki_{cis} = 43 μM with 80% PSS). This difference could be increased or reduced depending on the additives used. Assays with subtilisin, revealed an strong additive dependence, without evidence of light modulation inhibition.[214] Later it was proven certain decomposition for boronate esters derivates with UV irradiation of several durations, presenting different activities and reversed reponses in some cases.[221] After boronate derivatives, three α–keto esters candidates were tested (ortho-, meta-, para- α–ketoester) showing more potency in cis than in trans isomer. The optical difference in strenght of inhibition ranged from 2 to 3 times upon irradiation, caused by the ortho–substituted dye at most.[221, 222] Changing the α–ketoester group for trifluoromethylketone gave the best result controlling the inhibition of chymotrypsin optically. UV irradiation exhibit nearly five times more potency for 4–sulfonamido–4'–bromoazobenzene than after visible light.[223] With those results in hand, an inmobilized version was developed, onto a gold surface attaching the ligands by CuAAC (Cu (I) Azide–Alkyne Cycloaddition) reaction.[224] A combination of trifluoromethylketones and methylketones were synthesized and attached. The heterogenous catalyst was analysed, showing up to 3 times better inhibition for cis methylketones and 5.3 times for cis poliethylene glycol trifluoromethylketone derivates, obtaining indeed slighly better results than the homogenous version.[225]

Among photo–sensitized serine proteases, a wide variety of photoswitches have been developed and tested in order to photocontrol either hydrolytic activity or inhibition in the active site. Each corresponding heterogenous version was developed and optimized. Quaternary ammonium dibromide azo derivative allowed the highest photocontrol of hydrolytic chymotrypsin rate, being the first attempt, more than 40 years ago. For enzyme inhibition a list of aldehydes, boronates, α–methylketones and trifluromethylketones were tested reaching a higher optical enzymatic inhibition with trifluoromethylketone moiety, as shown in the inmobilized version, for promising bio assay applications.[10, 214, 218-225]

5.5 Carboxylic ester hydrolases

These proteins, previously called cholesterol estearase enzymes, are responsible for the lipolytic cleavage to give a carboxylate and alcohol as the products. They are found normally in the mammalian liver and in the gastrointestinal tract, taking part in the degradation process of toxins or drugs and in the digestion and absortion of lipid and nutrients respectively.[226, 227]

30 years ago, Ueda et al. published a study towards an optical control of phospholipase A2 (EC 3.1.1.4) with a substituted tripeptide sequence by unnatural aminoacids, pending an azobenzene (AzoF–AMPA). They observed a loss of hydrolytic activity in trans and a partial recovery upon UV irradiation. Unlike with photoresponsive endonucleases, synthetic photoswitches, have not been explored with carboxylic estearases, which might solve some drawbacks inherent about genetic engineering techniques and allow the development of therapeutic applications.

5.6 Endonucleases

They belong to the hydrolytic enzyme family that cleave the phophodiester bond of DNA sequences. The cleavage can be random or site-specific, mediated by the so-called restriction enzymes, that recognizes the methylated position where it starts. According to the mechanism of action, they are divided in Type I, II and III, wich Type II (EC 3.1.21.4), are particularly useful in the laboratory to generate recombinant DNA for genetic modifications into bacteria, plants or animal cells.[183, 228]

Early attempts at photocontrolling endonucleases took advantage of unnatural aminoacids. Genetic engineering techniques allowed the introduction of synthetic phenylazophenylalanine aminoacid into Ribonuclease S (RNaseS) but rather modest activity changes were observed.[229-231] However, only recent synthetic photoswitches were significantly successful for the same purpose.

Homodimeric restriction enzyme PvuII was cysteine–crosslinked by bismaleimide azo switch in between faces, in attachment positions T49C and N62C. Light irradiation with 365 – 470 nm, allowed complete cis – trans isomerization respectively, showing a 16 fold increase in hydrolytic activity. Those results are directed towards the investigation of other DNA recognition modules, including zinc fingers, for in vivo gene targeting.[232]

One year after a similar approach came up using the same azo bis–maleimide switch but mono–derivatized with 2–mercaptoethanol (MAB–OH) and cysteine (MAB–cys), applied

into SsoII restriction enzyme. They presented a molecular gate strategy where two molecules of the same derivative were attached in the homodimer interface positions R174C/A224C for MAB–OH and S171C/S171C for MAB–cys, in the presence of Ni^{2+} ions. 365 nm light irradiation opened the nano–gate increasing two fold the enzymatic activity rate and reverted with blue light.[233]

In between the first and the second successful approaches, a supported version appeared in 2002. The photoresponsive polymers thus serve as actuators that reversibly respond to distinct optical signals to switch the polymer–enzyme aggregates on and off. Two successful azobenzene containing polymers were synthesized (DMAAm and DMAA) by free radical copolymerization. UV irradiation (350 nm) causes a polymer collapse, blocking the substrate acces to endonuclease 12A nearly complete. Its extended state (420 nm irradiation) results in enzymatic activity recovering, but losing 40% from the previous irradiation cycle. Despite the losse in the performance, the polymer switching is very robust and reversible, being attractive in a wide variety of applications as microfluidics, drug encapsulation therapeutics, etc.[234]

5.7 Lipases

Enzymatic lipases hydrolyse a fatty acid into neutral acid and alcohol group similar to the products obtained with carboxyl estearases. They have been extensively applied to chemical processes, from laboratories to industrial plants.[235]

The photocontrol of the hydrolytic activity of lipases has been achieved for the first time as a result of this thesis. In particular, the optical control of lipase enantioselectivity was demonstrated in supported agarose beads. Using genetic techniques, different cysteine point mutations close to the active center were introduced and conjugated with maleimide–reactive azo and iodo–spyro dyes, after inmobilizing lipase 2 (Bacillus Thermocathenolatus) into the support. Optical regulated hydrolytic activity for azobenzene (365 cis and 460 nm trans) and spyropiran (380 mero and 500 nm spyro) showed a discrete change (up to 1.5 fold UV/vis) with both switches and at different mutated positions. However, HPLC analysis showed bigger difference in enantiopreference depending on the dye, the position and the substrate used. Hydroslyis of 2–butyryloxy–2–phenylacetic acid in position 320C with spyropiran, the S enantiomer is favored under visible light and in position 295C with azobenzene, the S enantiomer is favored under UV light. Enantioselectivity changes were also observed in the hydrolysis of 1–phenyl–ethyl acetate

catalyzed in position 187C and 320C for spyropiran where the R enantiomer is favored under visible light. In particular, positon 187C showed 3 times higher enantioselectivity with visible light than with UV light and approached that of the native enzyme. Those results were supported by computational calculations, in accordance with geometrical or hydrophobic switch changes towards the applied substrate.[236]

CHAPTER 4: Photo–modulation of lipase enantioselectivity

This work is the result of a collaboration between Dr. Fernando López and Prof. Pau Gorostiza, encompassed within the FPI subprogram framework supported by the Spanish Ministery EEBB-I-12-04884, carried out from april to october of 2012 in the laboratories of Prof. José Manuel Guisán under the supervision of Dr. Fernando López Gallego (Instituto de Catálisis y Petroleoquímica (ICP), Campus Universidad Autónoma de Madrid (UAM)). Experimental assays design and measurements with spiropyran dye were done by Dr. Fernando López. My contribution to this work was the synthesis of azobenzene compounds and their corresponding tests. Víctor Rojas under the supervision of Prof. Carme Rovira were responsible for computational simulation experiments (Department of Organic Chemistry, Universitat de Barcelona (UB)), to compare the experimental results obtained and disclose certain mechanistic insights. The publication: *Optical Control of Enzyme enantioselectivity is Solid Phase*. ACS Catal., **2014**, *4* (3) 1004-1009, reproduce the content shown herein.

1. OBJECTIVES

The aim of this chapter is to control with light the rate and enantioselectivity of an enzyme. For that purpose, a genetically engineered lipase 2 (from Bacillus Thermocathenolatus) anchored with azobenzene and spiropyran molecules into its catalytic site will serve to analyse the light-effect modulation of lipase 2 catalytic properties, depending on the nature of the photochromic molecule and the position occupied.

2. BACKGROUND

Isolated enzymes can catalyse organic transformations with both high yield and high enantioselectivity under mild conditions. However, *in situ* modulation of catalytic properties has proven to be a great challenge, as indicated by the lack of methods to regulate enzyme enantioselectivity during *in vitro* biotransformations. The dynamic control of enzyme selectivity for *in vitro* reactions schemes is thus an unmet need, especially in the context of cascade reactions catalyzed by multienzyme systems, in wich biocatalysts must be switched on and off *in situ* according to system requirements. Optical control[3] offers the possibility to remotely manipulate enzyme activity using spatiotemporally designated patterns of illumination.[37] Moreover, the immobilization of these engineered biocatalysts would enable their reuse as well as their incorporation into nanodevices.[237] Here, we present a rational approach to conjugate photochromic compounds to an immobilized enzyme in a site-directed manner and demonstrate for the first time the possibility of regulation of its enantioselectivity with light.

Lipases are serin–threonin hydrolases that naturally catalyze the hydrolysis of lipids and are widely applied in chemical processes from research laboratories to industrial plants.[235] Most lipases present a hydrophobic active site shielded by an amphiphilic domain (named as “lid”) that triggers the catalytic mechanism in the presence of hydrophobic substrates.[238] This class of enzymes is the paradigm of enantioselective biocatalysis, and their hydrolytic rate and enantiomeric excess can be enhanced by adjusting the position of the substrate into the hydrophobic cavity.[239] A plethora of methodologies to alter the lipase catalytic mechanism have been devised, including enzyme engineering, reaction media engineering, immobilization, and chemical modification.[239-241] We have recently reported the alteration of both activity and selectivity of lipase 2 from *Bacillus thermocathenolatus* (BTL2) using site-directed chemical modification in the solid–phase.[242] Building upon this methodology, we pursued photocontrol of BTL2 catalytic properties by tethering a photochromic group inside the enzyme active center.

3. RESULTS AND DISCUSSION

3.1– Site Directed Chemical Modification of BTL2 in Solid Phase

We chemically modified BTL2 with different photochromic molecules. As a result of the reversible transformation of the photochromic group anchored to the protein scaffold, we expected the active center conformation to change under different illumination conditions (**Figure 1. I**). To test whether those changes availed in altering the enzyme activity, we evaluated several positions located at the substrate binding pocket and at two compounds displaying different photochromic processes (**Figure 1. II**). In particular, an iodoacetate–spiropyran (**57,** **Figure 1**) and an azobenzene–methylthiosulfonate (**58,** **Figure 1**) were specifically conjugated to a unique cysteine at positions 17, 187, 245, 295, and 320 of BTL2. These positions were rationally choosen because they are important either for the substrate binding (17, 245 and 320) or for the lid aperture during the catalysis (187 and 295) (supporting information, Figure S1 and Table S1*)*.[238] The unique cysteine at the specific position was introduced by directed mutagenesis using a cysteine-less BTL2 variant that was created in previous work[242] to avoid unespecific chemical modification.

Both catalytic rate and enantioselectivity were assayed toward a survey of esters, under different light conditions (see the Supporting Information for details on the synthesis, mutagenesis, purification and site-selective chemical modification in solid phase of the enzymes). The conjugation took place in the solid phase by incubating the immobilized BTL2 in a photochromic compound solution. The yield of the chemical modification was evaluated by thiol titration. As an example, 94 ± 9 (%) of the BTL2 active centers were modified with molecule **57** at position 245. The conjugation procedure was simplified by solid–phase preparation since excess reagents and solvents could be easily removed by vacuum filtration. The site-directed chemical modification was confirmed by mass spectrometry (supporting information, Figure S2)

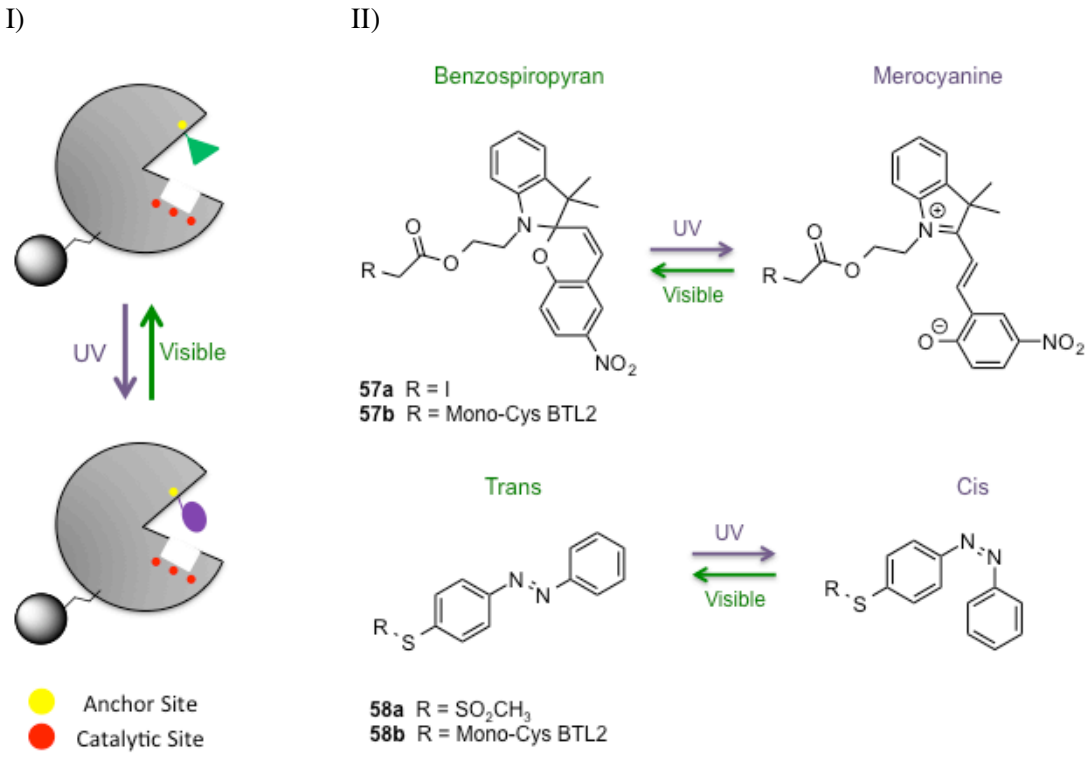

Figure 1. **I)** Site-directed chemical modification of BTL2 with phoswitchable molecules. Reversible conformational changes of semisynthetic binding pocket induced by light. BTL2 immobilized on agarose beads activated with cyanogen bromide groups has been site-directed-modified with photoswitchable molecules. Since the photosentitive molecules have been closely anchored to the catalytic residues, enzyme properties can be modulated. **II)** Photochromic properties of different immobilized bioconjugates. Photoswichable equilibrium undergone by spiropyran **(57)** and azobenzene **(58)** molecules. The spiropyran compound is activated by an iodoacetate reactive group **(57a)** to specifically react to cysteines on the protein structure, resulting in covalent and irreversibly anchored **(57b)** bioconjugates. In the same way, the azobenzene compound was activated with methylthiosulfonate groups (MTS) **(58a)** that selectively react to cysteine, as well, but form covalent and reversible bioconjugates **(58b)**.

3.2– Spectroscopic Characterization of the Photo-sensitive Biocatalysts

The photochromic biocatalysts were spectroscopically characterized under different illumination conditions. Ultraviolet (UV) light transforms the apolar spyropyran **57** into the planar, polar merocyanine form (**Figure 1. I**) and causes the isomerization of azo derivate **58** from the extended *trans* configuration to the bent *cis* form (**Figure 1. II**). In both cases, the initial state is reversibly recovered under visible illumination or after thermal relaxation in darkness (**Figure 2. I, II**). It is noteworthy that photochromic molecules tethered to immobilized BTL2 (**57b** and **58b**) presented absorbance spectra similar to those of the

molecules in solution. UV light increased the absorbance of compound **57** at 550 nm, as previously reported[243] (**Figure 2. I, inset**) and decreased the absorbance compound **58** at 350 nm, as described for similar azobenzenes[244] (**Figure 2. II, inset**). However, the half-life of thermal relaxation and the stationary state achieved in the dark by both photochromic molecules were substantially altered by coupling to the protein.[18] For example, after UV illumination, the soluble **57a** relaxation rate under darkness was 20% faster than the same molecule anchored to position 245 in the BTL2 active site (**57b**). In fact, 80% of soluble **57a** was relaxed after 24 h in darkness, but only 60% relaxation was observed after 24 h for **57a** conjugated to the protein scaffold (**57b**). Moreover, **57a** and **57b** preparations only were partially relaxed in the dark and required visible illumination to completely convert them back to the spiropyran form (**Figure 2. I** and supporting information Figure S3A). Therefore, the alteration of the "reversible photo-equilibrium" suggests that the protein environment could stabilize the polar merocyanine, as previously reported.[10]

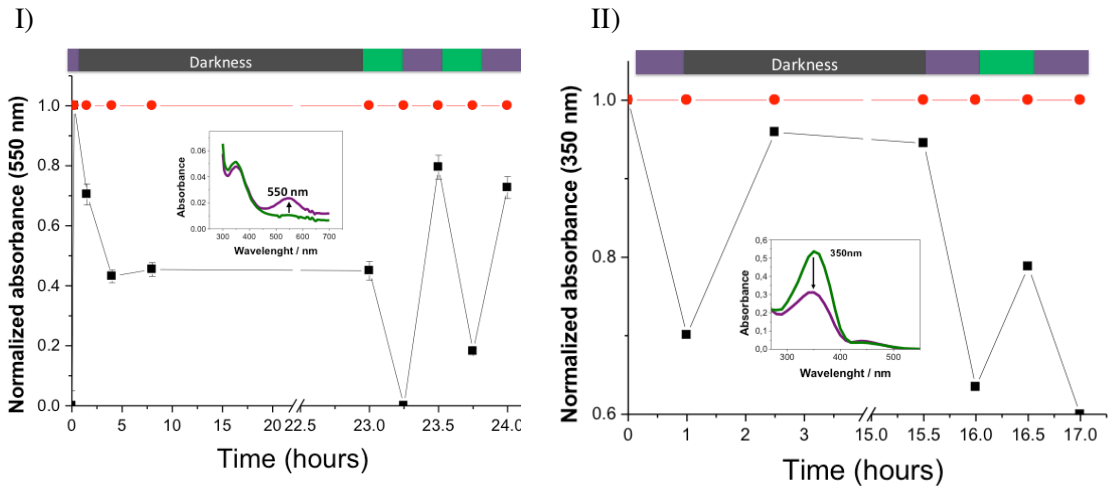

Figure 2. Spectroscopic characterization of immobilized BTL2 bioconjugates modified with either spiropyran **(I)** or azobenzene **(II)** molecules (see Supporting Information). Inset figure depicts the absorbance spectrum of solid bioconjugates illuminated with either visible (green line) or UV (violet line) light. The arrows point out the effect of the light switch on the absorbance maximum of the different molecules. The main graph represents the evolution of active site states under different light conditions. Red circles correspond to wild type and, consequently, non-modified BTL2; black squares, to BTL2-modified at position 245. After illuminating solid photochromic bioconjugates with UV lights, the relaxation of the excited compound was monitored along the time in darkness. Afterward, the solid preparations were subjected to light cycles to study the photocommutability of the anchored molecules into the active site environment.

3.3– Effect of Light on Immobilized BTL2 Catalytic Properties

Catalytic reactions with several conjugated BTL2 variants were carried out under different illumination conditions, and the activities were measured using colorimetric assays. **Figure 3. I** and **II** show the hydrolytic activity of different immobilized bioconjugates under UV and visible light. In general, conjugation of photochromic molecules led to a reduction in lipase activity, but several variants displayed a catalytic rate that was moderately light–dependent, thus validating the strategy to photocontrol an enzyme with a shielded active site. As an example, BTL2 conjugated with **57** at positions 187 and 245 (BTL2–187C-**57** and BTL2–245C-**57**) and with **58** at position 245 (BTL2–245C-**58**) presented a relative 1.5-fold higher activity under UV light than under visible light (**Figure 3. I** and **II**). These results demonstrate that the anchoring site of the photochromic group in the lipase is critical to control its hydrolytic activity with light, and constitute the first demonstration of enzyme photoregulation in solid state using porous materials as carriers. The choice of agarose beads as carriers was key because its transparency allows light passing through the pores and illuminating the enzymes attached to the solid structure, thereby activating the photochromic molecules anchored to the protein.

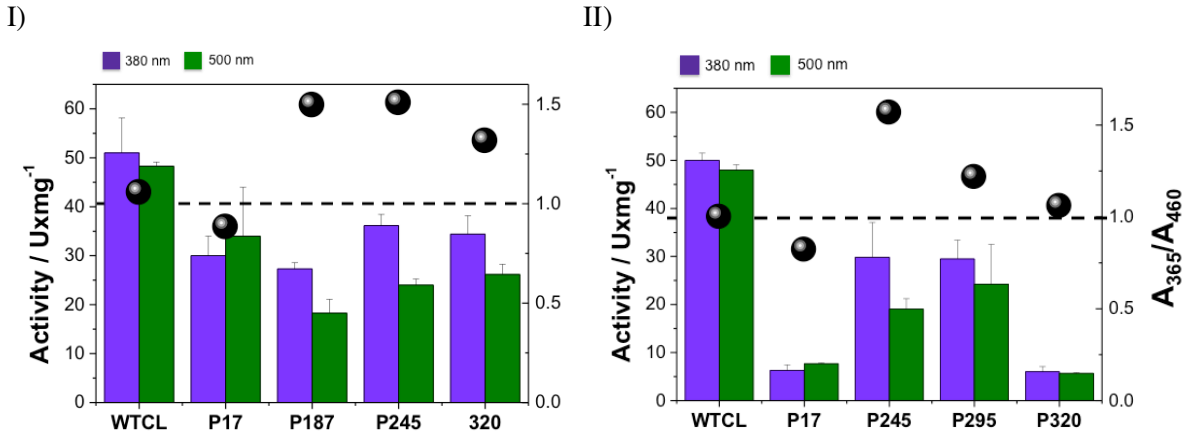

Figure 3. Analysis of the enzyme properties of photoswitchable lipase under different illumination conditions. Esterase activity of different immobilized variants of BTL2 modified with either **57a (I)** or **58a (II)** compounds under light at different wavelengths. Hydrolytic activity of the different chemically modified BTL2 variants were measured under either visible light (green bars)(500 and 460 nm for **57b** and **58b** bioconjugates respectively) or UV light (violet bar) (380 and 365 nm for **57b** and **58b** bioconjugates, respectively). The spherical points show the photocommutation ratio defined as the coefficient between the specific enzyme activity under UV and visible lights. Values close to 1 mean a non-photocommutable lipase, and ratios higher or lower than 1 mean photocommutable lipases.

These novel results prompted us to examine enzyme enantioselectivity, arguably one of the most outstanding properties of lipases.[239] To that goal, we tested racemic mixtures as substrates and measured the chirality of the products yielded by different BTL2 bioconjugates under UV and visible illumination. The enantioselectivity of modified BTL2 variants toward two different racemic esters, 2-butyryloxy-2-phenylacetic acid (***rac*-59**) and 1-phenyl-ethyl acetate (***rac*-60**), is shown in Figure 4 I and II, respectively. In the first case, site-directed modification of BTL2 with compound **57** tended to preferentially hydrolyze the *S* enantiomer, inverting the natural preference by the *R* enantiomer displayed by the native enzyme. In contrast, modification with compound **58** enhanced the enantiomeric excess values of the native enzyme (see complete results in supporting information Tables S2 and S3). Photocontrol of the enantioselectivity depended both on the conjugation site and on the nature of photochromic molecule unlike activity that depend only on the conjugation position. In this regard, the enantioselectivity was the inverse of the result for the hydrolysis of ***rac-59*** using BTL2–320C-**57** (the *S* enantiomer is favored under visible light) and BTL2–295C-**58** (the *S* enantiomer is favored under UV light) (**Figures 3. I** and supporting information Figure S4). On the other hand, enantioselectivity changes were also observed in the hydrolysis of ***rac-60*** catalyzed by BTL2–187C-**57** y BTL2–320C-**57** (the *R* enantiomer is favored under visible light) (**Figure 3. II**). In particular, the enantioselectivity of BTL2–187C-**57** toward ***rac-60*** under visible light was three times higher than under UV light, thus being approached to the native enzyme.

Position 320 located at the binding pocket and the contact region between the lid domain and the active site are "hot-spots" to anchor photochromic molecules that effectively modulated the enzyme enantioselectivity by the action of the light. Similarly, chemical modification of position 320 of BTL2 with alkanes modified both the activity and the enantioselectivity of the immobilized BTL2.[242]

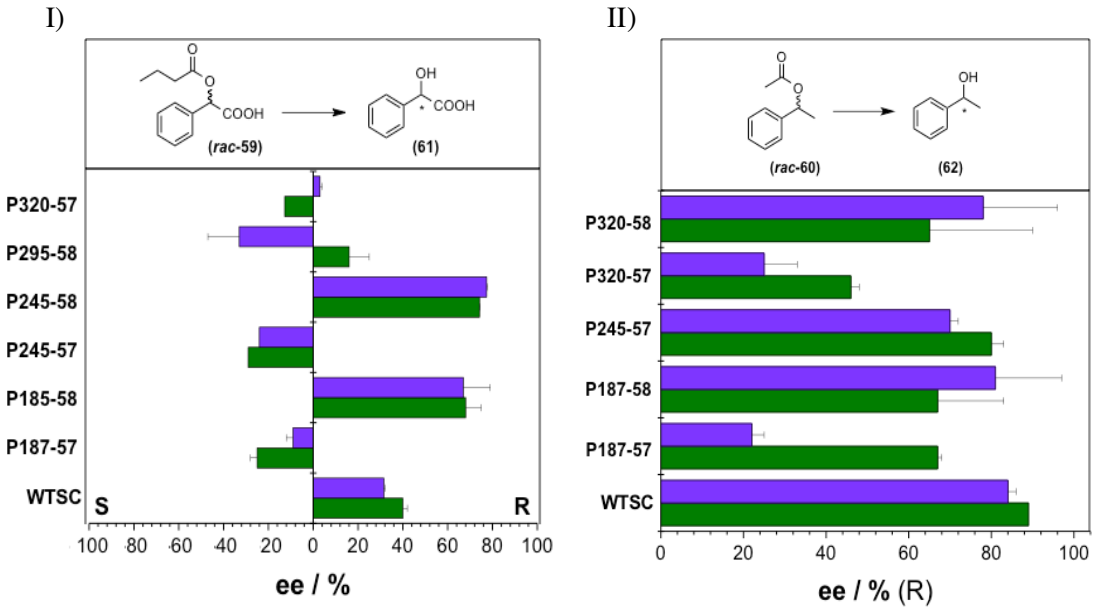

Figure 4. Selective hydrolysis of 2-butyryloxy-2-phenylacetic acid (***rac-59***) **(I)** and 1-phenyl-ethyl acetate (***rac-60***) (**II**) to their corresponding chiral alcohols 3-phenyl-2-hydroxypropionic acid (**61**) and 1-phenyl ethanol (**62**) were catalyzed by different BTL2 bioconjugates modified with either **57a** or **58a** compounds. Effect of light on the lipase selectivity was determined by measuring the enantiomeric excess (ee %) of the different bioconjugates modified at different positions under either visible (green bars) or UV (violet bars) light. For bioconjugates **57b**, visible and UV wavelengths were 500 and 380 nm. For bioconjugates **58b**, they were 460 and 365 nm for visible and UV light, respectively.

In principle this approach can be expanded to other enantioselective enzymes, regardless the morphology of their active site, and the catalytic mechanism as well as the activity of several enzimes (endonucleases, carbonic anhydrase, etc.)[34, 229, 232] can be modulated by light. Therefore, these light-driven changes in enzyme enantioselectivity constitute a breakthrough in the regulation of biocatalysis for *in vitro* applications. This complements engineered[245] and artificial[246-248] enzyme strategies to provide reversibility and remote control and largely outperforms previous attempts using additives in the reaction media.[242] Moreover, this work demonstrates for the first time that light can also modulate enzyme properties in the solid phase as well as it does in solution. The resulting photochromic immobilized biocatalysts might be used in a fix-bed reactor for a continous process that is able to respond to external signals, such as the light. This opens new opportunities for the regulation of biocatalytic systems formed by isolated enzymes.

3.4– Effect of Light on Catalytic Versatility of the Photochromic Biocatalysts

Since photoisomerization is expected to produce subtle changes in the catalytic site, we evaluated the photocontrol of the catalytic versatility of these novel biocatalysts. For that purpose, we performed a kinetically controlled transesterification reaction using glycerol (**63**) and methyl butyrate (**64**) as substrates (**Figure 5**). It has been reported that BTL2 catalyzes the transesterification reaction, yielding the corresponding glyceryl butyrate (**65**). However, the enzyme can also hydrolyze **64,** yielding butyric acid (**66**), undesirably lowering the synthetic product yield.[249] From a mechanistic point of view this reaction is highly interesting because it reveals that the lipase can act as synthetase and hydrolase in the same reaction. The ratio between synthesis and hydrolysis depends on the catalytic properties of the enzyme, and thus, it could be, in principle, regulated by light. To test this possibility, we carried out the transesterification reaction using immobilized BTL2–P245-**57** and different light cycles. Figure 2. I shows how BTL2 properties were altered by light while the unmodified native lipase was insensitive to illumination. Although UV light promotes an active site configuration that can hydrolyze and synthesize at similar rates, visible light leads to an enzyme that hydrolyzes three times better than it synthesizes. In the light statistical analysis of these results, differences between synthetic and hydrolytic ratios were much more significant under visible light than under UV light; therefore, the synthesis/hydrolysis ratio can be dynamically controlled by light, enabling the temporal control of catalytic performance of BTL2 in mechanistic terms.

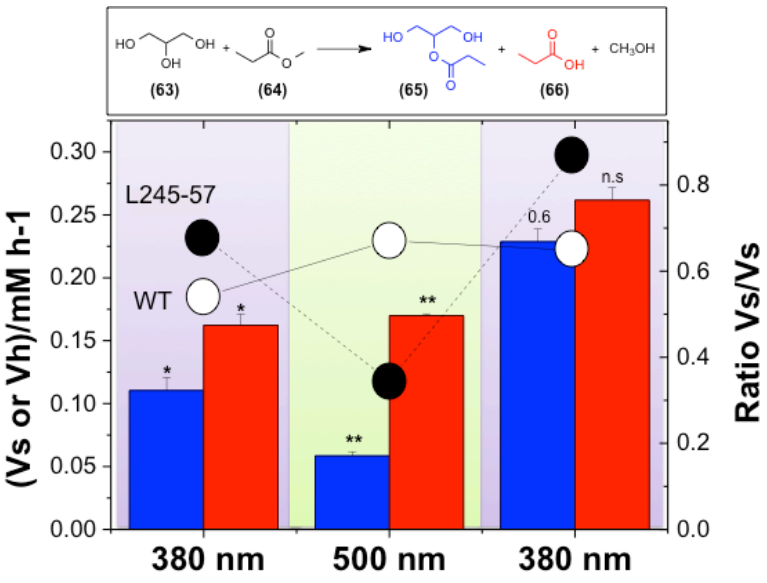

Figure 5. Kinetic controlled synthesis of 2-O-butyril-glycerol **(65)** catalyzed by BTL2 modified with **57a** at position 245. The light was switched every 30 min during the reaction, and the substrates and the product have been analyzed by HPLC to study the simultaneous hydrolytic and synthetic reactions. Synthetic (blue bars) and hydrolytic (red bars) rates represented in this figure were determined under different light conditions. Error bars show the standard deviation of two independent measurements subject to *t* test analysis, where (*)$p < 0.05$, (**)$p < 0.01$ are the significant differences between hydrolytic and synthetic rates and n.s. means no significant differences between those rates. The black circles and solid black line represent the ratio between the synthetic and the hydrolytic activity of the photoswitchable bioconjugate and the white circles and dashed black line show the same ratio for the unmodified wild type enzyme.

3.5 In Silico Studies of Photosensitive Bioconjugates. Binding Mode of Substrate to the Active Site under Different Light Conditions

Due to the success of this approach was built on rational design but also on testing empirically several attachment positions and reaction conditions, we turned to computer simulations of the best photocontrolled lipase variants to identify the principles that could help in the optimization of further design. In particular, we asked whether the observed enantiomeric excesses for the different bioconjugates can be explained by the influence of photoisomerization on the spatial availability within the active site by altering the substrate-binding properties (energy and conformation) or by conformational changes in the enzyme structure. To this aim, molecular dynamics (MD) simulations were performed on the lipase modified with either spiropyran or azobenzene molecules. Separate docking calculations with the *R* and *S* enantiomers of the 2-butyryloxy-2-phenylacetic acid (***rac-59***) substrate were also carried out. MD simulations have successfully been used to model conformational motions in lipases,[250] including substrate binding.[251] The current MD simulations show that bioconjugation with **57** and **58** does not perturb the protein folding, and the substrate binding pocket does not change significantly. Since the reactions were performed under nonsaturating conditions (1 mM), binding energy differences should reflect differences in reactivity. Analysis of the most populated substrate docking poses (among the ones well oriented for catalysis) (**Figure 6**) shows that the *R/S* enantiomers have a similar binding energy for the bioconjugates with little enantiomeric excess (Figure 6B: BTL2–320C-**57** in the merocyanine state, and Figure 6C: BTL2–295C-**58** in the *trans* configuration). In contrast, the two enantiomers are well separated in terms of binding energy for the bioconjugates for which the highest enantiomeric excess was measured

(**Figure 6A**: BTL2–320C-**57** in the spiropyran state, and **Figure 6D**: BTL2–295C-**58** in the *cis* configuration). Furthermore, the *S* enantiomer is clearly favored with respect to the *R* enantiomer not only in terms of energy but also in terms of structure (closeness of the substrate to the catalytic residues), with the effect being more pronounced for BTL2–295C-**58** under UV-light and in the *cis* conformation (**Figure 6** and supporting information, Table S4). Therefore, the simulations support that the highest enantiomeric excesses are experimentally observed for these two bioconjugates: BTL2–320C-**57**(top) and BTL2–295C-**58** (bottom) under visible (left) and UV (right) light.

Several strategies have been devised to control the catalytic rate of enzymes with light,[3] including unspecific conjugation of photochromic compounds,[10] diffusible photochromic ligands,[252] and site-specific incorporation of photochromic unnatural aminoacids.[229] However, photocontrol of chirality has remained elusive, despite the wide biochemical and biotechnological importance of enantioselective enzymes and knowledge of their structure and catalytic mechanisms.

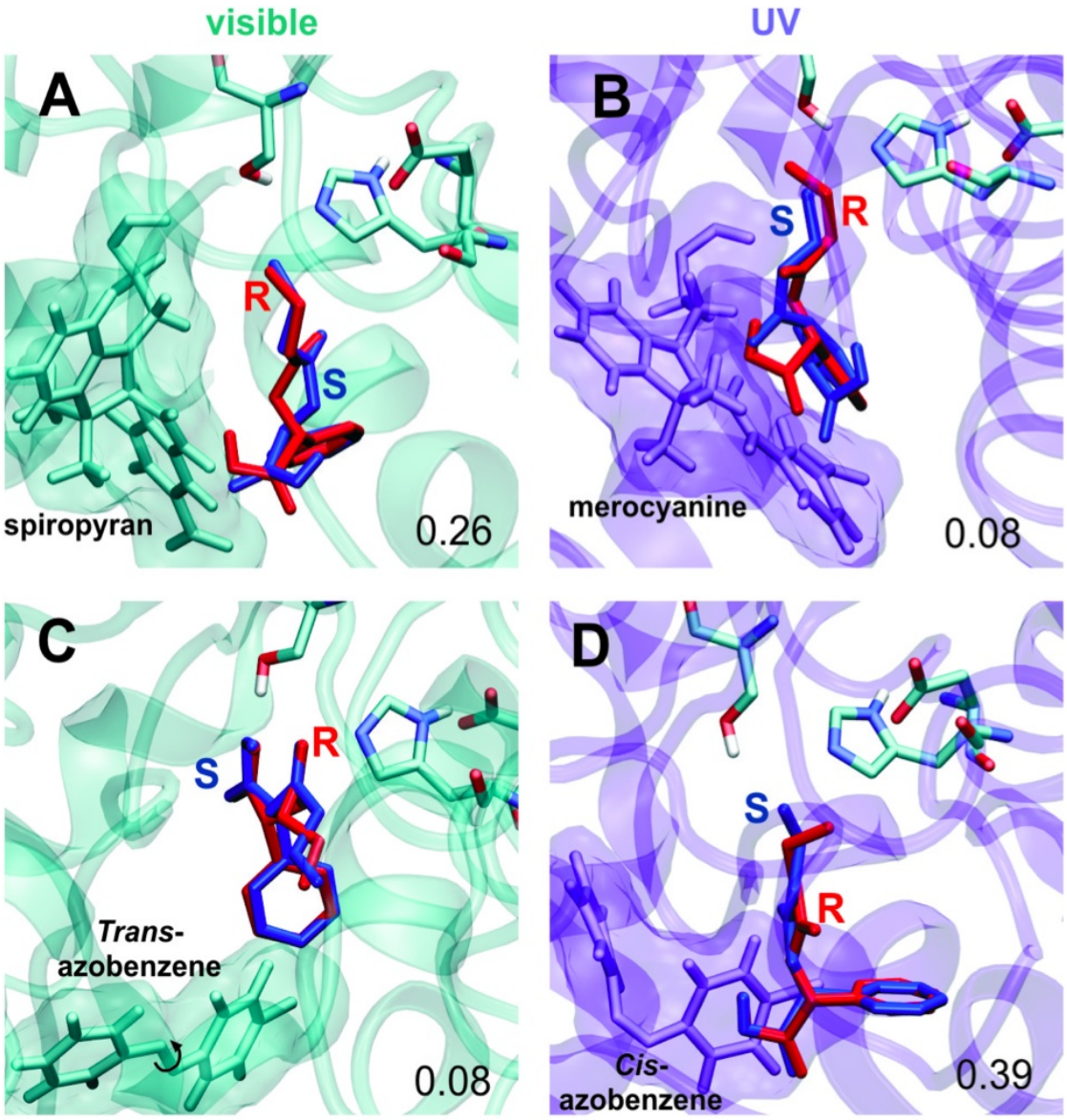

Figure 6. Most populated docking modes of (*R,S*)-2-butyryloxy-2-phenylacetic acid (*rac-59*) in the active site of the bioconjugates BTL2-P320C-57(top) and BTL2-P295C-58 (bottom) under visible (left) and UV (right) light. The differences in binding energies between the *R* and *S* enantiomers are indicated on the figures (positive values indicate binding that favors the *S* enantiomer). Adapted from Víctor Rojas

Here, we have presented a rational approach to nanoengineer immobilized enzymes by site-directed chemical modification with photochromic compounds. We have demonstrated how such chemical modifications enable optical regulation of BTL2 catalytic properties in different reaction schemes. The strategy of conjugating photochromic compounds in the binding pocket has allowed manipulation of the steric hindrance of the cavity and achievement of an enantioselective molecular fit in certain cases. Structural modeling and simulations provide a good basis to understand the experimental results, pinpointing the

atomic-scale structural elements that are key to photoregulate BTL2 activity and selectivity. In particular, light acts as an external stimulus that influences the active site spatial availability rather than promoting a conformational change in the protein tertiary structure (see supporting information Figure S5).

In this way, light remotely alters the substrate binding because the binding pocket is differently but reversibly shaped by a photocontrolled molecular adaptor. The combination of experiments and simulations suggests that the approach could be extended to other structurally well-characterized enzymes or multienzymatic complexes, providing reversible and noninvasive modulation of different biocatalytic properties *in-pot*. This novel form of enzymatic photoregulation might be useful to externally control a branching point in cascade enzymatic reactions. For example, in one-pot multienzymatic complexes, light would act as an external stimulus, selecting the products to be fed as substrates into subsequent enzymatic steps. This function is analogous to that of demultiplexer devices in electronic circuits (see supporting information, Figure S6) and has been recently demonstrated in organic molecular devices.[253] The enzyme with photoswitchable enantioselectivity described here thus constitutes the first demonstration of a protein-based demux.[254]

4. CONCLUSIONS

- We have presented a method to control the catalytic properties of a lipase with light that is based on the site-directed chemical conjugation of photochromic molecules into the catalytic cavity.

- Despite the relatively small changes in activity (**Figure 3**), the selectivity of the enzyme was modulated for the first time with light, using azobenzene (**58**) and spiropyran (**57**) molecules. The position, the photochromic compound selected and the substrate used, are crucial for the resulting effect (**Figure 4**).

- In particular BTL2–320-**57** and BTL2–295-**58** derivates for ***rac-59*** substrate, show a change in the enantiopreference with light. For the first one, the *S* enantiomer is

favoured under UV light. In contrast, the *R* enantiomer is favored under UV light for the second. However, BTL2–187-**57** and BTL2–320-**57** for ***rac-60*** share the same enantiopreference but the enantiomeric excess can be optically modulated (**Figure 4**).

- Transesterification experiments using inmobilized BTL2–245-**57** showed a dynamic synthesis/hydrolysis optical ratio control. Similar synthesis-hydrolysis rates were observed with UV light. However in visible light, the enzyme can hydrolyse three times better than it can synthesize (**Figure 5**).

- Molecular dynamics simulations indicated that conjugating photochromic compounds in the active site allows manipulation of the steric hindrance and binding energy of the substrates, leading to an enantioselective molecular fit in certain cases, in accordance with the experimental results obtained (**Figure 6**).

5. SUPPORTING INFORMATION

INDEX

SUPPLEMENTARY EXPERIMENTAL DETAILS

5.1– General experimental methods

Materials: Agarose beads activated with cyanogen bromide groups were supplied by GE healthcare (Uppsala, Sweden). Triton X-100, p-nitrophenyl butyrate (p-NPB), nitrosobenzene, 4,4'-diaminothiobenzene, Acetic acid (AcOH), sodium sulfinate, I_2, 2-(butyryloxy)-2-phenylacetic acid, 1-phenylethyl acetate, were purchased from Sigma Chem. Co (St. Louis, MO, USA). Other reagents and solvents were of analytical grade. *(3',3'-dimethyl-6-nitrospiro[chromene-2,2'-indolin]-1'-yl)ethyl 2-iodoacetate*, was synthesized as described.[243] LED lamps and power supply used for irradiation of compound **1** at 380/500 nm and compound **2** at 365/460 nm were custom-made by FCTècnics (Sant Adrià de Besòs, Spain)

Bacterial Strains, Plasmids and Enzyme expression: Escherichia coli strain DH5*α* (laboratory stock) was used for routine cloning procedures. Overproduction of BTL2 variants were carried out using BL21 (DE3) (laboratory stock). The *E. Coli* strains were routinely cultured at 37ºC in Luria-Bertani (LB) broth using ampicillin (150 µg/mL) as a resistance marker. The overexpression and purification of BTL2 variants were carried out as previously described by López-Gállego et al.[242]

Site-directed mutagenesis to create the mono-cysteine variants of BTL2. Site directed mutagenesis protocol was used to construct five BTL2 mutants (F17C, C64S, V187C, L245C and I320C). Mutants F17C, V187C, L245C and I320C were made by using BTL2 *C64S/C295S* as template. While for the mutant C64S (having an unique cysteine in position 295), we used the native *BTL2* gene as template. Briefly, to introduce the amino acid change, the corresponding pair of oligonucleotides was used as primer pair in a PCR reaction using a specific plasmid as template and Prime Start HS Takara DNA polymerase. The product of the PCR was digested with *Dpn*I that exclusively restricts methylated DNA. *E. coli* DH5α cells were transformed directly with the digested product. The plasmids bearing the mutated *btl2* genes were identified by sequencing and then transformed into *E. coli* BL21(DE3) cells to express the corresponding proteins. Mutations F17C, C64S, V187C, L245C and I320C were previosly described elsewhere by our group.[3, 237, 255]

Enzyme activity assay. Both immobilized and soluble lipase activity of BTL2 variants (5 μL in a 1/50 suspension) were spectrophotometrically measured by using 0,25 mM of p-nitrophenyl butyrate (p-NPB) as a substrate. The colorimetric product (p-nitrophenol) was quantified at different times by measuring the absorbance at 405 nm. The enzyme activity was calculated based on the product extinction coefficient ($\varepsilon = 5{,}15\ mM^{-1}$). The assay was carried out in 96-well microplates with a final volume of 205 μL, under different illumination conditions, based on the photochromic compounds used.

Immobilization of BTL2 variants: Firstly the Ag-CNBr was activated with a solution at pH 2 following the supplier instruction (GE healthcare, USA). The immobilization was carried out by the addition of 1g of agarose activated with cyanogen bromide groups to 10 mL of enzyme solution (12-87 U/mL) dissolved in 25 mM sodium phosphate buffer at pH 8. The suspension was gently stirred for 1h at 25 °C. Then, the support was vacuum filtered and washed with 25 mM sodium phosphate buffer at pH 8 and incubated for 2h with 1 M of ethanolamine solution at pH 8. Finally, the immobilized preparation was washed with abundant distilled water.

Conjugation with iodoacetate-spiropyran: 1 g of immobilized BTL2 variant was incubated with 10 mL of conjugation solution at 25 ºC under gentle stirring for 2 h. The conjugation solution was formed by 0,1 mM iodoacetate-spiropyran, 20% DMSO, 0,02% Triton X-100 and 10 mM Tris-HCl at pH 8.

Conjugation with azo-methylthiosulfonate: 1 g of immobilized BTL2 variant was incubated with 10 mL of conjugation solution at 25ºC under gentle stirring for 2 h. The conjugation solution was formed by 0,1 mM azo-methylthiosulfonate, 25% acetonitrile, 0,02% Triton X-100 and 10 mM Tris-HCl at pH 8. After conjugation with the different photochromic molecules, the immobilized preparations were exhaustively washed with water and then equilibrated with with 10 mM Tris-HCl at pH 7. Finally, all samples were stored at 4 ºC

Trypsin digestion procedure: 0.1 g of solid bioconjugates were incubated with 0.5 mL of guanidine 6 M in 12.5mM Tris-HCl buffer at pH 8, for 1h. Then, the guanidine was removed by vacuum filtration and the solid was washed with 100 volumes of 50 mM Tris-HCl buffer at pH 7.6. Afterwards this solid was incubated with 0.2 mL of trypsin solution for 12-16 h at 25 °C. Trypsin was dissolved in 50 mM Tris-HCl buffer at pH 7.6. The concentration of trypsin in such solution kept the ratio protease/protein 1:100-1:20. Finally the suspension was filtered and the supernatant was collected and stored at -20 °C for further mass spectrometry analysis.

Hydrolysis of chiral esters under different illumination conditions: 1-5 mM of different racemic esters (***rac*-59** and ***rac*-60**) were dissolved in 10 mM Tris-HCl buffer at pH 7. 10 μL (1/3 suspension) of different immobilized and photoconjugated BTL2 variants were exposed to different illumination conditions and reactions were triggered with 200 μL of the corresponding substrate solution. Hydrolysis reactions were incubated under the corresponding illumination conditions and 25 °C. Afterwards, the reactions were stopped at different end-point times by centrifugation removing the solid biocatalysts. The resulting supernatant was analyzed by HPLC under different conditions. HPLC equipment (Spectra Physics SP 100 coupled with a Diodos detector Spectra Physics SP 8450) was coupled to Kromasil C8 column (15 cm x 0.46 cm) supplied by Análisis Vínicos (Spain) to calculate the reaction conversion. The mobile phase was 35% acetonitrile in 10 mM of ammonium phosphate buffer at pH 3.2 for *rac-59* and *rac-60* respectively. The analyses were performed at a flow of 1 mL/min by recording the absorbance at two wavelengths of 254 and 210 nm. On the other hand, the enantiomeric excess (*e.e.*) of the different enantiomers of **61** and **62** were also determined by HPLC analysis on a chiral column (OD-R) using a mixture isocratic mobile phase 10 mM ammonium phosphate buffer and 5% acetonitrile at pH 2.3 and 7 as mobile phase, respectively. The analyses were performed at a flow of 0.5 ml/min by recording the absorbance at 210 nm.

*Kinetically controlled synthesis of 2-O-butyril glycerol***.** 0.1 g of different immobilized BTL2 and conjugated variants was incubated with 2 mL of a reaction mixture consisting of 90% glycerol in 10 mM Tris-HCl buffer and 50 mM methyl butyrate at pH 7. The reaction was carried out with gently stirring at 25 °C and samples of supernatants were withdrawn at different times. The samples were analyzed by HPLC (Spectra Physics SP 100 coupled with a Diodos detector Spectra Physics SP 8450) using a Kromasil C8 column (15 cm x 0.46 cm) supplied by Análisis Vínicos (Spain). The isocratic mobile phase was 0.025 mM acetic acid and 30% of acetonitrile dissolved in distilled water at pH 3.7. The analyses were performed at a flow of 0.7 ml/min by recording the absorbance at 210 nm.

5.2– Synthesis of azo-derivatives activated with cysteine-reactive groups

See the supporting information of chapter 1, section 5.2 for general instrumentation and methods.

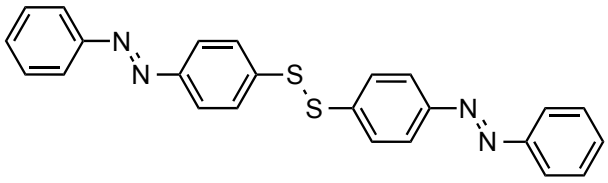

(1,2-bis(4-((E)-phenyldiazenyl)phenyl)disulfane). Modified protocol.[256] To a flask containing 4,4'-diaminothiobenzene (0.2 g, 0.81 mmol) dissolved in AcOH (0.32 M), nitrosobenzene (0.3 g, 2.81mmol) was slowly added (over a period of 10 min.). At this point we can see a colour change from fluorescence yellow to an orange-brownish solution. The reaction was kept without stirring for 5 days at room temperature. After that, the crude was dissolved in CH_2Cl_2 (30 mL) and extracted with HCl solution (1M) (2 × 30 mL), then washed with water (2 × 30 mL) and brine (2 × 30 mL). Residual H_2O was removed with $MgSO_4$, and the organic solvent was evaporated. The residue obtained was crystallized in a dimeric form with hot THF obtaining an orange solid (0.24 g, 69 %). **mp** 164-167 ºC. **IR (ATR)**: 1508, 1478, 1103, 1069, 1018, 1006, 827, 765, 538, 527 cm^{-1}. **^{1}H NMR** (400 MHz, $CDCl_3$): δ 7.90–7.87 (m, 8H), 7.66–7.63 (m, 4H), 7.52–7.46 (m, 6H). **^{13}C NMR** (100 MHz, $CDCl_3$): δ 152.7, 151.8, 140.02, 131.3, 129.3, 127.7, 123.8, 123.1. **HRMS** calculated for $C_{24}H_{19}N_4S_2$ $[M+H]^+$: 427.1046. Found: 427.1034.

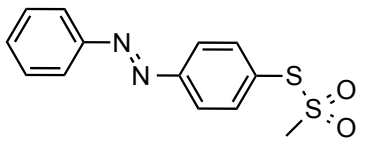

(E)-S-(4-(phenyldiazenyl)phenyl) methanesulfonothioate)(58a).[257] A mixture of sodium sulfinate (0.150 g, 1.47 mmol) and 1,2-bis(4-((*E*)-phenyldiazenyl) phenyl) disulfane (0.196 g, 0.46 mmol) were dissolved in CH_2Cl_2 (0.2 M) with vigorous stirring. Once all solid particles were dissolved, I_2 (0.245 g, 0.97 mmol) was added and the reaction continued stirring for 22 h. After, the reaction mixture was partitioned with CH_2Cl_2 and water (50

mL). The organic layer was separated and washed with a saturated solution of $Na_2S_2O_3$ (2 x 50 mL), then H_2O (2 × 50 mL) and brine (2 × 50 mL). To remove the remaining water, Na_2SO_4 was used, and the organic solvent was evaporated under reduced pressure. The solid obtained was purified by crystallization using a THF/Hexane solvent mixture. The resulting product appeared as a bright orange solid (0.075 g, 56 %). **mp** 157-162 ºC. **IR (ATR)**: 1512, 1475, 1296, 1093, 934, 830, 543, 479 cm^{-1}. **^{1}H NMR** (400 MHz, $CDCl_3$): δ 8.01–7.94 (m, 4H), 7.88–7.86 (m, 2H), 7.58–7.53 (m, 3H), 3.23 (s, 3H). **^{13}C NMR** (100 MHz, $CDCl_3$): δ 154.1, 152.5, 137.1, 132.0, 130.2, 129.4, 124.1, 123.3, 47.9. **HRMS** calculated for $C_{13}H_{13}O_2N_2S_2$ $[M+H]^+$: 293.0412. Found: 293.0410.

5.3– Selected NMR spectras

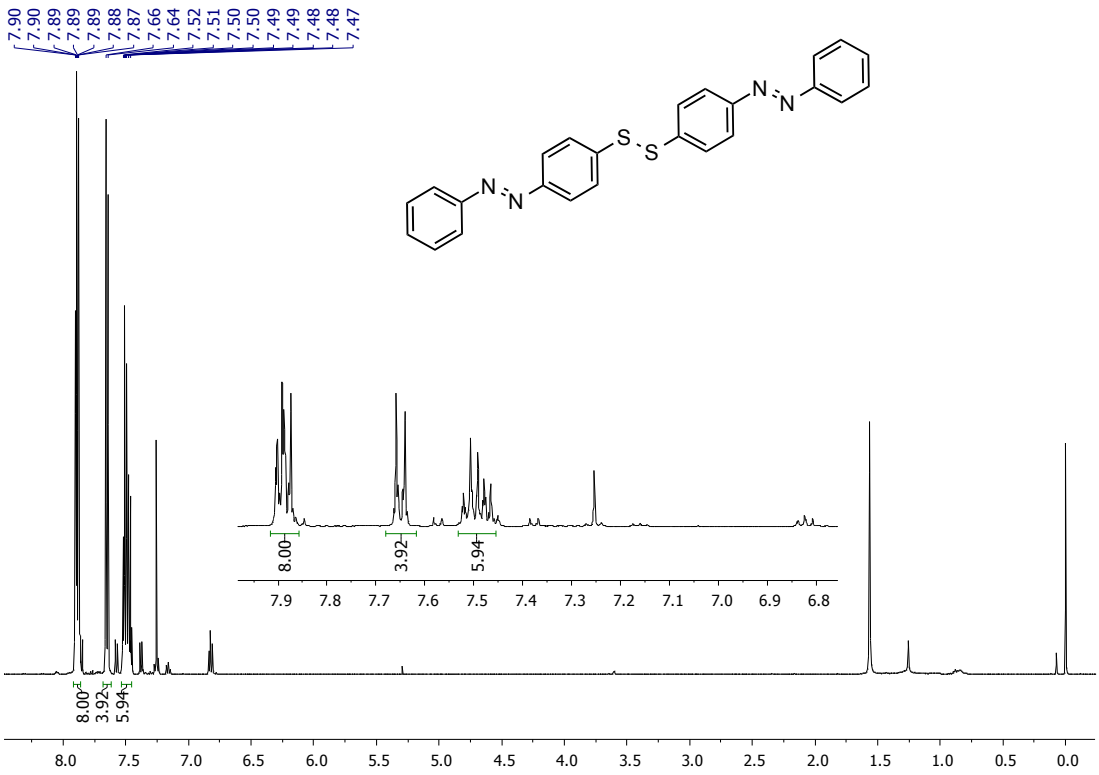

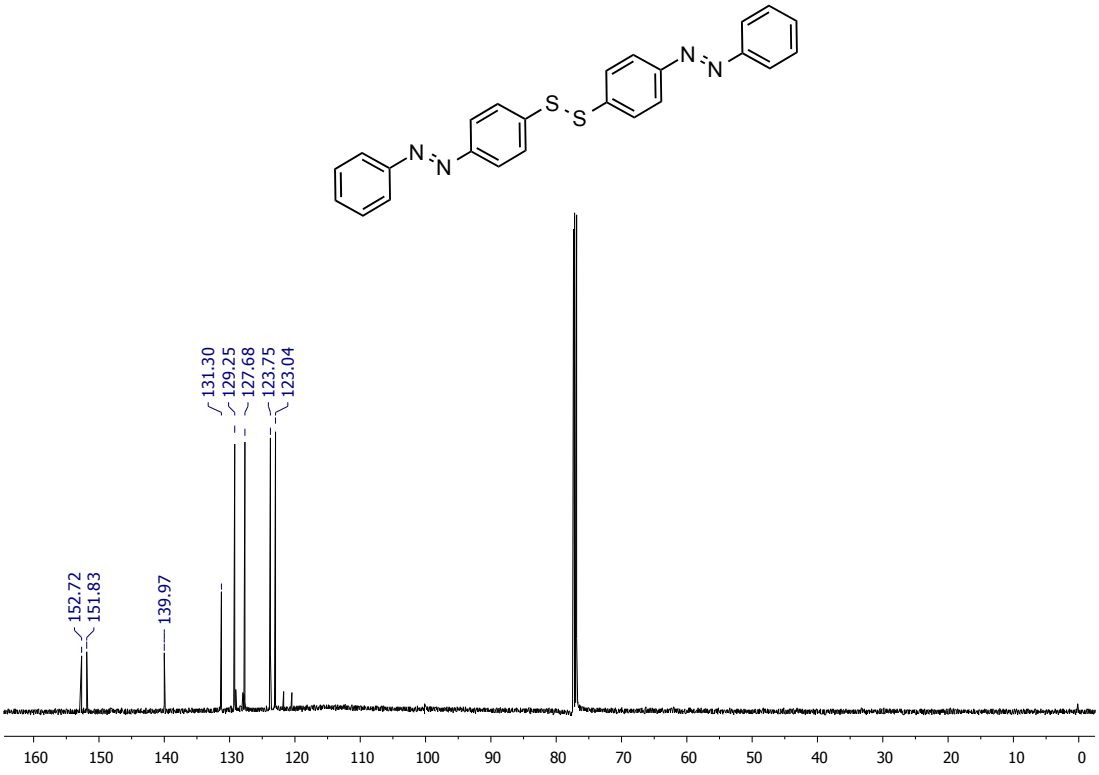

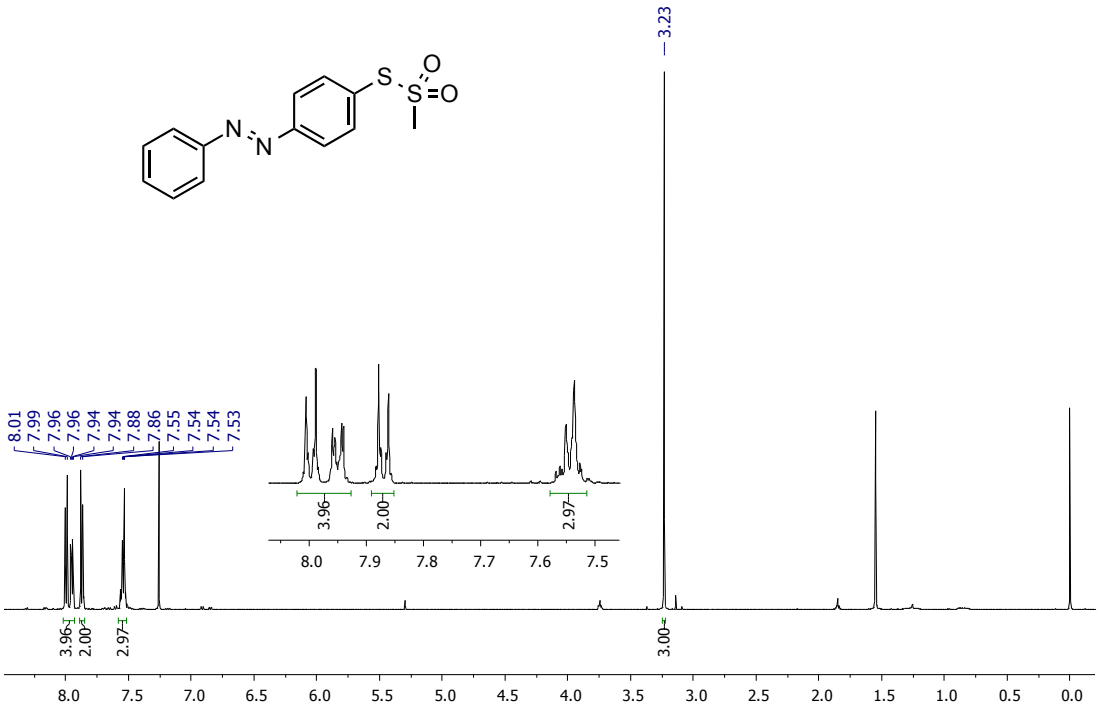

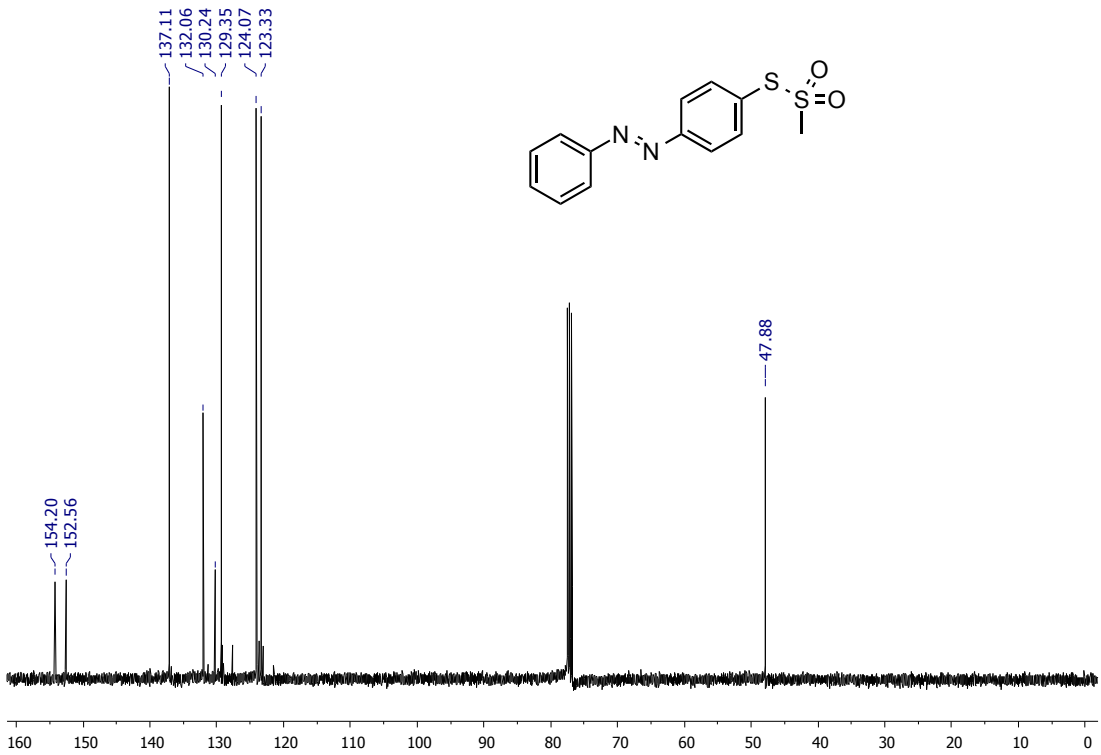

5.4– Solid-phase conjugation of BTL2 variants with photochromic molecules

The immobilized BTL2 variants were reduced by incubation of the solid derivatives with 5 mM DTT and 0.02% Triton X-100 solution at pH 8 and 25 ºC for 45 min. Then, the derivates were exhaustively washed using vacuum filtration in order to remove the DTT excess, and finally equilibrated with 25 mM sodium phosphate pH 8. Later on, the reduced solid preparations were conjugated with photochromic molecules through specific reaction between the unique cysteine residue of BTL2 variants and the reactive groups linked to the photochromic molecules.

5.5– Spectroscopic characterization of photochromic compounds both in solution and in solid state biconjugated to immobilized BTL2

Suspensions of different immobilized BTL2 variants conjugated to different photochromic molecules (**57 or 58**) were prepared in 25 mM sodium phosphate at pH 7. Experiments were carried out in 96-wells microplates at pH 7 and 25 ºC under different light cycles

(UV, visible or darkness) regarding to the photochromic molecule tethered to the BTL2. We measured the spectrum of the different variants under the different light conditions along the time. Similar experiment was carried out with soluble **57** and **58** molecules and their spectrums were monitored as well. The normalized absorbance was calculated as follows:

$$\text{Normalized Absorbance} = (Abs_X - A_{blank})/Abs_{max}$$

Abs_X: Absorbance of the sample under certain illumination conditions

Abs_{blank}: Absorbance of the non conjugated lipase immobilized on agarose beads under certain illumination conditions. In the case of the soluble molecules, this is the absorbance of the media where the measurements were carried out

Abs_{max}: Maximun absorbance measured under either UV or visible illumination conditions. In the case of molecule **57**, the maximum absorbance was determined under 380 nm illumination, while in the case of molecule **58** was under 365 nm.

5.6– Simulations

Four systems were built to simulate the different states of the photochromic groups under the UV (merocyanine and *cis*-azobenzene isomer) and visible (spiropyran and *trans*-azobenzene) light conditions. The wild-type protein (PDB code 2W22, at 2.20 Å resolution) was conjugated to spiropyran and merocyanine photochrome molecules through a I320C mutation. *Cis* and *Trans* azobenzene were manually linked to the protein at the Cys295 residue through a S-S bridge. Hydrogen atoms were added using the standard tools of AMBER[258] and the protein was solvated by a box of water molecules of size 100.2 x 79 x 82.2 $Å^3$.

The protein was modeled with the FF99SB force field.[259] To parametrize the photochromic groups, geometry optimizations and charge calculations at the B3LYP/6-31G* level of theory were performed using the Gaussian09[260] and AmberTools packages. Water

molecules were described with the TIP3P force field.[261] Formal charges of +2 were assigned to calcium and zinc cations.

Molecular dynamics (MD) simulations of the four systems were performed to for the four bioconjugate systems (lipase-merocyanine, lipase-trans-azobenzene and lipase-cis-azobenzene) using NAMD software.[262] The MD simulations were carried out for each system in different steps. First, all water molecules were minimized. Then, the whole system (protein + solvent) were relaxed. To gradually reach the desired temperature of 300 K in the MD simulation, the system was coupled to a thermostatic bath in 130 ps of MD simulation at constant volume and 50 ps more at constant pressure. The MD simulations were extended to ~ 50 ns, until the RMSD remains constant (*Figure S7*).

Docking calculations were perfomed on the equilibrate systems, choosing one representative conformation in the flat RMSD region. All water molecules were excluded. The Autodock 4.2.5.1 software was used with a Lamarckian genetic search algorithm to get different binding conformations of *R* and *S* butyrate isomers. Binding modes were ranked by a scoring function implemented in Autodock with a RMSD tolerance 1 Å, which allows a separation of conformations corresponding to *S* or *R* configurations. A 40 x 40 x 40 Å grid centered on the catalytic residues (Asp 318, His 359 and Ser 114) and the corresponding photochromic groups were used. Gasteiger atom charges were assigned to the protein using AutoDock tools.[263]

SUPPLEMENTARY FIGURES

Figure S1. Localization of the bioconjugation positions into the BTL2 active site. The figures shows the position of the target residues (oranges) where we have tethered different photochromic molecules. The "lid" domain is colored in red and the catalytic serine (S113) in yellow.

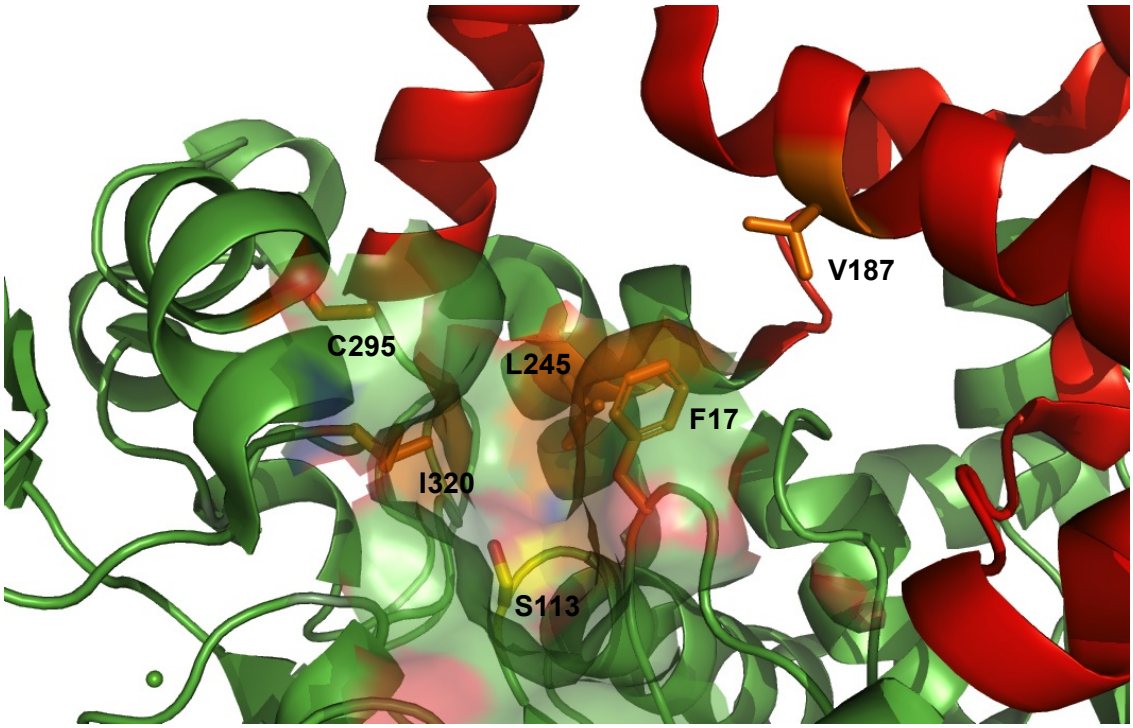

Figure S2. Mass spectroscopic analysis of immobilized BTL2-L245C conjugated with iodoacetate spiropyran. The tryptic peptide containing a cysteine at position 245 was modified with the photochromic molecule, but surprisingly we found both forms spiropyrans (visible form) (A) and merocyanine (UV form) (B). This fact can be explained because the solid bioconjugates were subjected to UV light conditions and stored in darkness at 4 ºC. These suggestions that the relaxation was not completed and thus we found both forms of the photochromic compounds. This insight agrees with the Figure 2. I, where it can be seen how the relaxation in darkness reaches an equilibrium where both photochromic forms are present.

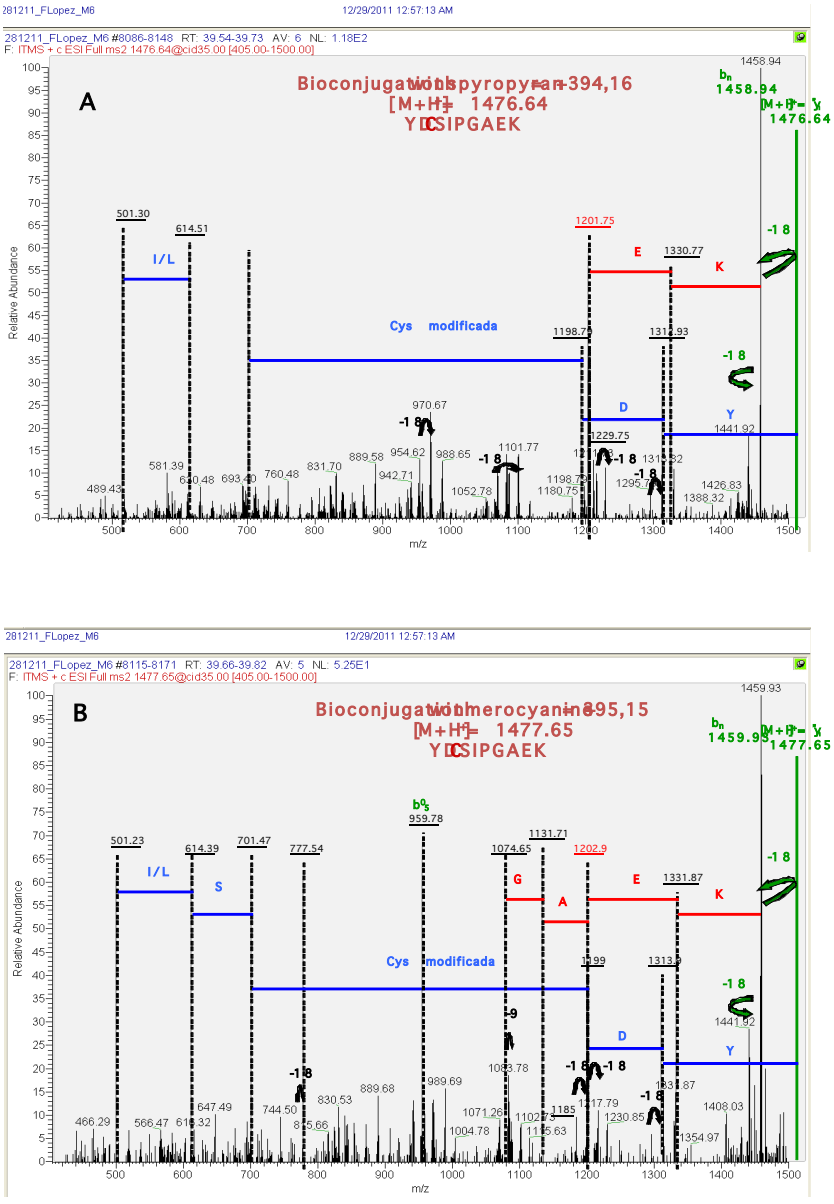

Figure S3. Spectroscopic characterization of soluble spiropyran (A) or azobenzene (B) molecules. 100 μM spiropyran was disolved in 25 mM sodium phosphate and 25% DMSO at pH 7, while 0.1 mM of azobenze was disolved in 25 mM sodium phosphate and 33% acetonitrile at pH 7. Normalized absorbance at 550 and 350 nm was monitored under different illumination conditions along the time (supporting information point 4 describes how to calculate the normalized absorbance from the raw data). The green bars depict the illumination period under visible light, 500 and 460 nm for spiropyran and azobenzene respectively. The violet bars depict UV illumination periods at 380 and 365 nm for spiropyran and azobenzene respectively. The grey bar represents the incubation of spiropyran in darkness.

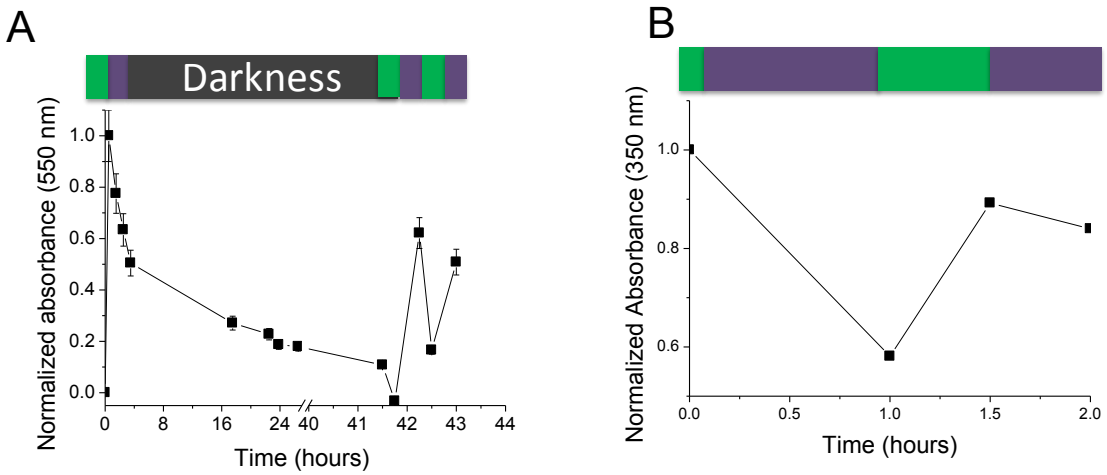

Figure S4. HPLC Chromatograms of enantioselective hydrolysis of rac-59. The peaks represent the different enantiomers of the product: 3-phenyl-2-hydroxy-propionic acid (**61**).

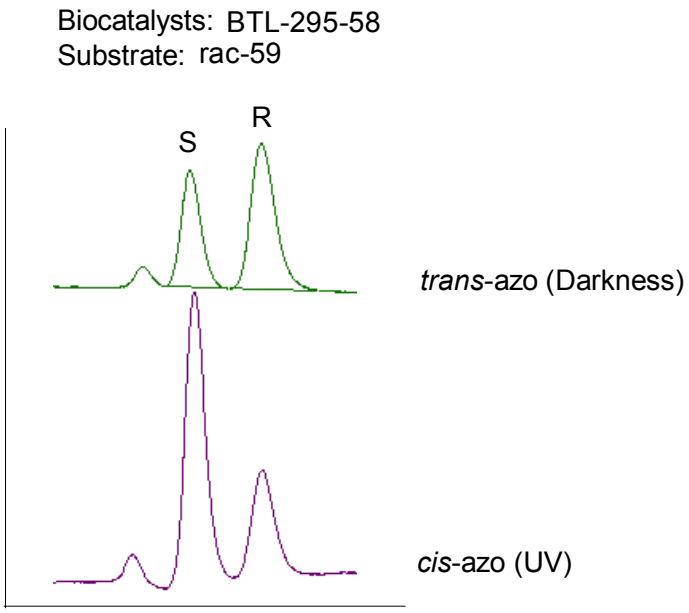

Figure S5. Structural superposition of the lipase-*trans*-azobenzene (green) and lipase-*cis*-azobenzene (violet) bioconjugates. The structures correspond to an average of the last 5 ns of MD simulation. The catalytic residues are shown in orange.

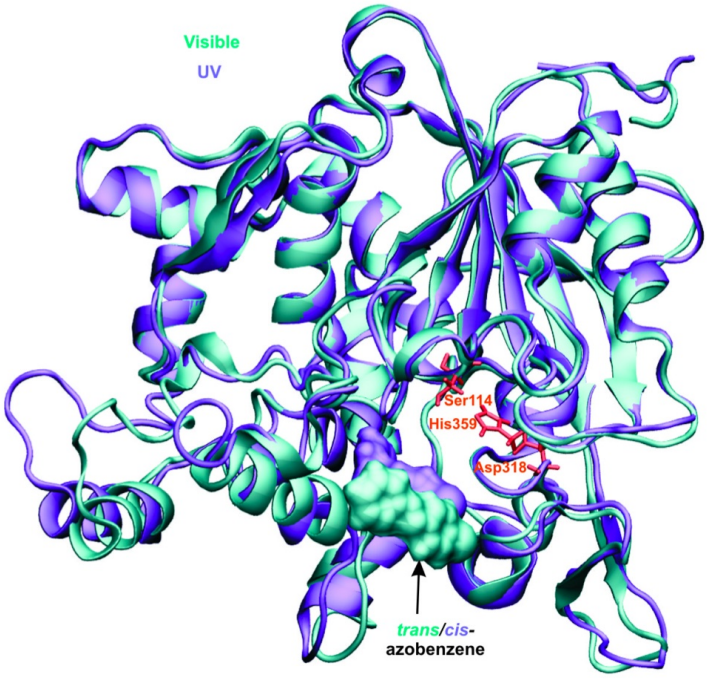

Figure S6. Analogy between the demultiplexer concept and the photochromic lipase. The diagram illustrates that the optical control of enantioselectivity in the hydrolysis of rac-59 using BTL2-P295-58 is analogous to the function of demultiplexer devices in electronic circuits, and constitutes the first demonstration of a protein-based demux. The input signal is given by rac-59, which is converted preferentially to isomer *S* (output 1) under 380nm light, and to isomer *R* (output 2) under 500 nm light.

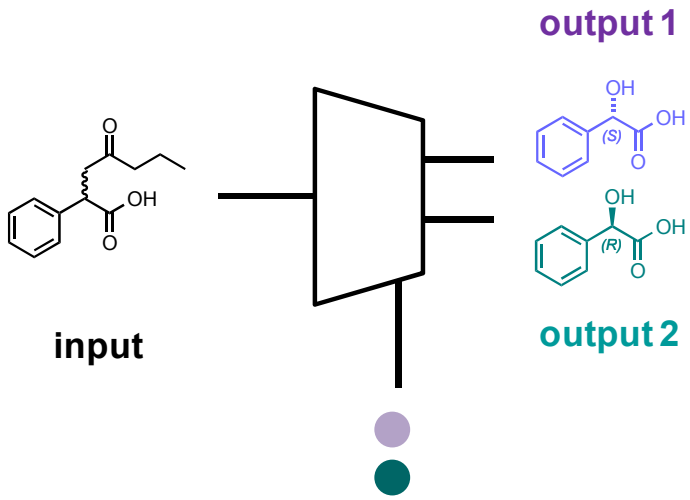

The corresponding truth table of a 1:2 demultiplexer is the following (*see Figure 4. I for the quantification*):

Input	wavelength	output 1	output 2
0	380 nm	0	0
0	500 nm	0	0
1	380 nm	1	0
1	500 nm	0	1

Figure S7. Time variation of the RMSD of backbone atoms of the four bioconjugate systems investigated (lipase-spiropyran (red), lipase-merocyanine (green), lipase-*trans*-azobenzene (pink) and lipase-*cis*-azobenzene (blue)) during the course of MD simulations carried out in explicit water.

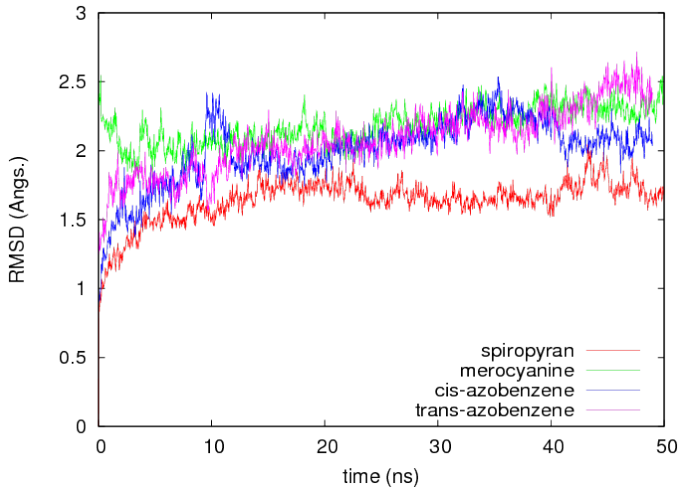

SUPPLEMENTARY TABLES

Table S1. Design of biconjugation positions in the BTL2 primary sequence. Superindex ([1]) indicates that the mutation was created by using the cysteine-less BTL2 double mutant C64S/C295S, and superindex ([2]) indicates that the mutation was created by using the native BTL2 variant.

Bioconjugation position	Mutation	Native residue	Transferred residue
17	17[1]	F	C
187	187[1]	V	C
320	320[1]	I	C
245	245[1]	L	C
295	64[2]	C	S

Table S2. Enantiomeric excess percentages (*ee* %) of different mono-cystein mutants and the wild type variant of BTL2. The hydrolysis reactions were carried out as methods section describes. (*ee* %) values were calculated at reaction yields lower than 25%. (1) WTSC variant is the wild type BTL2 where native cysteine at positions 64 and 295 have been changed by serine residues. (2) All these variants have been constructed from the template WTSC, thus the resulting variant only contains one cysteine at the indicated position. Therefore these variants are triple mutants. (3) This variant has been constructed by using wild type BTL2 as template by only changing the native cysteine at position 65 by a serine. Therefore, the resulting variant will have one of the two native cysteines; the cysteine at position 295

Substrate	**WTSC[1]**	**V187C[2]**	**L245C[2]**	**C64S[3]**	**I320C[2]**
rac-59	40±2 *(R)*	66±1*(R)*	50±8*(R)*	15±4*(R)*	35±9*(R)*
rac-60	84±2 *(R)*	31±2 *(R)*	71±10 *(R)*	Nd	90±16 *(R)*

Table S3. Enantiomeric excess percentages (*ee* %) of different immobilized BTL2 variants conjugated with different photochromic molecules. The hydrolysis reactions were carried out as methods section describes. (*ee* %) values were calculated at reaction yields lower than 25%. For compound 57, the reactions were carried out under 500 nm (Visible) and 380 nm (UV light) as illumination conditions. For compound 58, the reactions were carried out under 460 nm (Visible) and 365 nm (UV light).

Bioconjugate		Substrate			
		rac-59		rac-60	
Position	Photochromic compound	Visible	UV	Visible	UV
P187	57	25±3 (S)	9±3 (S)	67±1 (R)	22±3 (R)
	58	68±7 (R)	67±12 (R)	67±26 (R)	81±26 (R)
P245	57	29±3 (S)	24±3 (S)	80±3 (R)	70±2 (R)
	58	74±1 (R)	77±1 (R)	61±3 (R)	82±4 (R)
P295	58	16±9 (R)	33±14 (S)	nd	nd
P320	57	13±3 (S)	3±1 (R)	46±2 (R)	25±8 (R)
	58	80±2 (R)	71±10 (R)	65±25 (R)	78±20 (R)

Table S4. Results of the docking calculations of (R,S)-2-butyryloxy-2-phenylacetic acid (rac-59) in the active site of the bioconjugates investigated. Only the docking poses corresponding to configurations well oriented for catalysis are considered. For each docking mode, its relative population, the binding energy and the distance between the substrate and the catalytic serine residue (measured from the serine hydroxyl oxygen to the substrate carbonyl carbon atom) is reported.

bioconjugate	**enantiomer**	**conformation**	**population**	**Binding energy (Kcal/mol)**	**distance (Å)**
lipase-spiropyran	R	1	8	-4,04	6,16
	S	1	54	-4,30	6,25
lipase-merocyanine	R	1	58	-5,15	6,05
	S	1	76	-5,23	7,30
lipase-trans-azobenzene	R	1	20	-5,51	4,36
	S	1	14	-5,59	4,49
	S	2	34	-4,93	9,23
lipase-cis-azobenzene	R	1	52	-4,09	9,20
	R	2	33	-4,08	6,77
	S	1	64	-4,47	6,43

GENERAL CONCLUSIONS

- Two approaches were designed and attempted to build photoswitchable tethered ligands (PTL) of endogenous GluK2 receptors. Only arylazide compound **14** based on photoreactive groups was synthesized and *in vitro* tested with Ca^{2+} imaging technique.

- The results revealed that molecule **14** shows an intact glutamate part, displaying reversible binding activity comparable to the one with free glutamate in Ca^{2+} imaging tests. However, **14** failed to photosensitize GluK2 under the tested conditions.

- We re-designed and extended compound **14** to provide photocontrol of endogenous glutamate receptors by direct conjugation by means of a two-component modular strategy to generate *in situ* the complete PTLs.

- To generate directly the PTLs we used a fast adapted version of CuAAC reaction and screened different reactive groups and lenghts in order to optimize the best candidate with no information available about the distance and covalent labeling. Among the library of compounds obtained, **33** and **40** bearing a NHS-ester reactive group showed the largest inward currents in GluK1 receptors (*cis*-active receptor).

- A convergent approach was designed to synthesize benzodiazepine-PCLs bearing an azo group for the photomodulation of GABAA receptors. Two analogues were synthesized (**41** and **43**) from the common precursor **47**. Compound **42** was also attempted but it was isolated as a mixture of **41** (ratio 3:1 respectively, determined by NMR).

- The properties of **41**, **42** and **43** were determined and common isomerization wavelenghts and fast relaxation behaviour under physiological conditions were observed for these compounds. In contrast, their different solubility character depends on the group polarity of the PCL, significant for biological tests.

- We have presented a method to control the catalytic properties of a lipase with light that is based on the site-directed chemical conjugation of photochromic molecules (azobenzene **58** and spiropyran **57**) into the catalytic cavity.

- In particular BTL2–320-**57**, and BTL2–295-**58** derivates show a change in the enantiopreference between UV and visible light for substrates ***rac-59*** and ***rac-60***. However, for BTL2–187-**57**, BTL2–320-**57** they share the same enantiopreference but the enantiomeric excess can be optically modulated

REFERENCES

1. Beharry, A.A. & Woolley, G.A. Azobenzene photoswitches for biomolecules. *Chemical Society Reviews* 40, 4422-4437 (2011).
2. García-Amorós, J. & Velasco, D. Recent advances towards azobenzene-based light-driven real-time information-transmitting materials. *Beilstein Journal of Organic Chemistry* 8, 1003-1017 (2012).
3. Volgraf, M., Banghart, M. & Trauner, D. in Molecular Switches. (ed. B.L.F and W.R. Browne) (Wiley - VHC Verlag GmbH & Co, 2011).
4. Szymanski, W., Beierle, J.M., Kistemaker, H.A.V., Velema, W.A. & Feringa, B.L. Reversible photocontrol of biological systems by the incorporation of molecular photoswitches. *Chemical Reviews* 113, 6114-6178 (2013).
5. Irie, M. Diarylethenes for memories and switches. *Chemical Reviews* 100, 1685-1716 (2000).
6. Asano, T. & Okada, T. Further kinetic evidence for the competitive rotational and inversional Z-E isomerization of substituted azobenzenes. *The Journal of Organic Chemistry* 51, 4454-4458 (1986).
7. Schanze, K.S., Mattox, T.F. & Whitten, D.G. Solvent effects on the thermal cis-trans isomerization and charge-transfer absorption of 4-(diethylamino)-4'-nitroazobenzene. *The Journal of Organic Chemistry* 48, 2808-2813 (1983).
8. Willner, I., Lion-Dagan, M., Marx-Tibbon, S. & Katz, E. Bioelectrocatalyzed amperometric transduction of recorded optical signals using monolayer-modified Au electrodes. *Journal of the American Chemical Society* 117, 6581-6592 (1995).
9. Karube, I., Nakamoto, Y., Namba, K. & Suzuki, S. Photocontrol of urease-collagen membrane activity. *Biochim Biophys Acta* 429, 975-981 (1976).
10. Aizawa, M., Namba, K. & Suzuki, S. Light-induced enzyme activity changes associated with the photoisomerization of bound spiropyran. *Archives of Biochemistry and Biophysics* 182, 305-310 (1977).
11. Nakamoto, Y., Karube, I. & Suzuki, S. *J. Ferment. Technol.* 53, 595 (1975).
12. Griffiths, J. II. Photochemistry of azobenzene and its derivatives. *Chemical Society Reviews* 1, 481-493 (1972).

13. Merino, E. Synthesis of azobenzenes: the coloured pieces of molecular materials. *Chemical Society Reviews* 40, 3835-3853 (2011).
14. Spörlein, S. et al. Ultrafast spectroscopy reveals subnanosecond peptide conformational dynamics and validates molecular dynamics simulation. *Proceedings of the National Academy of Sciences* 99, 7998-8002 (2002).
15. Ihalainen, J.A. et al. Folding and unfolding of a photoswitchable peptide from picoseconds to microseconds. *Proceedings of the National Academy of Sciences* 104, 5383-5388 (2007).
16. Murakami, H., Kawabuchi, A., Kotoo, K., Kunitake, M. & Nakashima, N. A Light-driven molecular shuttle based on a rotaxane. *Journal of the American Chemical Society* 119, 7605-7606 (1997).
17. Cooper, A. Biophysical Chemistry. (Royal Society of Chemistry, 2004).
18. Rau, H. Photoisomerization of azobenzenes. *Photochemistry and Photophysics* 2, 119 - 143 (1990).
19. Tiberio, G., Muccioli, L., Berardi, R. & Zannoni, C. How does the trans-cis photoisomerization of azobenzene take place in organic solvents *ChemPhysChem* 11, 1018-1028 (2010).
20. Dokic, J. et al. Quantum chemical investigation of thermal cis-to-trans isomerization of azobenzene derivatives: substituent effects, solvent effects, and comparison to experimental data. *The Journal of Physical Chemistry A* 113, 6763-6773 (2009).
21. Gabor, G. & Fischer, E. Spectra and cis-trans isomerism in highly dipolar derivatives of azobenzene. *The Journal of Physical Chemistry* 75, 581-583 (1971).
22. Brode, W.R., Gould, J.H. & Wyman, G.M. The relation between the absorption spectra and the chemical constitution of dyes. XXVI. Effect of solvent and of temperature on the cis-trans isomerization of azo dyes. *Journal of the American Chemical Society* 75, 1856-1859 (1953).
23. Brode, W.R., Gould, J.H. & Wyman, G.M. The Relation between the Absorption Spectra and the Chemical Constitution of Dyes. XXV. Phototropism and cis-trans Isomerism in Aromatic Azo Compounds. *Journal of the American Chemical Society* 74, 4641-4646 (1952).
24. Samanta, S., McCormick, T.M., Schmidt, S.K., Seferos, D.S. & Woolley, G.A. Robust visible light photoswitching with ortho-thiol substituted azobenzenes. *Chemical Communications* 49, 10314-10316 (2013).

25. Wyart, C. et al. Optogenetic dissection of a behavioural module in the vertebrate spinal cord. *Nature* 461, 407-410 (2009).
26. Caporale, N. et al. LiGluR restores visual responses in rodent models of inherited blindness. *Mol Ther* 19, 1212-1219 (2011).
27. Levitz, J. et al. Optical control of metabotropic glutamate receptors. *Nat Neurosci* 16, 507-516 (2013).
28. Tye, K.M. & Deisseroth, K. Optogenetic investigation of neural circuits underlying brain disease in animal models. *Nat. Rev. Neurosci*. 304, 435-438 (2012).
29. Schoenberger, M., Damijonaitis, A., Zhang, Z., Nagel, D. & Trauner, D. Development of a new photochromic ion channel blocker via azologization of fomocaine. *ACS Chemical Neuroscience* 5, 514-518 (2014).
30. Ellis-Davies, G.C.R. Caged compounds: photorelease technology for control of cellular chemistry and physiology. *Nat Meth* 4, 619-628 (2007).
31. Pittolo, S. et al. An allosteric modulator to control endogenous G protein-coupled receptors with light. *Nat Chem Biol* 10, 813-815 (2014).
32. Fenno, L., Yizhar, O. & Deisseroth, K. The development and application of optogenetics. *Annual Review of Neuroscience* 34, 389-412 (2011).
33. Gorostiza, P. et al. Mechanisms of photoswitch conjugation and light activation of an ionotropic glutamate receptor. *Proceedings of the National Academy of Sciences* 104, 10865-10870 (2007).
34. Harvey, J.H. & Trauner, D. Regulating enzymatic activity with a photoswitchable affinity label. *ChemBioChem* 9, 191-193 (2008).
35. Bautista-Barrufet, A., Izquierdo-Serra, M. & Gorostiza, P. in Novel Approaches for Single Molecule Activation and Detection. (eds. F. Benfenati, E. Di Fabrizio & V. Torre) 169-188 (Springer Berlin Heidelberg, 2014).
36. Alivisatos, A.P. et al. The brain activity map. *Science* 339, 1284-1285 (2013).
37. Gorostiza, P. & Isacoff, E.Y. Optical switches for remote and non-invasive control of cell signaling. *Science* 322, 395-399 (2008).
38. Kramer, R.H., Mourot, A. & Adesnik, H. Optogenetic pharmacology for control of native neuronal signaling proteins. *Nat Neurosci* 16, 816-823 (2013).
39. Gorostiza, P. & Isacoff, E. Optical switches and triggers for the manipulation of ion channels and pores. *Molecular BioSystems* 3, 686-704 (2007).
40. Gorostiza, P. & Isacoff, E.Y. Nanoengineering ion channels for optical control. *Physiology* 23, 238-247 (2008).

41. Szobota, S. & Isacoff, E.Y. Optical control of neuronal activity. *Annu. Rev. Biophys*. 39, 329-348 (2010).
42. Szobota, S., McKenzie, C. & Janovjak, H. Optical control of ligand-gated ion channels. *Methods Mol. Biol*. 998, 417-435 (2013).
43. Mourot, A., Fehrentz, T. & Kramer, R. in Chemical Neurobiology, Vol. 995. (ed. M.R. Banghart) 89-105 (Humana Press, 2013).
44. Connolly, C.N. & Wafford, K.A. The Cys-loop superfamily of ligand-gated ion channels: the impact of receptor structure on function. *Biochem Soc Trans* 32, 529-534 (2004).
45. Ortells, M.O. & Lunt, G.G. Evolutionary history of the ligand-gated ion-channel superfamily of receptors. *Trends Neurosci*. 18, 121-127 (1995).
46. Hilf, R.J.C. & Dutzler, R. A prokaryotic perspective on pentameric ligand-gated ion channel structure. *Current Opinion in Structural Biology* 19, 418-424 (2009).
47. Brejc, K. et al. Crystal structure of an ACh-binding protein reveals the ligand-binding domain of nicotinic receptors. *Nature* 411, 269-276 (2001).
48. Changeux, J.P. & Edelstein, S.J. Allosteric receptors after 30 years. *Neuron* 21, 959-980 (1998).
49. Yip, G.M.S. et al. A propofol binding site on mammalian GABA(A) receptors identified by photolabeling. *Nat Chem Biol* 9, 715-720 (2013).
50. Hille, B. Ion channels of excitable membranes, Vol. 507. (Sinauer Sunderland, MA, 2001).
51. Bartels, E., Wassermann, N.H. & Erlanger, B.F. Photochromic activators of the acetylcholine receptor. *Proc Natl Acad Sci USA* 68, 1820-1823 (1971).
52. Silman, I. & Karlin, A. Acetylcholine receptor: covalent attachment of depolarizing groups at the active site. *Science* 164, 1420-1421 (1969).
53. Lester, H.A. & Chang, H.W. Response of acetylcholine receptors to rapid photochemically produced increases in agonist concentration. *Nature* 266, 373-374 (1977).
54. Chabala, L.D. & Lester, H.A. Activation of acetylcholine receptor channels by covalently bound agonists in cultured rat myoballs. *J Physiol* 379, 83-108 (1986).
55. Tochitsky, I. et al. Optochemical control of genetically engineered neuronal nicotinic acetylcholine receptors. *Nat Chem* 4, 105-111 (2012).
56. Gereau, R.W. & Swanson, G.T. The Glutamate Receptors. (Humana Press Inc., 2008).

57. Traynelis, S.F. et al. Glutamate receptor ion channels: structure, regulation, and function. *Pharmacol. Rev.* 62, 405-496 (2010).

58. Felder, C., Graul, R., Lee, A., Merkle, H.-P. & Sadee, W. The venus flytrap of periplasmic binding proteins: An ancient protein module present in multiple drug receptors. *AAPS PharmSci* 1, 7-26 (1999).

59. Sobolevsky, A.I., Rosconi, M.P. & Gouaux, E. X-ray structure, symmetry and mechanism of an AMPA-subtype glutamate receptor. *Nature* 462, 745-756 (2009).

60. Doumazane, E. et al. Illuminating the activation mechanisms and allosteric properties of metabotropic glutamate receptors. *Proceedings of the National Academy of Sciences* 110, 1416-1425 (2013).

61. Volgraf, M. et al. Allosteric control of an ionotropic glutamate receptor with an optical switch. *Nat Chem Biol* 2, 47-52 (2006).

62. Kienzler, M.A. et al. A red-shifted, fast-relaxing azobenzene photoswitch for visible light control of an ionotropic glutamate receptor. *J Am Chem Soc* 135, 17683-17686 (2013).

63. Volgraf, M. et al. Reversibly caged glutamate: a photochromic agonist of ionotropic glutamate receptors. *J Am Chem Soc* 129, 260-261 (2007).

64. Numano, R. et al. Nanosculpting reversed wavelength sensitivity into a photoswitchable iGluR. *Proc Natl Acad Sci USA* 106, 6814-6819 (2009).

65. Reiter, A., Skerra, A., Trauner, D. & Schiefner, A. A photoswitchable neurotransmitter analogue bound to its receptor. *Biochemisty* 52, 8972-8974 (2013).

66. Stawski, P., Sumser M Fau - Trauner, D. & Trauner, D. A photochromic agonist of AMPA receptors. *Angew Chem Int Ed Engl* 51, 5748-5751 (2012).

67. Janovjak, H., Szobota, S., Wyart, C., Trauner, D. & Isacoff, E.Y. A light-gated, potassium-selective glutamate receptor for the optical inhibition of neuronal firing. *Nat Neurosci* 13, 1027-1032 (2010).

68. Szobota, S. et al. Remote Control of Neuronal Activity with a Light-Gated Glutamate Receptor. *Neuron* 54, 535-545 (2007).

69. Li, D., Hérault, K., Isacoff, E.Y., Oheim, M. & Ropert, N. Optogenetic activation of LiGluR-expressing astrocytes evokes anion channel-mediated glutamate release. *The Journal of Physiology* 590, 855-873 (2012).

70. Izquierdo-Serra, M., Trauner, D., Llobet, A. & Gorostiza, P. Optical control of calcium-regulated exocytosis. *Biochimica et Biophysica Acta (BBA) - General Subjects* 1830, 2853-2860 (2013).
71. Izquierdo-Serra, M., Trauner, D., Llobet, A. & Gorostiza, P. Optical modulation of neurotransmission using calcium photocurrents through the ion channel LiGluR. *Frontiers in Molecular Neuroscience* 6 (2013).
72. Abrams, Z.e.R., Warrier, A., Wang, Y., Trauner, D. & Zhang, X. Tunable oscillations in the Purkinje neuron. *Physical Review E* 85, 041905 (2012).
73. Kawate, T., Michel, J.C., Birdsong, W.T. & Gouaux, E. Crystal structure of the ATP-gated P2X4 ion channel in the closed state. *Nature* 460, 592-598 (2009).
74. Conley, E.C. & Brammar, W.J. Ion Channel Factsbook: Extracellular Ligand-Gated Channels. (Acad. Press, 1996).
75. Valera, S. et al. A new class of ligand-gated ion channel defined by P2X receptor for extracellular ATP. *Nature* 371, 516-519 (1994).
76. Zemelman, B.V., Nesnas, N., Lee, G.A. & Miesenbock, G. Photochemical gating of heterologous ion channels: remote control over genetically designated populations of neurons. *Proc Natl Acad Sci USA* 100 (2003).
77. Lima, S.Q. & Miesenböck, G. Remote control of behavior through genetically targeted photostimulation of Neurons. *Cell* 121, 141-152 (2005).
78. Zemelman, B.V., Lee, G.A., Ng, M. & Miesenbock, G. Selective photostimulation of genetically charged neurons. *Neuron* 33, 15-22 (2002).
79. Browne, L.E. et al. Optical control of trimeric P2X receptors and acid-sensing ion channels. *Proc Natl Acad Sci USA* 111, 521-526 (2014).
80. Lemoine, D. et al. Optical control of an ion channel gate. *Proc Natl Acad Sci USA* 110, 20813-20818 (2013).
81. Banghart, M., Borges, K., Isacoff, E., Trauner, D. & Kramer, R.H. Light-activated ion channels for remote control of neuronal firing. *Nat Neurosci* 7, 1381-1386 (2004).
82. Chambers, J.J., Banghart, M.R., Trauner, D. & Kramer, R.H. Light-induced depolarization of neurons using a modified shaker K^+ Channel and a Molecular Photoswitch. *Journal of Neurophysiology* 96, 2792-2796 (2006).
83. Fortin, D.L. et al. Optogenetic photochemical control of designer K^+ channels in mammalian neurons. *Journal of Neurophysiology* 106, 488-496 (2011).

84. Fortin, D.L. et al. Photochemical control of endogenous ion channels and cellular excitability. *Nat Meth* 5, 331-338 (2008).

85. Banghart, M.R. et al. Photochromic blockers of voltage-gated potassium channels. *Angew Chem Int Ed Engl* 48, 9097-9101 (2009).

86. Mourot, A., Fehrentz, T., Le Feuvre, Y., Smith, C. M., Herold, C., Dalkara, D., Nagy, F., Trauner, D., Kramer, R. H., Rapid optical control of nociception with an ion-channel photoswitch *Nat Meth* 9, 396-402 (2012).

87. Mourot, A. et al. Tuning photochromic ion channel blockers. *ACS Chem Neurosci* 2, 536-543 (2011).

88. Fehrentz, T. et al. Exploring the pharmacology and action spectra of photochromic open-channel blockers. *Chem Bio Chem* 13, 1746-1749 (2012).

89. Polosukhina, A. et al. Photochemical restoration of visual responses in blind mice. *Neuron* 75, 271-282 (2012).

90. Sandoz, G., Levitz, J., Kramer, R.H. & Isacoff, E.Y. Optical control of endogenous proteins with a photoswitchable conditional subunit reveals a role for TREK1 in GABA(B) signaling. *Neuron* 74, 1005-1014 (2012).

91. Venkatachalam, K. & Montell, C. TRP channels. *Annu. Rev. Biochem.* 76, 387-417 (2007).

92. Stein, M., Fehrentz, T., Gudermann, T. & Trauner, D. Optical control of TRPV1 channels. *Angew Chem Int Ed Engl* 52, 9845-9848 (2013).

93. Papagiakoumou, E., Begue, A., Leshem, B., Schwartz, O., Stell, B. M., Bradley, J., Oron, D., Emiliani, V., Functional patterned multiphoton excitation deep inside scattering tissue. *Nat Photon* 7, 274-278 (2013).

94. Denk, W., Strickler, J. & Webb, W. Two-photon laser scanning fluorescence microscopy. *Science* 248, 73-76 (1990).

95. Oron, D., Papagiakoumou, E., Anselmi, F. & Emiliani, V. Two-photon optogenetics. *Prog. Bain Res.* 196, 119-143 (2012).

96. Watson, B.O., Nikolenko, V. & Yuste, R. Two-photon imaging with diffractive optical elements. *Front. Neural Circuits* 3, 6 (2009).

97. Nagel, G. et al. Channelrhodopsin-2, a directly light-gated cation-selective membrane channel. *Proceedings of the National Academy of Sciences* 100, 13940-13945 (2003).

98. Nagel, G. et al. Channelrhodopsins: directly light-gated cation channels. *Biochem Soc Trans* 33, 863-866 (2005).

99. Lanyi, J.K. Halorhodopsin: a light-driven chloride ion pump. *Annu Rev Biophys Biophys Chem* 15, 11-28 (1986).

100. Schobert, B. & Lanyi, J.K. Halorhodopsin is a light-driven chloride pump. *J Biol Chem* 257, 10306-10313 (1982).

101. Bi, A. et al. Ectopic expression of a microbial-type rhodopsin restores visual responses in mice with photoreceptor degeneration. *Neuron* 50, 23-33 (2006).

102. Han, X. & Boyden, E.S. Multiple-color optical activation, silencing, and desynchronization of neural activity, with single-spike temporal resolution. *PLoS One* 2, 299 (2007).

103. Zhang, F. et al. Multimodal fast optical interrogation of neural circuitry. *Nature* 446, 633-639 (2007).

104. Arenkiel, B.R. et al. In vivo light-induced activation of neural circuitry in transgenic mice expressing channelrhodopsin-2. *Neuron* 54, 205-218 (2007).

105. Petreanu, L., Huber, D., Sobczyk, A. & Svoboda, K. Channelrhodopsin-2-assisted circuit mapping of long-range callosal projections. *Nat Neurosci* 10, 663-668 (2007).

106. Deisseroth, K. et al. Next-generation optical technologies for illuminating genetically targeted brain circuits. *J Neurosci* 26, 10380-10386 (2006).

107. Nagel, G. et al. Light activation of channelrhodopsin-2 in excitable cells of Caenorhabditis elegans triggers rapid behavioral responses. *Curr Biol* 15, 2279-2284 (2005).

108. Schroll, C. et al. Light-induced activation of distinct modulatory neurons triggers appetitive or aversive learning in Drosophila larvae. *Curr Biol* 16, 1741-1747 (2006).

109. Karlin, A., Prives, J., Deal, W. & Winnik, M. Affinity labeling of the acetylcholine receptor in the electroplax. *J Mol Biol* 61, 175-188 (1971).

110. Karlin, A. & Winnik, M. Reduction and specific alkylation of the receptor for acetylcholine. *Proc Natl Acad Sci U S A* 60, 668-674 (1968).

111. Armstrong, N. & Gouaux, E. Mechanisms for Activation and Antagonism of an AMPA-Sensitive Glutamate Receptor: Crystal Structures of the GluR2 Ligand Binding Core. *Neuron* 28, 165-181 (2000).

112. Mayer, M.L. Crystal Structures of the GluR5 and GluR6 Ligand Binding Cores: Molecular Mechanisms Underlying Kainate Receptor Selectivity. *Neuron* 45, 539-552 (2005).

113. Pedregal, C. et al. 4-Alkyl- and 4-cinnamylglutamic acid analogues are potent GluR5 kainate receptor agonists. *J Med Chem* 43, 1958-1968 (2000).
114. Knowles, J.R. Photogenerated reagents for biological receptor-site labeling. *Accounts of Chemical Research* 5, 155-160 (1972).
115. Brunner, J. Photochemical labeling of apolar phase of membranes. *Methods Enzymol* 172, 628-687 (1989).
116. Brunner, J. New photolabeling and crosslinking methods. *Annu Rev Biochem* 62, 483-514 (1993).
117. Kotzyba-Hibert, F., Kapfer, I. & Goeldner, M. Recent trends in photoaffinity labeling. *Angewandte Chemie International Edition* 34, 1296-1312 (1995).
118. Dorman, G. & Prestwich, G.D. Using photolabile ligands in drug discovery and development. *Trends in Biotechnology* 18, 64-77 (2000).
119. Knoll, F., Kolter, T. & Sandhoff, K. in Methods in Enzymology, Vol. Volume 311. (ed. J.Y.A.H. Alfred H. Merrill) 568-600 (Academic Press, 2000).
120. Singh, A., Thornton, E.R. & Westheimer, F.H. The photolysis of diazoacetylchymotrypsin. *J Biol Chem* 237, 3006-3008 (1962).
121. Vodovozova, E.L. Photoaffinity labeling and its application in structural biology. *Biochemistry (Mosc)* 72, 1-20 (2007).
122. Dorman, G. & Prestwich, G.D. Benzophenone photophores in biochemistry. *Biochemistry* 33, 5661-5673 (1994).
123. Hegarty, F.A. The Chemistry of Diazonium and Diazo Groups, Vol. Part 2. (Wiley, New York; 1978).
124. Angeli & Valori *Atti accad. Lincei* 22 (1913).
125. Entwistle, I.D., Gilkerson, T., Johnstone, R.A.W. & Telford, R.P. Rapid catalytic transfer reduction of aromatic nitro compounds to hydroxylamines. *Tetrahedron* 34, 213-215 (1978).
126. Muathen, I.A. *Indian J. Chem. Sect. B* 30, 522 (1991).
127. Makaryan, I.A., Savchenko, V.I. & Brikenshtein, K.A. *Bull. Acad. Sci. USSR Div. Chem. Sci. (Engl. Transl.)* 32, 692 (1983).
128. Fitzgerald, T.J., Doull, J. & DeFeo, F.G. Radioprotective activity of p-aminopropiophenone. Structure-activity investigation. *Journal of Medicinal Chemistry* 17, 900-902 (1974).
129. Wood, W.W. & Wilkin, J.A. A convenient synthesis of aryl nitroso compounds. *Synthetic Communications* 22, 1683-1686 (1992).

130. Caro, H. *Angew Chem* 11, 845 (1898).
131. Gowenlock, B.G. & Richter-Addo, G.B. Preparations of C-nitroso compounds. *Chemical Reviews* 104, 3315-3340 (2004).
132. Zhu, Z. & Espenson, J.H. Kinetics and mechanism of oxidation of anilines by hydrogen peroxide as catalyzed by methylrhenium trioxide. *The Journal of Organic Chemistry* 60, 1326-1332 (1995).
133. Sakaue, S., Sakata, Y., Nishiyama, Y. & Yshi, Y. *Chem. Lett.*, 289 (1992).
134. Defoin, A. Simple preparation of nitroso benzenes and nitro benzenes by oxidation of anilines with H_2O_2 catalysed with molybdenum salts. *Synthesis* 2004, 706-710 (2004).
135. Priewisch, B. & Ruck-Braun, K. Efficient preparation of nitrosoarenes for the synthesis of azobenzenes. *J Org Chem* 70, 2350-2352 (2005).
136. Zhu, W. & Ma, D. Synthesis of aryl azides and vinyl azides via proline-promoted Cu-(I)-catalyzed coupling reactions. *Chemical Communications*, 888-889 (2004).
137. Köhler, M., Burnashev, N., Sakmann, B. & Seeburg, P.H. Determinants of Ca^{2+} permeability in both TM1 and TM2 of high affinity kainate receptor channels: Diversity by RNA editing. *Neuron* 10, 491-500.
138. Grynkiewicz, G., Ponie, M. & Tsien, R.Y. A new generation of Ca^{2+} indicators with greatly improved fluorescense properties. *J Biol Chem* 260, 3440-3450 (1985).
139. Tsukiji, S., Miyagawa, M., Takaoka, Y., Tamura, T. & Hamachi, I. Ligand-directed tosyl chemistry for protein labeling in vivo. *Nat Chem Biol* 5, 341-343 (2009).
140. Wilding, T.J. & Huettner, J.E. Activation and desensitization of hippocampal kainate receptors. *The Journal of Neuroscience* 17, 2713-2721 (1997).
141. Partin, K.M., Patneau, D.K., Winters, C.A., Mayer, M.L. & Buonanno, A. Selective modulation of desensitization at AMPA versus kainate receptors by cyclothiazide and concanavalin A. *Neuron* 11, 1069-1082.
142. Flynn, D.L., Zelle, R.E. & Grieco, P.A. A mild two-step method for the hydrolysis of lactams and secondary amides. *The Journal of Organic Chemistry* 48, 2424-2426 (1983).
143. Ezquerra, J.S. et al. Stereoselective reactions of lithium enolates derived from N-BOC protected pyroglutamic esters. *Tetrahedron* 49, 8665-8678 (1993).
144. Yue, L. et al. Robust photoregulation of GABA(A) receptors by allosteric modulation with a propofol analogue. *Nat Commun* 3, 1095 (2012).

145. Jung, N. & Bräse, S. in Kirk-Othmer Encyclopedia of Chemical Technology (John Wiley & Sons, Inc., 2000).
146. Shao, C. et al. Copper (I) oxide and benzoic acid in water: a highly practical and efficient catalytic system for copper(I)-catalyzed azide-alkyne cycloaddition. *Tetrahedron Letters* 52, 3782-3785 (2011).
147. Norman, N. & Mathisen, H. The crystal structure of lower n-paraffins. II. n-hexane. *Acta Chem. Scand.* 15, 1755-1760 (1961).
148. Neher, E., Sakmann, B. & Steinbach, J.H. The extracellular patch clamp: a method for resolving currents through individual open channels in biological membranes. *Pflugers Arch.* 375, 218-228 (1978).
149. Izquierdo-Serra, M. in Nanoprobes & Nanoswitches. Photoswitchable glutamate receptors to control neurotransmission with light. (University of Barcelona (UB), 2014).
150. Ren, Z. et al. Cell Surface Expression of GluR5 Kainate receptors is regulated by an endoplasmic reticulum retention signal. *Journal of Biological Chemistry* 278, 52700-52709 (2003).
151. Chow, B.Y. et al. High-performance genetically targetable optical neural silencing by light-driven proton pumps. *Nature* 463, 98-102 (2010).
152. Kasparov, S. & Herlitze, S. Optogenetics at a crossroads? *Experimental Physiology* 98, 971-972 (2013).
153. Raster, P. et al. New GABA amides activating GABA(A) receptors. *Beilstein J Org Chem* 9, 406-410 (2013).
154. Lin, W.C. et al. Engineering a Light-Regulated GABA Receptor for Optical Control of Neural Inhibition. *ACS Chem Biol* (2014).
155. Stein, M. et al. Azo-propofols: photochromic potentiators of GABA(A) receptors. *Angew Chem Int Ed Engl* 51, 10500-10504 (2012).
156. Rudolph, U. & Knoflach, F. Beyond classical benzodiazepines: novel therapeutic potential of GABA(A) receptor subtypes. *Nat Rev Drug Discov* 10, 685-697 (2011).
157. Jones-Davis, D.M. & Macdonald, R.L. GABA(A) receptor function and pharmacology in epilepsy and status epilepticus. *Curr Opin Pharmacol* 3, 12-18 (2003).
158. Mohler, H. GABA(A) receptor diversity and pharmacology. *Cell Tissue Res* 326, 505-516 (2006).

159. Korpi, E.R., Grunder, G. & Luddens, H. Drug interactions at GABA(A) receptors. *Prog Neurobiol* 67, 113-159 (2002).

160. Hadjipavlou-Litina, D. & Hansch, C. Quantitative Structure-activity relationships of the benzodiazepines. A review and reevaluation. *Chemical Reviews* 94, 1483-1505 (1994).

161. Fehrentz, T., Schönberger, M. & Trauner, D. Optochemical Genetics. *Angewandte Chemie International Edition* 50, 12156-12182 (2011).

162. Raster, P. in Organische Chemie, Vol. PhD (Regensburg Universität, 2014).

163. Roth, H.J. & Adomeit, M. Photochemistry of nitrazepam. *Arch Pharm (Weinheim)* 306, 889-897 (1973).

164. Menezes, C.M. et al. Synthesis, biological evaluation, and structure-activity relationship of clonazepam, meclonazepam, and 1,4-benzodiazepine compounds with schistosomicidal activity. *Chem Biol Drug Des* 79, 943-949 (2012).

165. Mahajan, A., Kumar, V., Mansour, N.R., Bickle, Q. & Chibale, K. Meclonazepam analogues as potential new antihelmintic agents. *Bioorg Med Chem Lett* 18, 2333-2336 (2008).

166. Roets, E. & Hoogmartens, J. Thin-layer chromatography of the acid hydrolysis products of nineteen benzodiazepine derivatives. *Journal of Chromatography A* 194, 262-269 (1980).

167. Seno, H., Suzuki, O., Kumazawa, T. & Hattori, H. Rapid isolation with Sep-Pak C18 cartridges and wide-bore capillary gas chromatography of benzophenones, the acid-hydrolysis products of benzodiazepines. *J Anal Toxicol* 15, 21-24 (1991).

168. Giera, H., Lange, W., Meiers, M. & Pires, R. in Eur. Pat. Appl. (ed. E. A1) 2001).

169. Karramkam, M., Hinnen, F., Vaufrey, F. & Dollé, F. 2-, 3- and 4-[18F] Fluoropyridine by no-carrier-added nucleophilic aromatic substitution with K[18F]F-K222 – a comparative study. *Journal of Labelled Compounds and Radiopharmaceuticals* 46, 979-992 (2003).

170. Murashima, K. et al. Preparations, crystal structures, and magnetic properties of *N,N*-dipyridylaminoxyl as a new magnetic coupler and its one-dimensional cobalt (II) chains. *Inorganic Chemistry* 51, 4982-4993 (2012).

171. Sell, H., Näther, C. & Herges, R. Amino-substituted diazocines as pincer-type photochromic switches. *Beilstein Journal of Organic Chemistry* 9, 1-7 (2013).

172. Kumar, M. et al. Catalyst-free water mediated reduction of nitroarenes using glucose as a hydrogen source. *RSC Advances* 3, 4894-4898 (2013).

173. Sigel, E. Properties of single sodium channels translated by Xenopus oocytes after injection with messenger ribonucleic acid. *The Journal of Physiology* 386, 73-90 (1987).

174. McNaught, A.D. & Wilkinson, A. IUPAC. The Gold Book. Compendium of Chemical Terminology. (1997).

175. Bairoch, A. The ENZYME database in 2000. *Nucleic Acids Research* 28, 304-305 (2000).

176. Chiche, J. et al. Hypoxia-inducible carbonic anhydrase IX and XII promote tumor cell growth by counteracting acidosis through the regulation of the intracellular pH. *Cancer Research* 69, 358-368 (2009).

177. Supuran, C.T., Scozzafava, A. & Casini, A. Carbonic anhydrase inhibitors. *Medicinal Research Reviews* 23, 146-189 (2003).

178. Supuran, C.T. & Scozzafava, A. Carbonic anhydrases as targets for medicinal chemistry. *Bioorganic & Medicinal Chemistry* 15, 4336-4350 (2007).

179. Innocenti, A. et al. Investigations of the esterase, phosphatase, and sulfatase activities of the cytosolic mammalian carbonic anhydrase isoforms I, II, and XIII with 4-nitrophenyl esters as substrates. *Bioorganic & Medicinal Chemistry Letters* 18, 2267-2271 (2008).

180. Takaoka, Y., Tsutsumi, H., Kasagi, N., Nakata, E. & Hamachi, I. One-Pot and Sequential Organic Chemistry on an Enzyme Surface to Tether a Fluorescent Probe at the Proximity of the Active Site with Restoring Enzyme Activity. *Journal of the American Chemical Society* 128, 3273-3280 (2006).

181. Vomasta, D., Högner, C., Branda, N.R. & König, B. Regulation of Human Carbonic Anhydrase I (hCAI) Activity by Using a Photochromic Inhibitor. *Angewandte Chemie International Edition* 47, 7644-7647 (2008).

182. Vomasta, D., Innocenti, A., König, B. & Supuran, C.T. Carbonic anhydrase inhibitors: Two-prong versus mono-prong inhibitors of isoforms I, II, IX, and XII exemplified by photochromic cis-1,2-α-dithienylethene derivatives. *Bioorganic & Medicinal Chemistry Letters* 19, 1283-1286 (2009).

183. Voet, D., Voet, J.G. & Pratt, C.W. Fundamentals of biochemistry. (John Wiley & Sons, Inc., New York; 1999).

184. Siraganian, R.P., Zhang, J., Suzuki, K. & Sada, K. Protein tyrosine kinase Syk in mast cell signaling. *Molecular Immunology* 38, 1229-1233 (2002).

185. Turner, M., Schweighoffer, E., Colucci, F., Di Santo, J.P. & Tybulewicz, V.L. Tyrosine kinase SYK: essential functions for immunoreceptor signalling. *Immunology Today* 21, 148-154 (2000).

186. Kuil, J., van Wandelen, L.T.M., de Mol, N.J. & Liskamp, R.M.J. A photoswitchable ITAM peptidomimetic: Synthesis and real time surface plasmon resonance (SPR) analysis of the effects of cis–trans isomerization on binding. *Bioorganic & Medicinal Chemistry* 16, 1393-1399 (2008).

187. Kuil, J., van Wandelen, L.T.M., de Mol, N.J. & Liskamp, R.M.J. Switching between low and high affinity for the Syk tandem SH2 domain by irradiation of azobenzene containing ITAM peptidomimetics. *Journal of Peptide Science* 15, 685-691 (2009).

188. Reisinger, B. et al. Exploiting protein symmetry to design light-controllable enzyme inhibitors. *Angewandte Chemie International Edition* 53, 595-598 (2014).

189. Mdluli, K. & Spigelman, M. Novel targets for tuberculosis drug discovery. *Current Opinion in Pharmacology* 6, 459-467 (2006).

190. Shen, H. et al. A novel inhibitor of indole-3-glycerol phosphate synthase with activity against multidrug-resistant Mycobacterium tuberculosis. *FEBS Journal* 276, 144-154 (2009).

191. Weston, D.G., Kirkham, J. & Cullen, D.C. Photo-modulation of horseradish peroxidase activity via covalent attachment of carboxylated-spiropyran dyes. *Biochimica et Biophysica Acta (BBA) - General Subjects* 1428, 463-467 (1999).

192. Hohsaka, T., Kawashima, K. & Sisido, M. Photoswitching of NAD^+ mediated enzyme reaction through photoreversible antigen-antibody reaction. *Journal of the American Chemical Society* 116, 413-414 (1994).

193. Fujita, D., Murai, M., Nishioka, T. & Miyoshi, H. Light control of mitochondrial Complex I activity by a photoresponsive inhibitor. *Biochemistry* 45, 6581-6586 (2006).

194. Cass, A.E.G. et al. Ferrocene-mediated enzyme electrode for amperometric determination of glucose. *Analytical Chemistry* 56, 667-671 (1984).

195. Blanford, C.F. The birth of protein electrochemistry. *Chemical Communications* 49, 11130-11132 (2013).

196. Purves, D. & Lichtman, J.W. Principles of neural development. (Sinauer Associates, Incorporated, 1985).

197. Quinn, D.M. Acetylcholinesterase: enzyme structure, reaction dynamics, and virtual transition states. *Chemical Reviews* 87, 955-979 (1987).

198. Taylor, P. & Radic, Z. The Cholinesterases: From genes to proteins. *Annual Review of Pharmacology and Toxicology* 34, 281-320 (1994).

199. Lester, H.A., Krouse, M.E., Nass, M.M., Wassermann, N.H. & Erlanger, B.F. A covalently bound photoisomerizable agonist: comparison with reversibly bound agonists at Electrophorus electroplaques. *J Gen Physiol* 75, 207-232 (1980).

200. Lester, H.A. et al. Electrophysiological experiments with photoisomerizable cholinergic compounds: review and progress report. *Ann N Y Acad Sci* 346, 475-490 (1980).

201. Wilson, I.B. & Alexander, J. Acetylcholinesterase: reversible inhibitors, substrate inhibition. *Journal of Biological Chemistry* 237, 1323-1326 (1962).

202. Bieth, J., Vratsanos, S.M., Wassermann, N. & Erlanger, B.F. Photoregulation of biological activity by photochromic reagents, II. Inhibitors of acetylcholinesterase. *Proceedings of the National Academy of Sciences* 64, 1103-1106 (1969).

203. Bieth, J., Wassermann, N., Vratsanos, S.M. & Erlanger, B.F. Photoregulation of biological activity by photochromic reagents, IV. A model for diurnal variation of enzymic activity. *Proceedings of the National Academy of Sciences* 66, 850-854 (1970).

204. Deal, W.J., Erlanger, B.F. & Nachmansohn, D. Photoregulation of biological activity by photochromic reagents, III. Photoregulation of bioelectricity by acetylcholine receptor inhibitors. *Proceedings of the National Academy of Sciences* 64, 1230-1234 (1969).

205. Broichhagen, J., Jurastow, I., Iwan, K., Kummer, W. & Trauner, D. Optical control of acetylcholinesterase with a tacrine switch. *Angewandte Chemie International Edition* 53, 1-5 (2014).

206. Nakata, H. et al. Immunological rapid urease test using monoclonal antibody for Helicobacter Pylory. *J. Gastroenterol. Hepatol.* 19, 970-974 (2004).

207. Korbus, M., Balasubramanian, G., Muller-Plathe, F., Kolmar, H. & Meyer-Almes, F.J. Azobenzene switch with a long-lived cis-state to photocontrol the enzyme activity of a histone deacetylase-like amidohydrolase. *Biol Chem* 395, 401-412 (2014).

208. Huang, Y. & Wang, K.K.W. The calpain family and human disease. *Trends in Molecular Medicine* 7, 355-362 (2001).

209. Imahori, K. Calcium and Cell Function, Vol. 4. (Academic, New York; 1983).

210. Kay, J. Protease Role in Health and Disease. (Plenum, New York; 1983).

211. Chapman, H.A., Riese, R.J. & Shi, G.-P. Emerging roles for Cysteine proteases in human biology. *Annual Review of Physiology* 59, 63-88 (1997).

212. Willner, I., Rubin, S. & Riklin, A. Photoregulation of papain activity through anchoring photochromic azo groups to the enzyme backbone. *Journal of the American Chemical Society* 113, 3321-3325 (1991).

213. Willner, I. & Rubin, S. Reversible photoregulation of the activities of proteins. *Reactive Polymers* 21, 177-186 (1993).

214. Westmark, P.R., Kelly, J.P. & Smith, B.D. Photoregulation of enzyme activity. Photochromic, transition-state-analog inhibitors of cysteine and serine proteases. *Journal of the American Chemical Society* 115, 3416-3419 (1993).

215. Abell, A.D. et al. Investigation into the P3 binding domain of m-Calpain using photoswitchable diazo- and triazene-dipeptide aldehydes: new anticataract agents. *Journal of Medicinal Chemistry* 50, 2916-2920 (2007).

216. Hedstrom, L. Serine protease mechanism and specificity. *Chemical Reviews* 102, 4501-4524 (2002).

217. Tyndall, J.D.A., Nall, T. & Fairlie, D.P. Proteases universally recognize β-strands in their active sites. *Chemical Reviews* 105, 973-1000 (2005).

218. Erlanger, B.F., Wassermann, N.H., Cooper, A.G. & Monk, R.J. Allosteric activation of the hydrolysis of specific substrates by chymotrypsin. *European Journal of Biochemistry* 61, 287-295 (1976).

219. Willner, I., Rubin, S. & Zor, T. Photoregulation of α-chymotrypsin by its immobilization in a photochromic azobenzene copolymer. *Journal of the American Chemical Society* 113, 4013-4014 (1991).

220. Willner, I., Rubin, S., Shatzmiller, R. & Zor, T. Reversible light-stimulated activation and deactivation of α-chymotrypsin by its immobilization in photoisomerizable copolymers. *Journal of the American Chemical Society* 115, 8690-8694 (1993).

221. Pearson, D. & Abell, A.D. Photoswitch inhibitors of (small alpha)-chymotrypsin-increased substitution and peptidic character in peptidomimetic boronate esters. *Organic & Biomolecular Chemistry* 4, 3618-3625 (2006).

222. Harvey, A.J. & Abell, A.D. Azobenzene-containing, peptidyl α-ketoesters as photobiological switches of α-chymotrypsin. *Tetrahedron* 56, 9763-9771 (2000).

223. Pearson, D., Alexander, N. & Abell, A.D. Improved photocontrol of α-chymotrypsin activity: peptidomimetic trifluoromethylketone photoswitch enzyme inhibitors. *Chemistry – A European Journal* 14, 7358-7365 (2008).

224. Pearson, D., Downard, A.J., Muscroft-Taylor, A. & Abell, A.D. Reversible photoregulation of binding of α-chymotrypsin to a gold surface. *Journal of the American Chemical Society* 129, 14862-14863 (2007).

225. Pearson, D. & Abell, A.D. Structural optimization of photoswitch ligands for surface attachment of α-chymotrypsin and regulation of its surface binding. *Chemistry – A European Journal* 16, 6983-6992 (2010).

226. Rudd, E.A. & Brockman, H.L. Pancreatic carboxyl ester lipase (cholesterol estearase). (Elsevier Science, New York; 1984).

227. Hui, D. Molecular Biology of enzymes involved with cholesterol ester hydrolysis in mammalian tissues. *Biochim Biophys Acta* 1303, 1-14 (1996).

228. Cox, M., Nelson, D.R. & Lehninger, A.L. Lehninger principles of biochemistry. (San Francisco; 2005).

229. Liu, D., Karanicolas, J., Yu, C., Zhang, Z. & Woolley, G.A. Site-specific incorporation of photoisomerizable azobenzene groups into ribonuclease S. *Bioorganic & Medicinal Chemistry Letters* 7, 2677-2680 (1997).

230. Hamachi, I., Hiraoka, T., Yamada, Y. & Shinkai, S. Photoswitching of the enzymatic activity of semisynthetic ribonuclease S & prime; bearing phenylazophenylalanine at a specific Site. *Chemistry Letters* 27, 537-538 (1998).

231. James, D.A., Burns, D.C. & Woolley, G.A. Kinetic characterization of ribonuclease S mutants containing photoisomerizable phenylazophenylalanine residues. *Protein Engineering* 14, 983-991 (2001).

232. Schierling, B. et al. Controlling the enzymatic activity of a restriction enzyme by light. *Proceedings of the National Academy of Sciences* 107, 1361-1366 (2010).

233. Hien, L.T. et al. Restriction endonuclease SsoII with photoregulated activity—a "Molecular Gate" approach. *Bioconjugate Chemistry* 22, 1366-1373 (2011).

234. Shimoboji, T. et al. Photoresponsive polymer-enzyme switches. *Proc Natl Acad Sci USA* 99, 16592-16596 (2002).

235. Gröger, H., Asano, Y., Bornscheuer, U.T. & Ogawa, J. Development of biocatalytic processes in Japan and Germany: From research synergies to industrial applications. *Chemistry – An Asian Journal* 7, 1138-1153 (2012).

236. Bautista-Barrufet, A. et al. Optical control of enzyme enantioselectivity in solid phase. *ACS Catalysis* 4, 1004-1009 (2014).

237. Bolivar, J.M., Wiesbauer, J. & Nidetzky, B. Biotransformations in microstructured reactors: more than flowing with the stream? *Trends in Biotechnology* 29, 333-342 (2011).

238. Carrasco-López, C. et al. Activation of bacterial thermoalkalophilic lipases is spurred by dramatic structural rearrangements. *Journal of Biological Chemistry* 284, 4365-4372 (2009).

239. Berglund, P. Controlling lipase enantioselectivity for organic synthesis. *Biomol Eng* 18, 13-22 (2001).

240. Fernandez-Lorente, G. et al. Solid-phase chemical amination of a lipase from bacillus thermocatenulatus to improve its stabilization via covalent immobilization on highly activated glyoxyl-agarose. *Biomacromolecules* 9, 2553-2561 (2008).

241. Palomo, J.M. et al. Modulation of the enantioselectivity of lipases via controlled immobilization and medium engineering: hydrolytic resolution of mandelic acid esters. *Enzyme and Microbial Technology* 31, 775-783 (2002).

242. López-Gallego, F., Abian, O. & Guisán, J.M. Altering the Interfacial Activation Mechanism of a Lipase by Solid-Phase Selective Chemical Modification. *Biochemistry* 51, 7028-7036 (2012).

243. Kocer, A., Walko, M., Meijberg, W. & Feringa, B.L. A Light-Actuated Nanovalve Derived from a Channel Protein. *Science* 309, 755-758 (2005).

244. Pozhidaeva, N., Cormier, M.E., Chaudhari, A. & Woolley, G.A. Reversible Photocontrol of Peptide Helix Content:,Äâ Adjusting Thermal Stability of the Cis State. *Bioconjugate Chemistry* 15, 1297-1303 (2004).

245. Giger, L. et al. Evolution of a designed retro-aldolase leads to complete active site remodeling. *Nat Chem Biol* 9, 494-498 (2013).

246. Coelho, P.S., Brustad, E.M., Kannan, A. & Arnold, F.H. Olefin Cyclopropanation via Carbene Transfer Catalyzed by Engineered Cytochrome P450 Enzymes. *Science* 339, 307-310 (2013).

247. Köhler, V. et al. OsO4–Streptavidin: A Tunable Hybrid Catalyst for the Enantioselective *cis*-Dihydroxylation of Olefins. *Angewandte Chemie International Edition* 50, 10863-10866 (2011).

248. Hyster, T.K., Knörr, L., Ward, T.R. & Rovis, T. Biotinylated Rh (III) Complexes in Engineered Streptavidin for Accelerated Asymmetric C-H Activation. *Science* 338, 500-503 (2012).

249. Acosta, A., Filice, M., Fernandez-Lorente, G., Palomo, J.M. & Guisan, J.M. Kinetically controlled synthesis of monoglyceryl esters from chiral and prochiral acids methyl esters catalyzed by immobilized Rhizomucor miehei lipase. *Bioresource Technology* 102, 507-512 (2011).

250. Barbe, S. et al. Insights into lid movements of Burkholderia cepacia lipase inferred from molecular dynamics simulations. *Proteins: Structure, Function, and Bioinformatics* 77, 509-523 (2009).

251. Lafaquière, V. et al. Control of Lipase Enantioselectivity by Engineering the Substrate Binding Site and Access Channel. *ChemBioChem* 10, 2760-2771 (2009).

252. Yamada, M.D., Nakajima, Y., Maeda, H. & Maruta, S. Photocontrol of Kinesin ATPase Activity Using an Azobenzene Derivative. *Journal of Biochemistry* 142, 691-698 (2007).

253. Erbas-Cakmak, S., Bozdemir, O.A., Cakmak, Y. & Akkaya, E.U. Proof of principle for a molecular 1 : 2 demultiplexer to function as an autonomously switching theranostic device. *Chemical Science* 4, 858-862 (2013).

254. Balzani, V., Credi, A. & Venturi, M. in Molecular Devices and Machines 259-311 (Wiley-VCH Verlag GmbH & Co. KGaA, 2008).

255. Gorostiza, P. & Isacoff, E. Optical Switches for Remote and Noninvasive Control of Cell Signaling. *Science* 322, 395-399 (2008).

256. Ohlsson, J., Wolpher, H., Hagfeldt, A. & Grennberg, H. New dyes for solar cells based on nanostructured semiconducting metal oxides: Synthesis and characterisation of ruthenium (II) complexes with thiol-substituted ligands. *Journal of Photochemistry and Photobiology A: Chemistry* 148, 41-48 (2002).

257. Fujiki, K., Tanifuji, N., Sasaki, Y. & Yokoyama, T. New and Facile Synthesis of Thiosulfonates from Sulfinate/Disulfide/I2 System. *Synthesis* 2002, 0343-0348 (2002).

258. Pearlman, D.A. et al. AMBER, a package of computer programs for applying molecular mechanics, normal mode analysis, molecular dynamics and free energy calculations to simulate the structural and energetic properties of molecules. *Computer Physics Communications* 91, 1-41 (1995).

259. Wang, J., Wolf, R.M., Caldwell, J.W., Kollman, P.A. & Case, D.A. Development and testing of a general amber force field. *Journal of Computational Chemistry* 25, 1157-1174 (2004).

260. Frisch, M.J. et al. (Gaussian, Inc., Wallingford, CT, USA; 2009).

261. Jorgensen, W.L., Chandrasekhar, J., Madura, J.D., Impey, R.W. & Klein, M.L. Comparison of simple potential functions for simulating liquid water. *The Journal of Chemical Physics* 79, 926-935 (1983).

262. Phillips, J.C. et al. Scalable molecular dynamics with NAMD. *Journal of Computational Chemistry* 26, 1781-1802 (2005).

263. Morris, G.M. et al. AutoDock4 and AutoDockTools4: Automated docking with selective receptor flexibility. *Journal of Computational Chemistry* 30, 2785-2791 (2009).

ABBREVIATIONS

Å: Angstroms

AcOH: Acetic acid

AMPA: α-amino-3-hydroxy-5-methyl-4-isoxazolepropionic acid

Ar: Argon

BSA: Bovine Serum Albumina

CNS: Central Nervous System

Con A: Concavaline A

Eq: Equivalents

GlyR: Glycine Receptors

HEK293: Human Embrionic kidney cell line

h: Hours

5-HT: Serotonin receptors

$\mathbf{K_{cat}}$: Catalytic constant

$\mathbf{K_D}$: Dissociation constant

$\mathbf{K_i}$: Inhibition constant

$\mathbf{K_m}$: Michaelis constant

LED: Light Emitting Diodes

mM: Milimolar

nAChR: Nicotinic acetylcholine receptors

NHS: N-Hydroxysuccinimide

nm: Nanometers

NMDA: N-methyl-D-Aspartate

quant: Quantitatively

rt: Room temperature

SPARK: Synthetic Photoisomerizable Azobenzene-regulated K^+

TM: Transmembrane

UPLC: Ultra Performance Liquid Chromatography

µs: Microseconds

UV: Ultra violet

Vis: Visible